

# Active Lévy Matter: Anomalous Diffusion, Hydrodynamics and Linear Stability

Andrea Cairoli\* and Chiu Fan Lee†

Department of Bioengineering, Imperial College London, London SW7 2AZ, United Kingdom

Anomalous diffusion, manifest as a nonlinear temporal evolution of the position mean square displacement, and/or non-Gaussian features of the position statistics, is prevalent in biological transport processes. Likewise, collective behavior is often observed to emerge spontaneously from the mutual interactions between constituent motile units in biological systems. Examples where these phenomena can be observed simultaneously have been identified in recent experiments on bird flocks, fish schools and bacterial swarms. These results pose an intriguing question, which cannot be resolved by existing theories of active matter: How is the collective motion of these systems affected by the anomalous diffusion of the constituent units? Here, we answer this question for a microscopic model of *active Lévy matter* – a collection of active particles that perform superdiffusion akin to a Lévy flight and interact by promoting polar alignment of their orientations. We present in details the derivation of the hydrodynamic equations of motion of the model, obtain from these equations the criteria for a disordered or ordered state, and apply linear stability analysis on these states at the onset of collective motion. Our analysis reveals that the disorder-order phase transition in active Lévy matter is critical, in contrast to ordinary active fluids where the phase transition is, instead, first-order. Correspondingly, we estimate the critical exponents of the transition by finite size scaling analysis and use these numerical estimates to relate our findings to known universality classes. These results highlight the novel physics exhibited by active matter integrating both anomalous diffusive single-particle motility and inter-particle interactions.

Active matter refers to systems comprising constitutive units with the ability to harvest energy from the environment and employ it to generate motion [1–6]. The mutual interactions of the active constituent units in these systems often cause the spontaneous emergence of collective behavior manifest as collective motion (flocking) [7–10], turbulence [11–19], and motility-induced phase separation [20–23]. Examples are widespread in nature: microorganisms swimming in ambient fluids [11, 13, 18, 24–26], cell tissues [27–32], the cellular cytoskeleton [6, 33, 34], and social groups of animals (from small-scale ones like ants and locusts to large-scale ones like birds, fish and even humans) [10, 35–38]. Furthermore, there has been wide interest in artificially engineering active systems. Numerous examples can be mentioned, such as collections of chemically self-propelled Janus particles [39] and swarming robots [40], and motility assays of self-assembled cytoskeletal components, especially cross-linked actin filaments or microtubules and motor proteins [41–43].

Being inherently out of equilibrium due to the continuous energy flux, active matter systems cannot be described within the framework of equilibrium statistical mechanics [44]. Instead, several agent-based microscopic models and hydrodynamic continuum theories have been formulated so far to capture the characteristic collective properties of these systems (e.g., see [4]). These hydrodynamic theories are usually derived by coarse-graining the many-body dynamics resulting from the underlying interacting active units [45–52], whose motion is typi-

cally assumed to be simple self-propulsion plus Gaussian fluctuations in their orientations and spatial positions [2, 4, 5, 53]. Alternatively, hydrodynamic theories have also been derived in full generality from first principles based on symmetry arguments [1, 8, 9, 54–59]. To incorporate the aforementioned microscopic fluctuations, these theories typically contain Gaussian noise terms, which are a manifestation of the celebrated *central limit theorem* [60], stating that the averaging over many fluctuations following a distribution with finite variance inevitably leads to a Gaussian distribution law.

In particular, flocking systems have been intensely studied in this respect [1, 4, 10]. The pioneering Vicsek model [7] first identified that (a) overdamped self-propelled particles with (b) noisy reorientation of the velocities and (c) short-range interactions favoring polar alignment of the velocities can self-organize into polar ordered states (flocks), where particles move on average in the same direction. This phase transition between disordered and ordered states is widely believed to be first-order: This result was first supported by numerical simulations of microscopic dynamics using either continuous or lattice based models implementing the basic ingredients (a)–(c), [61–64] (however their conclusions on the nature of the phase transition have been long debated [65–71]), and only later supported analytically by linear stability analysis of hydrodynamic theories [45–51]. The Vicsek model has been adapted over the years to include additional features such as particle cohesion [72, 73]; metric-free [74, 75], nematic [76, 77] and possibly mixed nematic-polar alignment interactions [78, 79]; density dependent velocities [80, 81]; inertial and non-Markovian orientational dynamics [82–86]; particle chirality [87–93]; and velocity reversals [94].

Nevertheless, an important setup has remained so far

\* andrea.cairoli@crick.ac.uk; current author’s affiliation: The Francis Crick Institute, London NW1 1AT, United Kingdom.

† c.lee@imperial.ac.uk

largely unexplored: Consider a population of active particles that, when their mutual interactions are switched off, can perform anomalous diffusive dynamics other than self-propulsion (see, e.g., [95–99] and references below). The following question arises naturally: How does this different single-particle diffusive dynamics of the active units affect the emergence, stability and universality of collective behavior, when particle interactions are switched back on?

Anomalous diffusion, which is generically characterized by a non linear position mean-square displacement (MSD) exhibiting possibly multiple scaling regimes [100] where  $\text{MSD}(t) \sim t^\beta$  with  $0 < \beta < 1$  for subdiffusion and  $1 < \beta < 2$  for superdiffusion ( $\beta = 1$  is normal diffusion), has been indeed widely observed experimentally for both transport processes in physical systems [96–98] and biological motion [99, 101–104]. While subdiffusion is typical for single particles whose motion is impeded, e.g. because they move in a crowded environment [105, 106], superdiffusion has been shown to optimize the search and foraging strategies of living organisms in specific environmental conditions [107–110], such that it can be potentially advantageous not only for single organisms per se but also when they belong to large interacting groups. Recent experiments have indeed measured superdiffusive dynamics manifest as power-law displacement distributions for individual organisms in bird flocks, fish schools and swarming bacteria [111–113], thus supporting the biological relevance of the scenario just depicted. Furthermore, such superdiffusive single-particle dynamics has been also shown to emerge as a result of non linear and non-Markovian effects [114]. Remarkably, these dynamics can be described, to first approximation, by models incorporating fluctuations with infinite variances, whose average has been shown to converge again to a universal distribution, called the  $\alpha$ -stable Lévy distribution, as guaranteed by the *generalized* central limit theorem [115].

Therefore, in this paper, we investigate the consequences of the anomalous superdiffusive dynamics on the collective properties of active matter. As a distinct notation, we will denote systems integrating anomalous superdiffusive behaviour and many-body particle interactions as *active Lévy matter* (ALM) [116]. Collective properties can be generically understood by formulating a hydrodynamic theory. However, while in ordinary active matter, symmetry considerations alone can sometimes be sufficient for the derivation of the hydrodynamic equations of motion (EOM), it is in contrast unclear how symmetry constrains the form of the hydrodynamic EOM for ALM. In particular, since fractional derivatives are expected to appear in these equations, the underlying model equations becomes non local and effectively long range and the typical way of truncating them by ignoring higher order derivatives may not be applicable.

To elucidate this issue, we will thus present the detailed derivation of the hydrodynamic EOM for ALM [116], by coarse-graining a microscopic model of polar alignment interacting active particles that perform superdif-

fusion akin to Lévy flights [117–119]. The Lévy flight is a Markovian random-walk model where superdiffusive behaviour is captured by fat-tailed jump-length distributions. Our setup differs from other models of ALM that have been previously proposed [120, 121], as ours is the only one that can permit the emergence of collective motion.

The Article is organized as follows. In Section I, we characterize the single-particle diffusive dynamics of our microscopic model of ALM in terms of the position mean-square displacement and the position statistics along any arbitrary direction. In Section II, we switch on the polar alignment interactions and derive the effective one-body Fokker-Planck equation that determines the joint statistics of the position and direction of motion of the active Lévy particles by employing the Bogoliubov-Born-Green-Kirkwood-Yvon (BBGKY) hierarchical method [122] and the stochastic calculus of Lévy processes [123]. In Section III, we show how to perform a Fourier angular expansion on this equation, and discuss the relevant terms that survive in the hydrodynamic limit, i.e., the limit  $k \rightarrow 0$  with  $k \equiv |\mathbf{k}|$  and  $\mathbf{k}$  the independent variable in Fourier space. This procedure yields the hydrodynamic description of our microscopic model of ALM, which is our first main result. Section IV presents the linear stability analysis on the characteristic disordered and ordered phases that are predicted by the hydrodynamic theory. Specifically, in Section IV A we show that the disordered phase is stable at linear level against small perturbations in all directions. Likewise, in Section IV B we discuss the stability of the ordered phase. First, we consider small longitudinal perturbations (i.e., in the direction of spontaneous symmetry breaking). Differently from ordinary active fluids, where a characteristic banding instability emerges at the onset of collective motion that renders the phase-transition first-order [61–64], our hydrodynamic theory predicts a stable ordered phase in the hydrodynamic limit (see Eq. (4.32)). Secondly, we demonstrate that the phase is stable at the onset also against transversal perturbations (i.e., in the direction orthogonal to the collective motion). These results, therefore, suggest that the order-disorder phase transition can be potentially critical in ALM. This prediction is the second main result of our study. A further confirmation of the criticality of the transition is presented in Sec. V, where we perform a finite size scaling analysis through extensive numerical simulations of the underlying microscopic dynamics. Correspondingly, we characterize numerically both static and dynamic critical exponents of the disorder-to-collective motion transition and use these numerical estimates to relate our findings to known universality classes. This numerical characterization of the critical properties of the transition is our third main result. Finally, in Section VI we draw conclusions and outline future perspectives.

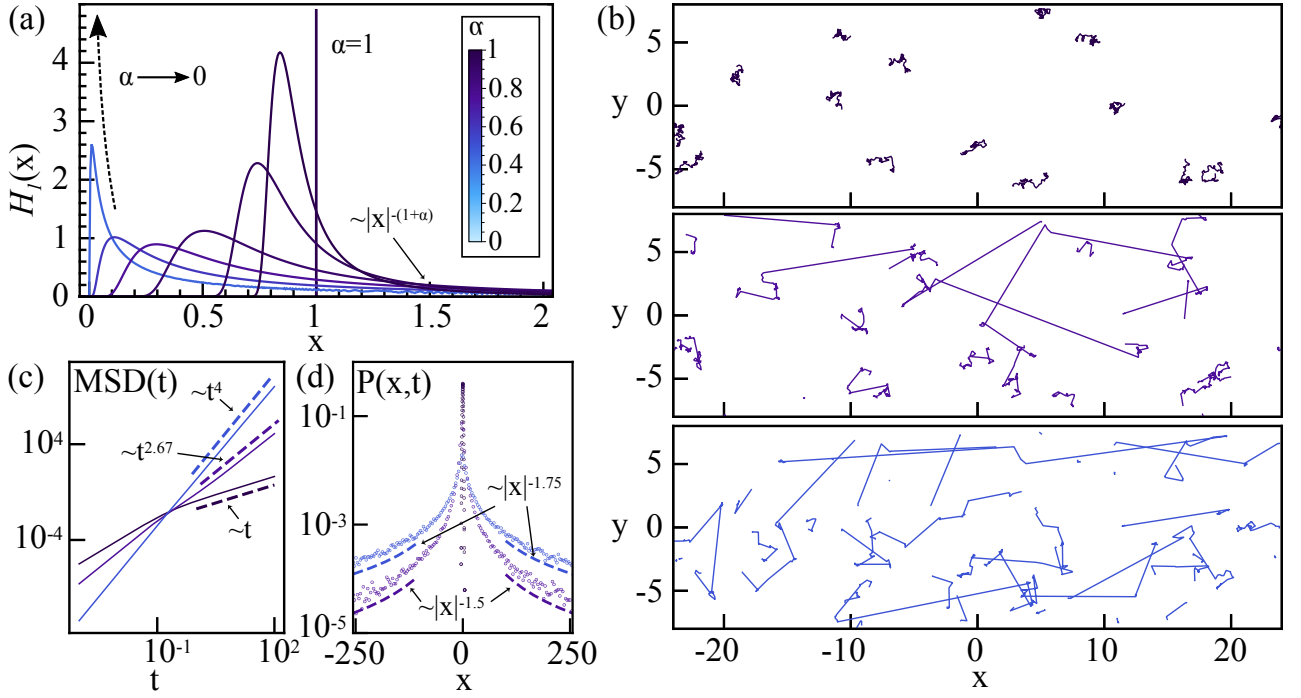


FIG. 1. (a) Scaling function  $H_1$  for different values of the stability index  $0 < \alpha < 1$ . The special case  $\alpha = 1$  where  $H_1(x) = \delta(x-1)$  is plotted for reference. (b) Exemplary trajectories of particles moving according to the dynamical model (1.1) in an asymmetric box  $6L \times 2L$  (here  $L = 8$ ) with periodic boundary conditions. Characteristic parameters are  $\alpha = \{1, 0.75, 0.5\}$  (top to bottom panel) and  $\sigma = 10$ . Large particle jumps induced by the Lévy stable displacement statistics are evident. (c) Mean-square displacement and (d) position statistics projected in the  $x$ -direction of the active Lévy particles. As we are interested in the characteristic features of the free diffusion of the active particles, we run the simulations for these panels without periodic boundary conditions. All the simulation parameters are defined as in panel (b).

## I. SINGLE PARTICLE DYNAMICS

We consider a single particle whose position  $\mathbf{r}(t)$  on a planar surface is described by the Langevin equations:

$$\dot{\mathbf{r}}(t) = \eta(t)\mathbf{n}(\theta(t)), \quad \dot{\theta}(t) = \xi(t) \quad (1.1)$$

with the unit vector  $\mathbf{n}(\theta) \equiv (\cos \theta, \sin \theta)$  prescribing its direction of motion. We define the noises  $\xi$  and  $\eta$ , and respectively  $\langle \cdot \rangle$  and  $\prec \cdot \succ$  the ensemble averages over their stochastic realizations, as follows: (i)  $\xi$  is a white Gaussian noise of variance  $\sigma$ , i.e.,  $\langle \xi(t) \rangle = 0$  and  $\langle \xi(t)\xi(t') \rangle = 2\sigma\delta(t-t')$ ; (ii)  $\eta$  is the formal derivative of the one-sided positive Lévy process  $L(t) \equiv \int_0^t \eta(t') dt'$ . This process is thus a subordinator (i.e., a strictly non-decreasing Lévy process) and is specified by the characteristic function  $\prec e^{ikL(t)} \succ = e^{t\Psi(k)}$ , with the so called Lévy symbol [123]

$$\Psi(k) = ivk + \int_0^\infty (e^{ikz} - 1)\nu(dz), \quad (1.2)$$

where  $v \geq 0$  is the constant drift and  $\nu(dz)$  is the Lévy measure satisfying  $\nu(-\infty, 0) = 0$  and  $\int_0^\infty \min(z, 1)\nu(dz) < \infty$ . An important example of such

processes is represented by stable subordinators with stability parameter  $0 < \alpha < 1$ . These are defined by setting

$$v = 0, \quad \nu(dz) = \frac{\alpha}{\Gamma(1-\alpha)} \frac{dz}{z^{1+\alpha}}, \quad (1.3)$$

which yields  $\Psi(k) = k^\alpha$  [123]. When an explicit upper cutoff  $H$  is introduced in the Lévy measure, we obtain tempered Lévy stable subordinators; in this case

$$\nu(dz) = \frac{\alpha}{\Gamma(1-\alpha)} e^{-Hz} \frac{dz}{z^{1+\alpha}} \quad (1.4)$$

and consequently  $\Psi(k) = (k+H)^\alpha - H^\alpha$ . The characteristic functional of  $\eta$  is thus defined as [124]

$$G[h(t')] \equiv \langle e^{-\int_0^\infty h(t')\eta(t') dt'} \rangle = e^{-\int_0^\infty \Psi(h(t')) dt'} \quad (1.5)$$

with  $h$  an arbitrary test function. The noises  $\xi, \eta$  are assumed independent, and Itô prescription is chosen for the multiplicative term of Eq. (1.1).

The process  $L$  measures the total distance traveled by the active particles. Its statistics,  $Q(l, t) \equiv \langle \delta(l - L(t)) \rangle$ , is easily calculated by Fourier inversion of its characteristic function. For stable subordinators, in particular, we find the following characterization: For  $0 < \alpha < 1$

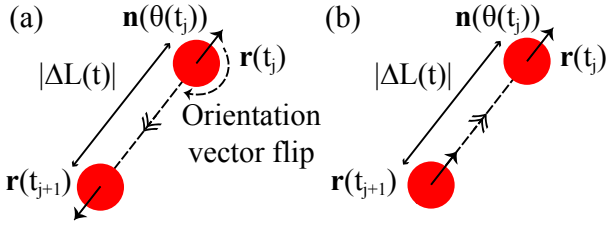


FIG. 2. Schematic of different interpretations for negative distributed displacements of active Lévy particles.

1,  $Q(l, t) = t^{-1/\alpha} H_1(lt^{-1/\alpha})$  with the scaling function  $H_1(x) \equiv (2\pi)^{-1} \int_{-\infty}^{\infty} e^{-i\omega x - (-i\omega)^\alpha} d\omega$  (see Fig. 1a). The function  $H_1$  is unimodal with maximum at the point  $x_m(\alpha)$  and heavy-tailed asymptotics for large  $x$ , i.e.,  $H_1(x) \sim x^{-(1+\alpha)}$  for  $x \rightarrow \infty$ , and satisfies  $H_1(x) \rightarrow 0$  for  $x \rightarrow 0^+$ . As  $\alpha \rightarrow 0$ ,  $x_m \rightarrow 0$  and  $H_1$  simultaneously sharpens at this point [125–128]. For  $\alpha = 1$ ,  $Q(l, t) = \delta(l - t)$  [95, 129]. In this case Eqs. (2.1) reduce to self-propelled dynamics with constant particle velocity [7]. Exemplary particle trajectories for different values of the characteristic parameter  $\alpha$  are shown in Fig. 1b.

When  $L$  is a stable subordinator, the dynamics described by the Langevin Eqs. (1.1) exhibits the following super-diffusive features (see Appendix A): (a) fractional moments  $\prec \langle |\mathbf{r}'(t)|^\delta \rangle \succ$  ( $0 < \delta < \alpha$ ) with  $\mathbf{r}'(t) \equiv \mathbf{r}(t) - \mathbf{r}(0)$  scale as  $\sim t^{\delta/\alpha}$ ; (b) moments of order  $\geq 1$  do not exist. Nevertheless, upon rescaling suitably the fractional moments, we obtain that the mean-square displacement  $\text{MSD}(t) \equiv \prec \langle [\mathbf{r}'(t)]^2 \rangle \succ$  scales as  $\sim t^{2/\alpha}$  for long times (see Fig. 1c); (c) the projected position statistics, e.g. in the direction  $\mathbf{e}_1 \equiv (1, 0)$ , which is defined as  $P(x, t) \equiv \prec \langle \delta(x - \mathbf{r}'(t) \cdot \mathbf{e}_1) \rangle \succ$ , has power-law asymptotic tail behaviour with the same characteristic exponent of  $H_1$ , i.e.,  $P(x, t) \sim |x|^{-(1+\alpha)}$  (see Fig. 1d).

We remark that the stochastic increments  $\Delta L(t) \equiv \int_t^{t+\Delta t} \eta(t') dt' = |\mathbf{r}(t + \Delta t) - \mathbf{r}(t)|$  with  $\Delta t$  an arbitrarily small time step, which measure the distance traveled by the active particle over the time interval  $[t, t + \Delta t]$  in the direction  $\mathbf{n}(\theta(t))$ , are non-negative with the definition chosen for the step size process  $\eta$ ; thus, the particle orientation vector is determined only by the dynamics of the angular variable  $\theta$  as prescribed by Eqs. (1.1). Nevertheless, more general Lévy processes generating both positive and negative increments, such as, e.g., symmetric Lévy stable processes with  $\Psi(k) = -|k|^\beta$  ( $0 < \beta < 2$ ), can also be used to define the step-size process by adopting a suitable interpretation of the negative increments. In fact, if  $\Delta L(t)$  is negative, two alternative scenarios can be identified (see schematic in Fig. 2). On the one hand, we can flip the orientation vector of the active Lévy particle, which is then displaced by  $|\Delta L(t)|$  (Fig. 2a); this choice inevitably increases the noise in the system, thus disallowing collective motion (verified numerically; not shown). On the other hand, we can keep the orientation vector unchanged and displace the particle by  $|\Delta L(t)|$  in the direction  $-\mathbf{n}(\theta(t))$  (Fig. 2b). This latter case is

reminiscent of the model studied by Mahault and collaborators [94], where ordinary self-propelled active particles can move in the direction opposite to their intrinsic polarity with some constant probability  $p$ .

## II. MANY-BODY SYSTEM WITH POLAR ALIGNMENT INTERACTIONS AND THE ONE-BODY FOKKER-PLANCK EQUATION

We now consider  $N$  active Lévy particles and switch on interactions between them that promote polar alignment of their orientation vectors. These are modeled by modifying the angular dynamics in (1.1) as

$$\dot{\mathbf{r}}_i(t) = \eta_i(t) \mathbf{n}(\theta_i(t)), \quad \dot{\theta}_i(t) = F_i(t) + \xi_i(t), \quad (2.1)$$

where the force  $F_i$  is defined as [7, 46]

$$F_i(t) \equiv \frac{\gamma}{\pi d^2} \sum_{j=1}^N H(d - |\mathbf{r}_{ij}|) \sin(\theta_j - \theta_i) \quad (2.2)$$

with  $\mathbf{r}_{ij} \equiv \mathbf{r}_i - \mathbf{r}_j$  the distance between particle  $i$ -th and  $j$ -th,  $d > 0$  the interaction range, and  $H$  the Heaviside function ( $H(x) = 1$  for  $x \geq 0$ ;  $H(x) = 0$  otherwise).

The one-body Fokker-Planck equation for the stochastic dynamics described by the Langevin equations (2.1) is derived by using the BBGKY hierarchical formalism [122]. Schematically this method consists in the following steps: (1.) one computes the  $N$ -body probability density function (PDF)  $P_N(\mathbf{X}, \Phi, t) \equiv \prec \langle \prod_{j=1}^N \delta(\mathbf{x}_j - \mathbf{r}_j(t)) \delta(\phi_j - \theta_j(t)) \rangle \succ$ , where we introduce the shorthand vector notation  $\mathbf{X} \equiv (\mathbf{x}_1, \dots, \mathbf{x}_N)$ ,  $\Phi \equiv (\phi_1, \dots, \phi_N)$ . (2.) One then derives an exact equation for the one-body PDF  $P(\mathbf{x}_1, \phi_1, t) \equiv N \int d^2 \mathbf{x}_2 d\phi_2 \dots d^2 \mathbf{x}_N d\phi_N P_N(\mathbf{X}, \Phi, t)$  by integrating out  $N - 1$  other degrees of freedom. The resulting equation naturally depends on the two-body PDF  $P_2(\mathbf{x}_1, \phi_1, \mathbf{x}_2, \phi_2, t) \equiv N(N - 1) \int d^2 \mathbf{x}_3 d\phi_3 \dots d^2 \mathbf{x}_N d\phi_N P_N(\mathbf{X}, \Phi, t)$ . (3.) Finally, one adopts a suitable approximation of the two-body distribution in terms of the one-body PDF in order to close the equation. We adopt here the *molecular chaos* approximation from the Boltzmann kinetic theory [130]; however we apply the approximation directly in the BBGKY formalism to close the equation. Specifically, in mathematical terms, the two-body distribution function is factorized into a product of two independent one-body densities

$$P_2(\mathbf{x}_1, \phi_1, \mathbf{x}_2, \phi_2, t) = P(\mathbf{x}_1, \phi_1, t) P(\mathbf{x}_2, \phi_2, t). \quad (2.3)$$

This approximation is particularly suited for dilute systems with long-range interactions between particles [131], but is nevertheless widely applied to self-propelled particle models for active matter, where in contrast the interactions are typically short-range [45–50, 52]. In light of this, the approximation is, in fact, even more justified for ALM than for ordinary (self-propelled) active matter, because the Lévy displacement statistics renders the short-range alignment interactions effectively long-range. Two

arguments support the validity of this statement: First, the large relocations of the active particles that are induced by their fat-tailed displacement statistics greatly facilitate the removal of the spatial correlations between them. This is evidenced by the rapid homogenization of the pair correlation function of the system observed in numerical simulations (see Sec. V, Fig. 5(a)). Second, these relocations ultimately invalidate the assumption that only interactions local in time and space between the constituent particles determine the macroscopic behaviour of the system, which is at the basis of the standard kinetic theory of dilute gases [130]. As a further consequence of the Lévy displacement statistics, in fact, even in dilute conditions there is a finite probability for more than one particle to jump in one time-step in the vicinity of another particle.

Step (1.) can be solved by employing the stochastic calculus of Lévy processes [123]. We thus rewrite the Langevin equations (2.1) in vector notation, i.e.,

$$\begin{pmatrix} \{d\mathbf{r}_i(t)\} \\ \{d\theta_i(t)\} \end{pmatrix} = \begin{pmatrix} \mathbf{0}_N \\ \{F_i(t)\} \end{pmatrix} dt + \begin{pmatrix} \text{diag}(\{\mathbf{n}(\theta_i(t))\}) & \mathbf{0}_N \\ \mathbf{0}_N & \sqrt{2\sigma}\mathbf{I}_N \end{pmatrix} \begin{pmatrix} \{dL_i(t)\} \\ \{dW_i(t)\} \end{pmatrix} \quad (2.4)$$

with  $dL_i(t) \equiv \eta_i dt$  the traveled distance of the active particle during the infinitesimal time interval  $[t, t + dt]$ , and  $dW_i(t) \equiv \xi_i dt$  the increment of the angular noise over the same time interval. The Fokker-Planck equation of the  $2N$  dimensional process  $(\{\mathbf{r}_i(t)\}, \{\theta_i(t)\})$  is

$$\frac{\partial}{\partial t} P_N(\mathbf{X}, \Phi, t) = (A^\dagger P_N)(\mathbf{X}, \Phi, t) \quad (2.5)$$

with  $A^\dagger$  the adjoint of its characteristic generator  $A$ . Because the noises  $\{L_i\}, \{W_i\}$  are independent,  $A$  can be written as the sum of its continuous  $A_c$  and càdlàg  $A_d$  parts ( $A_d$  is right continuous with left limits). In other words,  $(Ah)(\mathbf{X}, \Phi) = (A_c h)(\mathbf{X}, \Phi) + (A_d h)(\mathbf{X}, \Phi)$  for an arbitrary smooth function  $h(\mathbf{X}, \Phi)$  within its domain. These operators are respectively defined as

$$A_c h \equiv \sum_{j=1}^N \left[ v_j \mathbf{n}(\phi_j) \cdot \nabla_j + F_j(t) \frac{\partial}{\partial \phi_j} + \sigma \frac{\partial^2}{\partial \phi_j^2} \right] h, \quad (2.6)$$

$$A_d h \equiv \sum_{j=1}^N \int_0^\infty [-1 + \mathcal{T}_{z\mathbf{n}(\phi_j)}^+] h \nu(dz) \quad (2.7)$$

with the translation operator

$$\mathcal{T}_{z\mathbf{n}(\phi_j)}^\pm h \equiv h(\{\mathbf{x}_i\}_{i=1}^{j-1}, \mathbf{x}_j \pm z\mathbf{n}(\phi_j), \{\mathbf{x}_i\}_{i=j+1}^N, \Phi). \quad (2.8)$$

Their adjoint operators are easily computed. Considering two arbitrary smooth functions  $h_1, h_2$  and adopting the notation  $\int_{\mathbb{R}^2} \int_{-\pi}^\pi d\Phi d\mathbf{X} = \prod_{j=1}^N \int_{\mathbb{R}^2} \int_{-\pi}^\pi d\phi_j d\mathbf{x}_j$  we can

calculate

$$\begin{aligned} (A_c h_1, h_2) &= \int_{\mathbb{R}^2} \int_{-\pi}^\pi [(A_c h_1) h_2] d\Phi d\mathbf{X} \\ &= \sum_{j=1}^N \int_{\mathbb{R}^2} \int_{-\pi}^\pi h_2 \left[ \mathcal{L}_j + F_j(t) \frac{\partial}{\partial \phi_j} \right] h_1 d\Phi d\mathbf{X} \\ &= \sum_{j=1}^N \int_{\mathbb{R}^2} \int_{-\pi}^\pi h_1 \left[ \mathcal{L}_j^\dagger - \frac{\partial}{\partial \phi_j} F_j(t) \right] h_2 d\Phi d\mathbf{X} \\ &= (h_1, A_c^\dagger h_2), \end{aligned} \quad (2.9)$$

where the second and third lines are related by integration by parts, and we introduce the auxiliary operators

$$\mathcal{L}_j(\mathbf{x}_j, \phi_j) \equiv v_j \mathbf{n}(\phi_j) \cdot \nabla_j + \sigma \frac{\partial^2}{\partial \phi_j^2}, \quad (2.10)$$

$$\mathcal{L}_j^\dagger(\mathbf{x}_j, \phi_j) \equiv -v_j \mathbf{n}(\phi_j) \cdot \nabla_j + \sigma \frac{\partial^2}{\partial \phi_j^2}. \quad (2.11)$$

Similarly, for the operator  $A_d$  we obtain

$$\begin{aligned} (A_d h_1, h_2) &= \int_{\mathbb{R}^2} \int_{-\pi}^\pi [(A_d h_1) h_2] d\Phi d\mathbf{X} \\ &= \sum_{j=1}^N \int_{\mathbb{R}^2} \int_{-\pi}^\pi h_2 \int_0^\infty [-1 + \mathcal{T}_{z\mathbf{n}(\phi_j)}^+] h_1 \nu(dz) d\Phi d\mathbf{X} \\ &= \sum_{j=1}^N \int_{\mathbb{R}^2} \int_{-\pi}^\pi h_1 \int_0^\infty [-1 + \mathcal{T}_{z\mathbf{n}(\phi_j)}^-] h_2 \nu(dz) d\Phi d\mathbf{X}' \\ &= (h_1, A_d^\dagger h_2), \end{aligned} \quad (2.12)$$

where we use the change of variables  $\mathbf{x}'_j = \mathbf{x}_j + z\mathbf{n}(\phi_j)$ ,  $\mathbf{x}'_i = \mathbf{x}_i$  for  $i \neq j$  to rearrange the integrand terms. Thus,  $A^\dagger P_N \equiv (A_c^\dagger + A_d^\dagger) P_N$  with

$$A_c^\dagger P_N \equiv \sum_{j=1}^N \left[ \mathcal{L}_j^\dagger - \frac{\partial}{\partial \phi_j} F_j(t) \right] P_N, \quad (2.13)$$

$$A_d^\dagger P_N \equiv \sum_{j=1}^N \int_0^\infty [-1 + \mathcal{T}_{z\mathbf{n}(\phi_j)}^-] P_N \nu(dz). \quad (2.14)$$

Finally, substituting  $F_j$  as specified in Eq. (2.2) and Eqs. (2.13, 2.14) into Eq. (2.5), we obtain

$$\begin{aligned} \left( \frac{\partial}{\partial t} - \sum_{j=1}^N \mathcal{L}_j^\dagger \right) P_N &= - \sum_{j=1}^N \int_0^\infty [1 - \mathcal{T}_{z\mathbf{n}(\phi_j)}^-] P_N \nu(dz) \\ &\quad - \frac{\gamma}{\pi d^2} \sum_{j,m} H(d - |\mathbf{x}_{mj}|) \frac{\partial}{\partial \phi_j} [\sin(\phi_m - \phi_j) P_N] \end{aligned} \quad (2.15)$$

with the shorthand notation  $\mathbf{x}_{mj} \equiv \mathbf{x}_m - \mathbf{x}_j$ .

Step (2.) is straightforward. Only the integration of the fractional term requires special care. In details, we calculate the quantity  $N \prod_{m=2}^N \int_{\mathbb{R}^2} \int_{-\pi}^\pi \int_0^\infty [1 -$

$\mathcal{T}_{z\mathbf{n}(\phi_j)}^-]P_N \nu(dz) d\phi_m d\mathbf{x}_m$ . If  $j = 1$  this formula reduces to  $\int_0^\infty [1 - \mathcal{T}_{z\mathbf{n}(\phi_1)}^-]P \nu(dz)$ . Instead, if  $j \neq 1$  we obtain

$$\begin{aligned} & \int_{\mathbb{R}^2} \int_{-\pi}^\pi \int_0^\infty [1 - \mathcal{T}_{z\mathbf{n}(\phi_j)}^-]P(\mathbf{x}_j, \phi_j, t) \nu(dz) d\phi_j d\mathbf{x}_j \\ &= \int_{\mathbb{R}^2} \int_0^\infty \prec \langle [1 - \mathcal{T}_{z\mathbf{n}(\theta_j(t))}^-] \delta(\mathbf{x}_j - \mathbf{r}_j(t)) \rangle \succ \nu(dz) d\mathbf{x}_j \\ &= \int_0^\infty \prec \langle e^{i\mathbf{k} \cdot \mathbf{r}_j(t)} [1 - e^{iz\mathbf{k} \cdot \mathbf{n}(\theta_j(t))}] \rangle \succ \nu(dz) \Big|_{\mathbf{k}=0} \\ &= 0. \end{aligned} \quad (2.16)$$

Therefore, we obtain the equation

$$\begin{aligned} & \left( \frac{\partial}{\partial t} - \mathcal{L}_1^\dagger \right) P + \int_0^\infty [1 - \mathcal{T}_{z\mathbf{n}(\phi_1)}^-]P \nu(dz) = -\frac{\gamma}{\pi d^2} \times \\ & \times \frac{\partial}{\partial \phi_1} \int_{-\pi}^\pi \int_{\mathbb{R}^2} H(d - |\mathbf{x}_{12}|) \sin(\phi_2 - \phi_1) P_2 d\mathbf{x}_2 d\phi_2. \end{aligned} \quad (2.17)$$

Implementing the approximation (2.3) as prescribed in step (3.) finally yields

$$\left( \frac{\partial}{\partial t} - \tilde{\mathcal{L}}_1 \right) P + \int_0^\infty [1 - \mathcal{T}_{z\mathbf{n}(\phi_1)}^-]P \nu(dz) = 0 \quad (2.18)$$

where we define the operator  $\tilde{\mathcal{L}}_1$  as

$$\tilde{\mathcal{L}}_1 \equiv \mathcal{L}_1^\dagger + \frac{\partial}{\partial \phi_1} M[P] \quad (2.19)$$

and the functional of  $P$

$$\begin{aligned} M[P] &\equiv -\frac{\gamma}{\pi d^2} \int_{-\pi}^\pi \int_{\mathbb{R}^2} H(d - |\mathbf{x}_{12}|) \times \\ &\times \sin(\phi_2 - \phi_1) P(\mathbf{x}_2, \phi_2, t) d\mathbf{x}_2 d\phi_2. \end{aligned} \quad (2.20)$$

Taking the large-scale limit where  $d \simeq 0$ , this reduces to (see Appendix C for a formal derivation)

$$M[P] \simeq -\gamma \int_{-\pi}^\pi \sin(\phi_2 - \phi_1) P(\mathbf{x}_1, \phi_2, t) d\phi_2. \quad (2.21)$$

Eq. (2.18) with the specifics (2.19, 2.21) is the reduced one-body Fokker-Planck equation of the microscopic model (2.1). The remaining non local operator is specified by the prescribed statistics of the noise  $L_1$ .

For stable subordinators in particular Eq. (2.18) can be rewritten as (see Eq. (1.3))

$$\left( \frac{\partial}{\partial t} + \mathcal{D}_{\mathbf{n}(\phi)}^\alpha - \sigma \frac{\partial^2}{\partial \phi^2} - \frac{\partial}{\partial \phi} M[P] \right) P = 0, \quad (2.22)$$

where  $\mathcal{D}_{\mathbf{n}(\phi)}^\alpha$  is the fractional directional derivative [132]

$$\mathcal{D}_{\mathbf{n}(\phi)}^\alpha P \equiv \frac{\alpha}{\Gamma(1-\alpha)} \int_0^\infty [1 - \mathcal{T}_{z\mathbf{n}(\phi)}^-]P \frac{dz}{z^{1+\alpha}}. \quad (2.23)$$

Fractional advection-diffusion equations similar to Eq. (2.18) were first discussed by Meerschaert and collaborators [133]. Their model however did not account for

interactions between the moving particles, which could affect the time evolution of the velocity directions. Thus, the statistics of the velocity directions of the particles can be prescribed *a priori* in their case by specifying a probability measure  $M(d\mathbf{n})$  over the unit circle. The fractional operator thus simplifies to

$$\int_{\|\mathbf{n}\|=1} \int_0^\infty [1 - \mathcal{T}_{z\mathbf{n}}^-]P \nu(dz) M(d\mathbf{n}) \quad (2.24)$$

with  $P$  the particle position statistics (indeed the velocity direction is no longer needed to build a statistical description of the anomalous diffusion process). This is different from the scenario discussed here, where the velocity directions of the active particles are primitive statistical variables for the diffusion process, and their statistics must be inferred from the many-body dynamics.

### III. DERIVATION OF THE HYDRODYNAMIC EQUATIONS

The hydrodynamic description for the microscopic model (2.1) is obtained by performing a Fourier expansion of the distribution  $P$  with respect to the angular argument [45, 46, 48–50, 52]. We thus write

$$P(\mathbf{x}, \phi, t) \equiv \frac{1}{2\pi} \sum_{m \in \mathbb{Z}} f_m(\mathbf{x}, t) e^{-im\phi} \quad (3.1)$$

with the  $m$ -th order angular mode

$$f_m(\mathbf{x}, t) \equiv \int_{-\pi}^\pi e^{im\phi} P(\mathbf{x}, \phi, t) d\phi. \quad (3.2)$$

The slow macroscopic fields are the density

$$\rho(\mathbf{x}, t) \equiv \int_{-\pi}^\pi P(\mathbf{x}, \phi, t) d\phi, \quad (3.3)$$

the mean direction

$$\mathbf{p}(\mathbf{x}, t) \equiv \int_{-\pi}^\pi \mathbf{n}(\phi) P(\mathbf{x}, \phi, t) d\phi, \quad (3.4)$$

and the apolar nematic tensor

$$\mathbf{Q}(\mathbf{x}, t) \equiv \int_{-\pi}^\pi \left[ \mathbf{n}(\phi) \mathbf{n}(\phi) - \frac{1}{2} \mathbf{1} \right] P(\mathbf{x}, \phi, t) d\phi \quad (3.5)$$

with  $\mathbf{1}$  the  $2 \times 2$  identity matrix, which are determined by the lower order Fourier angular modes  $f_0$ ,  $f_1$  and  $f_2$ , respectively, as prescribed by the following relations:

$$\rho(\mathbf{x}, t) = f_0(\mathbf{x}, t), \quad (3.6)$$

$$\mathbf{p}(\mathbf{x}, t) = \begin{pmatrix} \text{Re } f_1(\mathbf{x}, t) \\ \text{Im } f_1(\mathbf{x}, t) \end{pmatrix}, \quad (3.7)$$

$$\mathbf{Q}(\mathbf{x}, t) = \frac{1}{2} \begin{pmatrix} \text{Re } f_2(\mathbf{x}, t) & \text{Im } f_2(\mathbf{x}, t) \\ \text{Im } f_2(\mathbf{x}, t) & -\text{Re } f_2(\mathbf{x}, t) \end{pmatrix}. \quad (3.8)$$

To determine the Fourier coefficients  $f_m$  we first take the spatial Fourier transform of Eq. (2.18)<sup>1</sup>. The latter transform is particularly advantageous to expand the non local integral operator. In details, we obtain

$$\frac{\partial}{\partial t} \hat{P} - \mathcal{F}\{\tilde{\mathcal{L}}_1 P\} + \int_0^\infty [1 - e^{i\zeta \mathbf{k} \cdot \mathbf{n}(\phi)}] \hat{P} \nu(d\zeta) = 0. \quad (3.9)$$

Secondly, we multiply both its sides by  $e^{im\phi}$  and integrate them in the angular variable  $\phi$ . This yields

$$\begin{aligned} \frac{\partial}{\partial t} \hat{f}_m - \int_{-\pi}^\pi e^{im\phi} \mathcal{F}\{\tilde{\mathcal{L}}_1 P\} d\phi \\ + \int_{-\pi}^\pi e^{im\phi} \int_0^\infty [1 - e^{i\zeta \mathbf{k} \cdot \mathbf{n}(\phi)}] \hat{P} \nu(d\zeta) d\phi = 0. \end{aligned} \quad (3.10)$$

To relate analytically the integrals appearing in this equation to the Fourier modes  $\hat{f}_m$ , we explicitly write out the angle specifying the direction of the Fourier variable, i.e., we substitute  $\mathbf{k} \equiv k \mathbf{n}(\phi)$  with  $k \equiv |\mathbf{k}|$  [134]. On the one hand, the first integral in its rhs is given by

$$\begin{aligned} \int_{-\pi}^\pi e^{im\phi} \mathcal{F}\{\tilde{\mathcal{L}}_1 P\} d\phi = \frac{v_1}{2} ik (e^{-i\psi} \hat{f}_{m+1} + e^{i\psi} \hat{f}_{m-1}) \\ - \sigma m^2 \hat{f}_m + \frac{m\gamma}{2} (\hat{f}_{m-1} \star \hat{f}_1 - \hat{f}_{m+1} \star \hat{f}_{-1}). \end{aligned} \quad (3.11)$$

On the other hand, using Eq. (3.1) we can expand the non local advective term as

$$\begin{aligned} \int_{-\pi}^\pi e^{im\phi} \int_0^\infty [1 - e^{i\zeta \mathbf{k} \cdot \mathbf{n}(\phi)}] \hat{P} \nu(d\zeta) d\phi = \\ \frac{1}{2\pi} \sum_{m' \in \mathbb{Z}} \hat{f}_{m'+m} \int_{-\pi}^\pi e^{-im'\phi} \int_0^\infty [1 - e^{i\zeta k \cos(\psi-\phi)}] \nu(d\zeta) d\phi, \end{aligned} \quad (3.12)$$

where we used the relation  $\mathbf{n}(\psi) \cdot \mathbf{n}(\phi) = \cos(\psi - \phi)$ . Finally, changing angular coordinate as  $\phi' = \psi - \phi$ , we obtain

$$\begin{aligned} \int_{-\pi}^\pi e^{im\phi} \int_0^\infty [1 - e^{i\zeta \mathbf{k} \cdot \mathbf{n}(\phi)}] \hat{P} \nu(d\zeta) d\phi = \\ \sum_{m' \in \mathbb{Z}} i^{m'} \hat{f}_{m'+m} e^{-im'\psi} C_{m'}(k, \alpha), \end{aligned} \quad (3.13)$$

where we define the  $(k, \alpha)$ -dependent coefficients

$$C_{m'} \equiv \frac{(-i)^{m'}}{2\pi} \int_{-\pi}^\pi e^{i\phi' m'} \int_0^\infty [1 - e^{i\zeta k \cos \phi'}] \nu(d\zeta) d\phi'. \quad (3.14)$$

In the hydrodynamic limit, the scaling behaviour of  $C_{m'}$  is determined by the corresponding scaling of the

Lévy measure  $\nu$  for large displacements. For a heavy-tailed measure  $\nu(dz) \sim z^{-1-\alpha} dz$ , such as for the Lévy stable subordinator (1.3), we can rescale  $z$  in Eq. (3.14) such that

$$C_{m'} \sim k^\alpha \Upsilon_{m'}(\alpha) \quad (3.15)$$

with  $\alpha$ -dependent numerical coefficients

$$\begin{aligned} \Upsilon_{m'} &\propto \frac{(-i)^{m'}}{2\pi} \int_{-\pi}^\pi e^{i\phi' m'} \int_0^\infty [1 - e^{iz' \cos \phi'}] \frac{dz'}{z'^{1+\alpha}} d\phi' \\ &\propto \frac{(-i)^{m'}}{2\pi} \int_{-\pi}^\pi e^{i\phi' m'} (-i \cos \phi')^\alpha d\phi', \end{aligned} \quad (3.16)$$

where any multiplicative constant in front of the integral is determined by the exact definition of the measure  $\nu$ . The scaling behaviour in the hydrodynamic limit (3.15) reveals that the collective properties of the system are only determined by the corresponding scaling properties of the tails of the microscopic step size distribution. In fact, while for  $0 < \alpha < 1$  this term is dominant, in the hydrodynamic limit, against the conventional advective term (i.e., the term  $\propto v_1$  in Eq. (3.11)), it becomes of the same order or sub-leading for  $\alpha \geq 1$ . In this latter case, therefore, no matter what specific step size distribution is chosen, the model is equivalent to an ordinary active fluid with constant self-propulsion velocity (again in the hydrodynamic limit). For Lévy stable distributed step sizes analytical formulas can be obtained straightforwardly (see Appendix D Eqs. (D.3, D.9)). In this specific case, numerical results suggest that these coefficients decay as  $m'^{-1-\alpha}$  for  $m' \rightarrow \infty$  (see Fig. 3), thus ensuring the convergence of the series expansion (3.13). These coefficients also satisfy the property

$$\Upsilon_{-m'} = (-1)^{m'} \Upsilon_{m'}, \quad (3.17)$$

or alternatively  $i^{-m'} \Upsilon_{-m'} = i^{m'} \Upsilon_{m'}$ .

In contrast, when  $\nu$  exhibits an upper cutoff  $H$  on its tails, such as for the tempered Lévy stable subordinator (1.4), different scenarios are predicted according to how the cutoff depends on the system size. Upon rescaling the integration variable, we obtain

$$C_{m'} \sim k^\alpha \int_{-\pi}^\pi e^{i\phi' m'} \int_0^\infty [1 - e^{iz' \cos \phi'}] e^{-\frac{z'}{Hk}} \frac{dz'}{z'^{1+\alpha}} d\phi'. \quad (3.18)$$

The scaling behaviour of this integral in the hydrodynamic limit thus depends on the exponential tempering factor, which in terms of the system size  $L$  can be written as  $e^{-z'/H} \sim e^{-z' L/H}$ . Three different scenarios are identified: (I) If  $H \gg L$ , in the hydrodynamic limit we have  $e^{-z' L/H} \sim 1$ . Thus, the model is effectively equivalent to the case of heavy-tailed  $\nu$ . (II) If  $H \ll L$ , in the hydrodynamic limit we obtain  $e^{-z' L/H} \sim 0$ , meaning that the terms originating from the non local advection do not contribute to the hydrodynamic EOM. In this case, the model is equivalent to ordinary active matter with self-propulsion

<sup>1</sup> The Fourier transform of a function  $f_1(\mathbf{x})$  is written as  $\hat{f}_1(\mathbf{k}) \equiv \mathcal{F}\{f_1(\mathbf{x})\}(\mathbf{k})$ . Correspondingly,  $\mathcal{F}^{-1}$  is the inverse transform. The symbol  $\star$  denotes the convolution of two such functions, i.e.,  $f_1(\mathbf{x}) \star f_2(\mathbf{x}) \equiv \int_{-\infty}^\infty f_1(\mathbf{x} - \mathbf{x}') f_2(\mathbf{x}') d\mathbf{x}'$ .

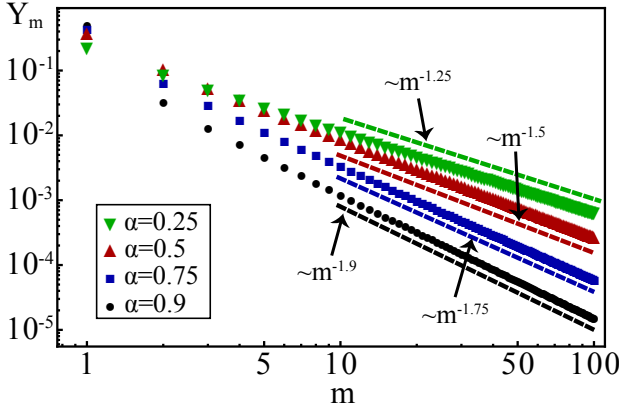


FIG. 3. Plot of the coefficients  $\Upsilon_m$  ( $m > 0$ ) for Lévy stable distributed step sizes (see Eq. (D.9)) for different values of the characteristic parameter  $\alpha$ . Numerical results suggest that  $\Upsilon_m$  scales as  $m^{-1-\alpha}$  for  $m \gg 1$  (dashed lines).

particle velocity  $v_1$  [7–9]. (III) If  $H \sim L$ , in the hydrodynamic limit we find  $e^{-z'L/H} \sim e^{-z'}$ . In this case, the model is expected to exhibit distinctive behaviour in the hydrodynamic limit than the other two regimes, but this special case will be discussed in future publications.

We now derive the hydrodynamic equations for a heavy-tailed measure  $\nu$ , and specifically we choose the Lévy stable subordinator (1.3). Using the relations (3.11) and (3.13), the scaling formulas for the coefficients  $C_m$  (3.15) and (3.16), and their property (3.17), we obtain the equations for the Fourier transform of the angular modes of  $P$

$$\begin{aligned} \frac{\partial}{\partial t} \hat{f}_m = & -(\Upsilon_0 k^\alpha + \sigma m^2) \hat{f}_m + \frac{\gamma m}{2} (\hat{f}_{m-1} \star \hat{f}_1 - \hat{f}_{m+1} \star \hat{f}_{-1}) \\ & - k^\alpha \sum_{m'=1}^{\infty} i^{m'} \Upsilon_{m'} (e^{-im'\psi} \hat{f}_{m+m'} + e^{im'\psi} \hat{f}_{m-m'}). \end{aligned} \quad (3.19)$$

These coupled non-linear equations clearly cannot be solved analytically for the entire hierarchy of angular modes; a suitable approximation scheme is thus required. In analogy with ordinary active matter [45, 46, 48–50, 52], Eqs. (3.19) prescribe that higher order angular modes are suppressed by the “mass” term  $\propto m^2$ , thus highlighting that only lower order modes are relevant to describe the macroscopic dynamical behaviour of the system. The fractional advection similarly enhances this damping by a term  $\propto \Upsilon_0 k^\alpha$ , which is however equal for all modes. In addition, it strengthens the coupling between the equations, which now extends to the entire hierarchy of angular modes, while for ordinary active matter it is limited only to the modes  $\hat{f}_1$ ,  $\hat{f}_{m-1}$  and  $\hat{f}_{m+1}$ . We remark that this coupling between the equations leaves the damping effect unaltered. All these observations suggest that we can adopt here the same approximation strategy usually employed in ordinary active matter [45, 46, 48–50, 52].

Therefore, we assume  $\hat{f}_m \approx 0$  for  $m > 2$ . Further recalling that  $\hat{f}_{-m} = \hat{f}_m^*$  (the superscript  $*$  denotes complex conjugation), we obtain the set of coupled equations

$$\begin{aligned} \frac{\partial}{\partial t} \hat{f}_0 = & -\Upsilon_0 k^\alpha \hat{f}_0 - i\Upsilon_1 k^\alpha (e^{-i\psi} \hat{f}_1 + e^{i\psi} \hat{f}_1^*) \\ & + \Upsilon_2 k^\alpha (e^{-i2\psi} \hat{f}_2 + e^{i2\psi} \hat{f}_2^*), \end{aligned} \quad (3.20)$$

$$\begin{aligned} \frac{\partial}{\partial t} \hat{f}_1 = & -(\Upsilon_0 k^\alpha + \sigma) \hat{f}_1 + \frac{\gamma}{2} (\hat{f}_0 \star \hat{f}_1 - \hat{f}_2 \star \hat{f}_1^*) \\ & - i\Upsilon_1 k^\alpha (e^{-i\psi} \hat{f}_2 + e^{i\psi} \hat{f}_0) + \Upsilon_2 k^\alpha e^{i2\psi} \hat{f}_1^* \\ & + i\Upsilon_3 k^\alpha e^{i3\psi} \hat{f}_2^*, \end{aligned} \quad (3.21)$$

$$\begin{aligned} \frac{\partial}{\partial t} \hat{f}_2 = & -(\Upsilon_0 k^\alpha + 4\sigma) \hat{f}_2 + \gamma (\hat{f}_1 \star \hat{f}_1) - i\Upsilon_1 k^\alpha e^{i\psi} \hat{f}_1 \\ & + \Upsilon_2 k^\alpha e^{i2\psi} \hat{f}_0 + i\Upsilon_3 k^\alpha e^{i3\psi} \hat{f}_1^* - \Upsilon_4 k^\alpha e^{i4\psi} \hat{f}_2^*. \end{aligned} \quad (3.22)$$

By further imposing  $\partial_t \hat{f}_2 \approx 0$ , Eq. (3.22) can be solved analytically for  $\hat{f}_2$  (see Appendix E). In detail,

$$\begin{aligned} \hat{f}_2 = & \gamma \hat{D}_0 (\hat{f}_1 \star \hat{f}_1) - \hat{D}_1 k^\alpha i e^{i\psi} \hat{f}_1 + \hat{D}_2 k^\alpha e^{i2\psi} \hat{f}_0 \\ & + \hat{D}_3 k^\alpha i e^{i3\psi} \hat{f}_1^* - \gamma \hat{D}_4 e^{i4\psi} (\hat{f}_1 \star \hat{f}_1)^*, \end{aligned} \quad (3.23)$$

with  $(k, \alpha)$ -dependent coefficients  $\hat{D}_j$  ( $j = 0, \dots, 4$ ) (see Appendix E, Eqs. (E.8), (E.9) and (E.13–E.15)). Their dependence on the Fourier variable  $k$  is studied in Fig. 4 (see Appendix E for asymptotic formulas). Finally, by substituting Eq. (3.23) into Eqs. (3.20) and (3.21) we derive closed analytical equations for the lower order modes  $\hat{f}_0$  and  $\hat{f}_1$  valid at all wavelengths (i.e.,  $\forall k \in \mathbb{R}$ ).

These equations potentially contain an infinite number of higher order terms in the wavelength number  $k$ , which are encapsulated in the coefficients  $\hat{D}_j$ . Our interest, however, is in the hydrodynamic limit of these equations, where only few of these terms are in fact relevant. To reveal these terms, we will thus expand all coefficients  $\hat{D}_j$  as power series of  $k^\alpha$  and keep only the first order terms, i.e., those that are  $\mathcal{O}(k^{2\alpha})$ . Within this expansion scheme, we can then write  $\hat{f}_2 \sim \hat{f}_2^{(0)} + k^\alpha \hat{f}_2^{(1)}$  with (see Appendix E, Eqs. (E.16–E.20))

$$\hat{f}_2^{(0)} = \frac{\gamma}{4\sigma} (\hat{f}_1 \star \hat{f}_1) \quad (3.24)$$

$$\begin{aligned} \hat{f}_2^{(1)} = & -\frac{\gamma \Upsilon_0}{(4\sigma)^2} (\hat{f}_1 \star \hat{f}_1) - \frac{\Upsilon_1}{4\sigma} i e^{i\psi} \hat{f}_1 + \frac{\Upsilon_2}{4\sigma} e^{i2\psi} \hat{f}_0 \\ & + \frac{\Upsilon_3}{4\sigma} i e^{i3\psi} \hat{f}_1^* - \frac{\gamma \Upsilon_4}{(4\sigma)^2} e^{i4\psi} (\hat{f}_1 \star \hat{f}_1)^*. \end{aligned} \quad (3.25)$$

This corresponds to an expansion of the nematic tensor as  $\mathbf{Q} \sim \mathbf{Q}^{(0)} + \mathbf{Q}^{(1)}$  with, respectively,

$$\hat{\mathbf{Q}}^{(0)} = \frac{1}{2} \begin{pmatrix} \text{Re } \hat{f}_2^{(0)} & \text{Im } \hat{f}_2^{(0)} \\ \text{Im } \hat{f}_2^{(0)} & -\text{Re } \hat{f}_2^{(0)} \end{pmatrix}, \quad (3.26)$$

$$\hat{\mathbf{Q}}^{(1)} = \frac{1}{2} \begin{pmatrix} \text{Re } \hat{f}_2^{(1)} & \text{Im } \hat{f}_2^{(1)} \\ \text{Im } \hat{f}_2^{(1)} & -\text{Re } \hat{f}_2^{(1)} \end{pmatrix}. \quad (3.27)$$

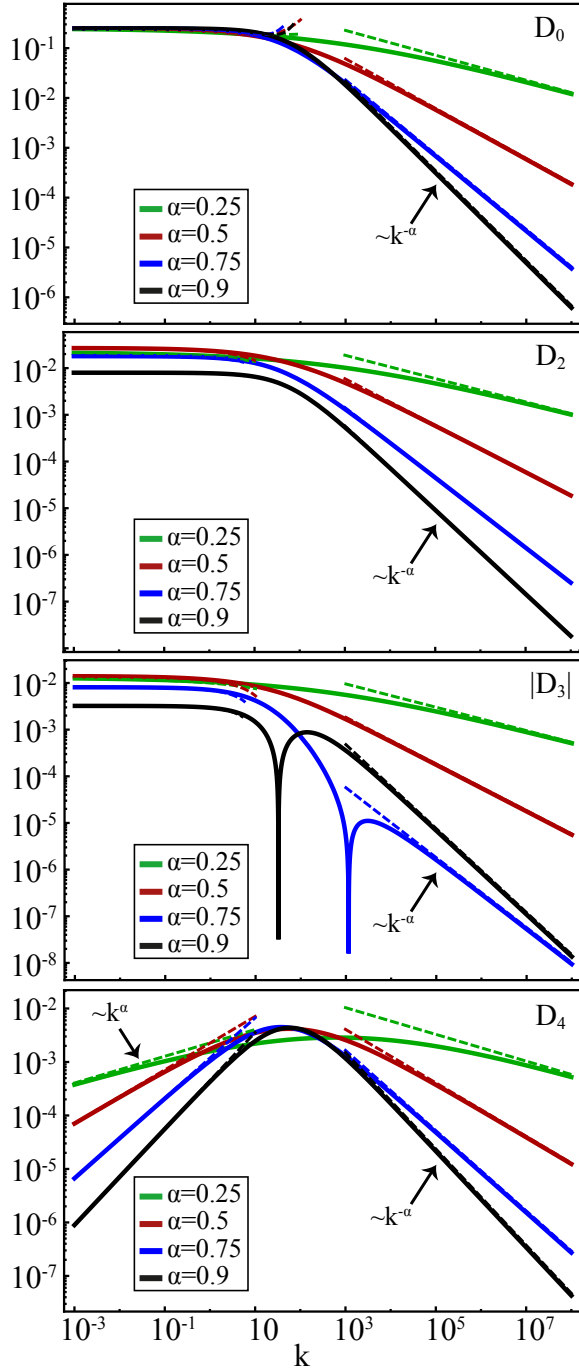


FIG. 4. Coefficients  $\hat{D}_j$  ( $j = 0, \dots, 4$ ) vs. the Fourier variable  $k$  for different values of  $\alpha$ .  $\hat{D}_1$  is not shown as it is qualitatively similar to  $\hat{D}_0$ . Their asymptotic behaviour in the limit of long and short wavelengths is highlighted (see Appendix E, Eqs. (E.16–E.20) and (E.21–E.25) respectively).

The hydrodynamic equations for  $\hat{f}_0$  and  $\hat{f}_1$  are thus

$$\begin{aligned} \frac{\partial}{\partial t} \hat{f}_0 &= -\Upsilon_0 k^\alpha \hat{f}_0 - \Upsilon_1 k^\alpha i(e^{-i\psi} \hat{f}_1 + e^{i\psi} \hat{f}_1^*) \\ &\quad + \frac{\gamma \Upsilon_2}{4\sigma} k^\alpha [e^{-i2\psi} (\hat{f}_1 \star \hat{f}_1) + e^{i2\psi} (\hat{f}_1 \star \hat{f}_1)^*], \end{aligned} \quad (3.28)$$

$$\begin{aligned} \frac{\partial}{\partial t} \hat{f}_1 &= -(\sigma + \Upsilon_0 k^\alpha) \hat{f}_1 + \frac{\gamma}{2} (\hat{f}_0 \star \hat{f}_1) - \frac{\gamma^2}{8\sigma} (\hat{f}_1 \star \hat{f}_1^*) \star \hat{f}_1 \\ &\quad - \Upsilon_1 k^\alpha i e^{i\psi} \hat{f}_0 + \Upsilon_2 k^\alpha e^{i2\psi} \hat{f}_1^* - \frac{\gamma \Upsilon_1}{4\sigma} k^\alpha i e^{-i\psi} (\hat{f}_1 \star \hat{f}_1) \\ &\quad + \frac{\gamma \Upsilon_3}{4\sigma} k^\alpha i e^{i3\psi} (\hat{f}_1 \star \hat{f}_1)^* - \frac{\gamma}{2} \hat{f}_1^* \star (k^\alpha \hat{f}_2^{(1)}). \end{aligned} \quad (3.29)$$

Finally, we perform the inverse Fourier transform of Eqs. (3.28, 3.29). To this aim, we define the fractional Riesz integral operator  $\mathbb{I}^\beta$  in terms of its Fourier transform  $\mathcal{F}\{(\mathbb{I}^\beta h)(\mathbf{x})\} \equiv k^{-\beta} \hat{h}(\mathbf{k})$  (for  $\text{Re } \beta > 0$ ). Its expression as a non local spatial integral in two dimensions is [135]

$$(\mathbb{I}^\beta h)(\mathbf{x}) \equiv \frac{1}{\mu'_2(\beta)} \int_{\mathbb{R}^2} h(\mathbf{x} - \boldsymbol{\zeta}) \frac{d\boldsymbol{\zeta}}{|\boldsymbol{\zeta}|^{2-\beta}} \quad (3.30)$$

with  $\mu'_2(\beta) \equiv 2^\beta \pi \Gamma(\beta/2) / \Gamma(2 - \beta/2)$  for  $\beta \neq 2(1 + l)$  ( $l > 0, l \in \mathbb{Z}$ ). Correspondingly, we introduce the fractional Riesz derivative  $\mathbb{D}^\beta$ , as the operator with Fourier representation  $\mathcal{F}\{(\mathbb{D}^\beta h)(\mathbf{x})\} \equiv k^\beta \hat{h}(\mathbf{k})$ . Its integral representation is (see [132], Sec. 25.4)

$$(\mathbb{D}^\beta h)(\mathbf{x}) = \frac{1}{c_l} \int_{\mathbb{R}^2} (\Delta_\zeta^l h)(\mathbf{x}) \frac{d\boldsymbol{\zeta}}{|\boldsymbol{\zeta}|^{2+\beta}} \quad (3.31)$$

with  $l > \beta$ ,  $\beta$ -dependent normalizing coefficients  $c_l$  and finite differences of the scalar function  $h$  either centered,

$$\Delta_\zeta^l h(\mathbf{x}) \equiv \sum_{m=0}^l (-1)^m \binom{l}{m} \mathcal{T}_{(\frac{l}{2}-m)}^- h(\mathbf{x}), \quad (3.32)$$

in which case  $c_l \equiv 2^{l-\beta} l! \int_{\mathbb{R}^2} (\sin \zeta_x)^l |\boldsymbol{\zeta}|^{-2-\beta} d\boldsymbol{\zeta}$ ; or non centered,

$$\Delta_\zeta^l h(\mathbf{x}) \equiv \sum_{m=0}^l (-1)^m \binom{l}{m} \mathcal{T}_{m\zeta}^- h(\mathbf{x}), \quad (3.33)$$

in which case  $c_l \equiv \int_{\mathbb{R}^2} (1 - e^{i\zeta_x})^l |\boldsymbol{\zeta}|^{-2-\beta} d\boldsymbol{\zeta}$ . These operators are the inverses of each other. Furthermore, we use the relations presented in Table I (see Section F for detailed proofs), with the vorticity field  $\boldsymbol{\omega}(\mathbf{r}, t) \equiv \nabla \times \mathbf{p}$  and the auxiliary non-linear  $(\mathbf{r}, t)$ -dependent vector fields  $\Xi_0$  and  $\Xi_1$  (below we introduce the notation  $p \equiv |\mathbf{p}|$ )

$$\Xi_0 \equiv 2[(\mathbf{p} \cdot \nabla) \mathbf{p} + (\nabla \cdot \mathbf{p}) \mathbf{p}] - \nabla p^2, \quad (3.34)$$

$$\begin{aligned} \Xi_1 &\equiv (\mathbf{p} \cdot \nabla) \nabla^2 \mathbf{p} + (\mathbf{p} \times \nabla) \times \nabla^2 \mathbf{p} \\ &\quad + 3[(\nabla \cdot \mathbf{p}) \nabla^2 \mathbf{p} + (\boldsymbol{\omega} \times \nabla^2 \mathbf{p}) - (\boldsymbol{\omega} \cdot \nabla) \boldsymbol{\omega}]. \end{aligned} \quad (3.35)$$

The hydrodynamic equations for the density and mean direction fields are thus

$$\left(\frac{\partial}{\partial t} + \Upsilon_0 \mathbb{D}^\alpha\right) \rho = 2\Upsilon_1 \mathbb{I}^{1-\alpha} (\nabla \cdot \mathbf{p}) - \lambda_2 \mathbb{I}^{2-\alpha} (\nabla \cdot \Xi_0); \quad (3.36)$$

$$\left(\frac{\partial}{\partial t} + \Upsilon_0 \mathbb{D}^\alpha\right) \mathbf{p} = [\kappa_0(\rho) - \xi p^2] \mathbf{p} + \Upsilon_1 \mathbb{I}^{1-\alpha} \nabla \rho + \lambda_1 \mathbb{I}^{1-\alpha} \Xi_0 - \Upsilon_2 \mathbb{I}^{2-\alpha} \nabla^2 \mathbf{p} + \lambda_3 \mathbb{I}^{3-\alpha} \Xi_1 - \mathbf{Q}^{(1)} \mathbf{p} \quad (3.37)$$

with the components of the tensor  $\mathbf{Q}^{(1)}$  specified by  $\mathbf{Q}_{xx}^{(1)} = \mathbf{Q}_1^{(1)} = -\mathbf{Q}_{yy}^{(1)}$  and  $\mathbf{Q}_{xy}^{(1)} = \mathbf{Q}_2^{(1)} = \mathbf{Q}_{yx}^{(1)}$  with (note that we absorbed a multiplicative factor  $\gamma$  in its definition)

$$\begin{aligned} \mathbf{Q}_j^{(1)} = & -B_0 \mathbb{D}^\alpha \mathbf{M}_{jl} p_l + \frac{\lambda_1}{2} \mathbb{I}^{1-\alpha} \mathbf{T}_{jl} p_l - \frac{\lambda_2}{4} \mathbb{I}^{2-\alpha} \mathbf{T}_{jl} \partial_l \rho \\ & + \frac{\lambda_3}{4} \mathbb{I}^{3-\alpha} \mathbf{T}_{jl} \nabla^2 p_l - B_4 \mathbb{I}^{4-\alpha} \mathbf{T}_{jl} \Xi_{1l}, \end{aligned} \quad (3.38)$$

where  $j, l = 1, 2$  and we identify  $p_1$  and  $p_2$  with the components of  $\mathbf{p}$  along the  $x$  and  $y$  axis, respectively. In the above, we introduce the  $(p_x, p_y)$ -dependent tensor function  $\mathbf{M}_{jl} \equiv (p_x \delta_{jl} + p_y \epsilon_{jl})$ , the differential matrix operator  $\mathbf{T}_{jl} \equiv \partial_x \delta_{jl} + \partial_y \epsilon_{jl}$ , the Kronecher symbol  $\delta_{jl}$  and the generator of counter-clock wise rotations  $\epsilon_{jl}$ , defined by  $\epsilon_{11} = 0 = \epsilon_{22}$  and  $\epsilon_{21} = 1 = -\epsilon_{12}$  (see Appendix F, Eq. (F.3)). In addition, we defined the function of the density field

$$\kappa_0(\rho) \equiv -\sigma + \frac{\gamma \rho}{2}, \quad (3.39)$$

the  $\alpha$ -dependent coefficients

$$\lambda_1 \equiv \frac{\gamma \Upsilon_1}{4\sigma}, \quad \lambda_2 \equiv \frac{\gamma \Upsilon_2}{2\sigma}, \quad \lambda_3 \equiv \frac{\gamma \Upsilon_3}{2\sigma}, \quad (3.40)$$

and  $\alpha$ -independent ones

$$B_0 \equiv \frac{\gamma^2 \Upsilon_0}{32\sigma^2}, \quad B_4 \equiv \frac{\gamma^2 \Upsilon_4}{16\sigma^2}, \quad \xi \equiv \frac{\gamma^2}{8\sigma}. \quad (3.41)$$

As a check on the validity of our hydrodynamic EOM, we write out explicitly these equations for  $\alpha = 1$ . In this case, one can show that (see Appendix D, Eq. (D.7))

$$\Upsilon_{m'} = (-i)^{m'+1} \frac{m' \sin(m' \pi)}{\pi(1 - m'^2)} = \begin{cases} 0 & m' \neq 1 \\ -1/2 & m' = 1 \end{cases}. \quad (3.42)$$

Therefore, introducing further auxiliary parameters

$$\zeta_0 \equiv \frac{3\gamma}{16\sigma}, \quad \lambda_0 \equiv \frac{5\gamma}{16\sigma}, \quad (3.43)$$

we obtain  $\mathbf{Q}_1^{(1)} = \lambda_0(\partial_y p_y - \partial_x p_x)/5$  and  $\mathbf{Q}_2^{(1)} = -\lambda_0(\partial_y p_x + \partial_x p_y)/5$ . Using these formulas, we can show that  $\mathbf{Q}^{(1)} \mathbf{p} = \lambda_0[(\nabla \cdot \mathbf{p}) \mathbf{p} - (\mathbf{p} \cdot \nabla) \mathbf{p} - \nabla p^2/2]/5$ . Therefore, Eqs. (3.36) and (3.37) reduce to a version of the hydrodynamic equations of ordinary active fluids derived by

Toner and Tu [8]

$$\frac{\partial}{\partial t} \rho = -\nabla \cdot \mathbf{p}, \quad (3.44)$$

$$\begin{aligned} \frac{\partial}{\partial t} \mathbf{p} = & [\kappa_0(\rho) - \xi p^2] \mathbf{p} - \frac{1}{2} \nabla (\rho - \lambda_0 p^2) \\ & - \lambda_0 (\nabla \cdot \mathbf{p}) \mathbf{p} - \zeta_0 (\mathbf{p} \cdot \nabla) \mathbf{p}. \end{aligned} \quad (3.45)$$

These are equations for an active inviscid fluid. In fact, the passive viscous term in ordinary active matter is of higher order (specifically, it is of order  $k^2$ ). Therefore, it cannot be captured within our approximation scheme.

Our hydrodynamic EOM are manifestly more complex than the Toner-Tu equations. Nevertheless, Eq. (3.36) can be interpreted as the counterpart of the conventional continuity equation expressing mass conservation. In fact, the rate of mass change over an infinitesimal time interval is given by

$$\frac{\partial}{\partial t} \int_{\mathbb{R}^2} \rho(\mathbf{r}, t) d\mathbf{r} = \frac{\partial}{\partial t} \hat{\rho}(\mathbf{k}, t) \Big|_{\mathbf{k}=0} = 0, \quad (3.46)$$

because  $\partial_t \hat{\rho}(\mathbf{k}, t) \propto k^\alpha$  (see Eq. (3.28)). Therefore, our hydrodynamic model conserves mass as required. Eq. (3.37) instead describes the time evolution of the director field  $\mathbf{p}$  by accounting for contributions due to the rotational diffusion of active particles, their anomalous displacement statistics and polar alignment interactions.

In more details, we can understand Eqs. (3.36) and (3.37) term by term. Starting from the former one, the term  $\mathbb{D}^\alpha \rho$  in its lhs describes the isotropic superdiffusion of the density field, which is a direct consequence of the Lévy stable distributed particle displacements. Its effect can be understood by calculating the solution of the equation with  $\mathbf{p} = 0$  for the initial condition  $\rho(\mathbf{r}, t = 0) = \delta(\mathbf{r} - \mathbf{r}_0)$ , which is

$$\rho(\mathbf{r}, t) = \frac{1}{(\Upsilon_0 t)^{2/\alpha}} H_2 \left( \frac{|\mathbf{r} - \mathbf{r}_0|}{(\Upsilon_0 t)^{1/\alpha}} \right) \quad (3.47)$$

with  $H_2(x) \equiv (2\pi)^{-1} \int_0^\infty k J_0(kx) e^{-k^\alpha} dk$  and  $J_0$  a Bessel function of the first kind [136]. This is a Lévy distribution with variance increasing over time; therefore, it displays the anomalous diffusive spreading of the underlying microscopic particles. Conversely, for ordinary active matter, the advective term is null in the absence of global polarization order and, consequently, the density remains localized at the origin forever. In addition, by recalling (3.31), we note that the kernel function specifying the non local character of this term can be defined as

$\mu_0(d\zeta) \propto |\zeta|^{-2-\alpha} d\zeta$ , which is the distribution of rotationally invariant stable variables in two dimensions with stability parameter  $\alpha$ . Interestingly, this is an isotropic probability distribution with the same tail scaling properties of the microscopic step size distribution.

The first term in the rhs of Eq. (3.36) is a fractional divergence, thus quantifying the flux of active particles. Indeed, taking its integral over some prescribed volume  $V \subset \mathbb{R}^2$ , we can write

$$\begin{aligned} \int_V \mathbb{I}^{1-\alpha}(\nabla \cdot \mathbf{p}) d\mathbf{r} &= \int_S \mathbb{I}^{1-\alpha} \mathbf{p} \cdot d\mathbf{S} \\ &= \int_{\mathbb{R}^2} \left( \int_S \mathbf{p}(\mathbf{r} + \zeta, t) \cdot d\mathbf{S} \right) |\zeta|^{-1-\alpha} \frac{d\zeta}{\mu'_1} \end{aligned} \quad (3.48)$$

with  $S$  the volume boundary and the positive coefficient  $\mu'_1(\alpha) \equiv \Gamma((1-\alpha)/2)/[2^\alpha \Gamma((3+\alpha)/2)]$  [135]. This expression can be interpreted straightforwardly: the inner integral measures the flux of active particles jumping into  $V$  from an arbitrary position  $\mathbf{r} + \zeta$ ; the outer integral is the average over all such jumps whose statistics is specified by the probability measure  $\mu_1(d\zeta) \equiv (2\Upsilon_1/\mu'_1)|\zeta|^{-1-\alpha} d\zeta$ , which we can show to be the distribution of one-dimensional  $\alpha$ -stable random variables. Thus, the non local character of this term is fully specified by the microscopic step size statistics. The second term can be interpreted, analogously, as a non-linear contribution to the active flux. In fact, we can write

$$\begin{aligned} \int_V \mathbb{I}^{2-\alpha}(\nabla \cdot \Xi_0) d\mathbf{r} &= \int_S \mathbb{I}^{2-\alpha} \Xi_0 \cdot d\mathbf{S} = \\ &= \int_{\mathbb{R}^2} \left( \int_S \Xi_0(\mathbf{r} + \zeta, t) \cdot d\mathbf{S} \right) |\zeta|^{-\alpha} \frac{d\zeta}{\mu'_2} \end{aligned} \quad (3.49)$$

with  $\mu'_2(\alpha) \equiv 2^{1-\alpha} \Gamma(1-\alpha/2)/\Gamma(1+\alpha/2)$  [135]. We can recognize the flux of the vector field  $\Xi_0$ , which depends non-linearly on  $\mathbf{p}$  [see Eq. (3.34)], averaged over all jumps with probability measure  $\mu_2(d\zeta) \equiv (\gamma \Upsilon_2/2\sigma \mu'_2) \zeta^{-\alpha} d\zeta$ . Differently from the other terms,  $\mu_2$  cannot be related as clearly to the microscopic step size distribution.

Likewise, we can also understand the term-by-term structure of Eq. (3.37). The first term in its rhs typically characterizes alignment interacting systems, but is here augmented by the anomalous diffusive term  $\Upsilon_0 \mathbb{D}^\alpha \mathbf{p}$ , similar to (3.36). The hydrodynamic pressure gradient  $\mathbb{I}^{1-\alpha} \nabla [\rho - (\gamma/4\sigma) p^2]$ , the convective term  $\mathbb{I}^{1-\alpha} (\mathbf{p} \cdot \nabla) \mathbf{p}$ , and the divergence-induced flow  $\mathbb{I}^{1-\alpha} (\nabla \cdot \mathbf{p}) \mathbf{p}$ , which are encapsulated in the term  $\mathbb{I}^{1-\alpha} \Xi_0$ , all have their counterparts in the Toner-Tu EOM, albeit modified with fractional derivative operators and possibly different multiplicative coefficients. Interestingly, their corresponding non local integral expressions all possess kernel functions that directly relate to the microscopic step size distribution, akin to the flux term in (3.36).

Conversely, the viscous-like term  $\mathbb{I}^{2-\alpha} \nabla^2 \mathbf{p}$ , the non linear term  $\mathbb{I}^{3-\alpha} \Xi_1$  and all those included through the nematic term  $\mathbf{Q}^{(1)} \mathbf{p}$ , have no counterparts in ordinary

active fluids. While for some of these terms the corresponding non-local integral expression is integrated over the same probability measures discussed previously, for other ones (such as those involving the operators  $\mathbb{I}^{3-\alpha}$  and  $\mathbb{I}^{4-\alpha}$ ) we need to introduce other non-trivial measures (not discussed further here). All these latter terms correspond to higher-order terms in the Fourier angular expansion.

Overall, this analysis highlights that, on the one hand, many terms in the hydrodynamic EOM of ALM can be inferred directly by simply knowing the Toner-Tu equations for ordinary active matter and the scaling properties of the microscopic step size distribution. Therefore, all these terms can potentially be derived by using symmetry considerations only. On the other hand, however, it shows that these equations also contain several higher order terms that exhibit not only non-linear fields contributions but also highly non trivial jump statistics (in the corresponding integral expression). These terms can thus be correctly identified only by applying a formal coarse-graining procedure.

#### IV. MEAN FIELD SOLUTIONS AND LINEAR STABILITY ANALYSIS

The mean-field solutions of Eqs. (3.36, 3.37), which we call  $\rho^*$  and  $\mathbf{p}^*$ , are obtained by solving the EOM for spatially homogeneous hydrodynamic fields. Clearly, not only ordinary but also fractional derivatives are null when applied on spatially homogeneous functions. Therefore, ALM is completely equivalent to ordinary active matter at the mean field level. In particular, their hydrodynamic EOM have the same mean field solutions: On the one hand, there exists a disordered gas phase with constant density and  $\mathbf{p}^* = 0$  for noise strengths  $\sigma \geq \sigma_t$  with the density dependent threshold  $\sigma_t(\rho^*) \equiv \gamma \rho^*/2$ ; on the other hand, for  $\sigma < \sigma_t$  a ordered liquid phase spontaneously emerges where collective motion is observed along an arbitrary direction  $\mathbf{e}_1$  with  $\mathbf{p}^* = \sqrt{\kappa_0(\rho^*)/\xi} \mathbf{e}_1$ .

We then consider a generic perturbation of these solutions  $\rho(\mathbf{r}, t) = \rho^* + \delta\rho(\mathbf{r}, t)$  and  $\mathbf{p}(\mathbf{r}, t) = \mathbf{p}^* + \delta\mathbf{p}(\mathbf{r}, t)$ , with  $\delta\rho, \delta\mathbf{p}$  expressed as plane waves

$$\delta\rho(\mathbf{r}, t) = \delta\rho_0 e^{st+i\mathbf{q}\cdot\mathbf{r}}, \quad \delta\mathbf{p}(\mathbf{r}, t) = \delta\mathbf{p}_0 e^{st+i\mathbf{q}\cdot\mathbf{r}}. \quad (4.1)$$

Using the linearity of the fractional operators, and the spatial homogeneity of the fields  $\rho^*$  and  $\mathbf{p}^*$ , we obtain the following equations for the perturbations:

$$\begin{aligned} \frac{\partial}{\partial t} \delta\rho &= -\Upsilon_0 \mathbb{D}^\alpha \delta\rho + 2\Upsilon_1 \mathbb{I}^{1-\alpha} (\nabla \cdot \delta\mathbf{p}) \\ &\quad - 2\lambda_2 \mathbb{I}^{2-\alpha} (\nabla \cdot \delta\Xi_0), \end{aligned} \quad (4.2)$$

$$\begin{aligned} \frac{\partial}{\partial t} \delta\mathbf{p} &= \left[ \frac{\gamma}{2} \delta\rho - 2\xi(\mathbf{p}^* \cdot \delta\mathbf{p}) \right] \mathbf{p}^* - \Upsilon_0 \mathbb{D}^\alpha \delta\mathbf{p} \\ &\quad + \Upsilon_1 \mathbb{I}^{1-\alpha} \nabla \delta\rho - \Upsilon_2 \mathbb{I}^{2-\alpha} \nabla^2 \delta\mathbf{p} \\ &\quad + 2\lambda_1 \mathbb{I}^{1-\alpha} \delta\Xi_0 + \lambda_3 \mathbb{I}^{3-\alpha} \delta\Xi_1 - \delta\mathbf{Q}^{(1)} \mathbf{p}^*, \end{aligned} \quad (4.3)$$

Original term	Manipulated term	Inv. Fourier transf.	$\mathbb{C} \rightarrow \mathbb{R}^2$	Eq.
$ik^\alpha(e^{-i\psi}\hat{f}_1 + e^{i\psi}\hat{f}_1^*)$	$-k^{\alpha-1}(\hat{\nabla}_{\mathbf{k}}^*\hat{f}_1 + \hat{\nabla}_{\mathbf{k}}\hat{f}_1^*)$	$-2\mathbb{I}^{1-\alpha}\text{Re}(\hat{\nabla}^*f_1)$	$-2\mathbb{I}^{1-\alpha}(\nabla \cdot \mathbf{p})$	(3.50)
$k^\alpha[e^{-i2\psi}(\hat{f}_1 \star \hat{f}_1) + c.c.]$	$-2k^{\alpha-2}\text{Re}[\hat{\nabla}_{\mathbf{k}}^{*2}(\hat{f}_1 \star \hat{f}_1)]$	$-2\mathbb{I}^{2-\alpha}\text{Re}(\hat{\nabla}^{*2}f_1^2)$	$-2\mathbb{I}^{2-\alpha}(\nabla \cdot \Xi_0)$	(3.51)
$ik^\alpha e^{i\psi}\hat{f}_0$	$-k^{\alpha-1}\hat{\nabla}_{\mathbf{k}}\hat{f}_0$	$-\mathbb{I}^{1-\alpha}\nabla f_0$	$-\mathbb{I}^{1-\alpha}\nabla\rho$	(3.52)
$ik^\alpha e^{-i\psi}(\hat{f}_1 \star \hat{f}_1)$	$-k^{\alpha-1}\hat{\nabla}_{\mathbf{k}}^*(\hat{f}_1 \star \hat{f}_1)$	$-\mathbb{I}^{1-\alpha}\hat{\nabla}^*f_1^2$	$-\mathbb{I}^{1-\alpha}\Xi_0$	(3.53)
$k^\alpha e^{i2\psi}\hat{f}_1^*$	$-k^{\alpha-2}\hat{\nabla}_{\mathbf{k}}^2\hat{f}_1^*$	$-\mathbb{I}^{2-\alpha}\hat{\nabla}^2f_1^*$	$-\mathbb{I}^{2-\alpha}\nabla^2\mathbf{p}$	(3.54)
$ik^\alpha e^{i\psi}\hat{f}_1$	$-k^{\alpha-1}(\hat{\nabla}_{\mathbf{k}}\hat{f}_1)$	$-\mathbb{I}^{1-\alpha}(\hat{\nabla}f_1)$	$-\mathbb{I}^{1-\alpha}\mathbf{T}\mathbf{p}$	(3.55)
$k^\alpha e^{i2\psi}\hat{f}_0$	$-k^{\alpha-2}(\hat{\nabla}_{\mathbf{k}}^2\hat{f}_0)$	$-\mathbb{I}^{2-\alpha}(\hat{\nabla}^2f_0)$	$-\mathbb{I}^{2-\alpha}\mathbf{T}\nabla\rho$	(3.56)
$ik^\alpha e^{i3\psi}\hat{f}_1^*$	$k^{\alpha-3}(\hat{\nabla}_{\mathbf{k}}^3\hat{f}_1^*)$	$\mathbb{I}^{3-\alpha}(\hat{\nabla}^3f_1^*)$	$\mathbb{I}^{3-\alpha}\mathbf{T}\nabla^2\mathbf{p}$	(3.57)
$ik^\alpha e^{i3\psi}(\hat{f}_1 \star \hat{f}_1)^*$	$k^{\alpha-3}\hat{\nabla}_{\mathbf{k}}^3(\hat{f}_1 \star \hat{f}_1)^*$	$\mathbb{I}^{3-\alpha}\hat{\nabla}^3f_1^{*2}$	$2\mathbb{I}^{3-\alpha}\Xi_1$	(3.58)
$k^\alpha e^{i4\psi}(\hat{f}_1 \star \hat{f}_1)^*$	$k^{\alpha-4}[\hat{\nabla}_{\mathbf{k}}^4(\hat{f}_1 \star \hat{f}_1)^*]$	$\mathbb{I}^{4-\alpha}(\hat{\nabla}^4f_1^{*2})$	$2\mathbb{I}^{4-\alpha}\mathbf{T}\Xi_1$	(3.59)

TABLE I. Summary of the identities used to calculate the inverse Fourier transform and the vector representation of Eqs. (3.28, 3.29). We define complex derivatives  $\hat{\nabla} \equiv \partial_x + i\partial_y$  and  $\hat{\nabla}^* \equiv \partial_x - i\partial_y$ , such that their Fourier transforms are  $\hat{\nabla}_{\mathbf{k}} \equiv -ike^{i\psi}$ ,  $\hat{\nabla}_{\mathbf{k}}^* \equiv -ike^{-i\psi}$ . In addition, we have introduced the differential matrix operator  $T_{ij} \equiv \partial_x\delta_{ij} + \partial_y\epsilon_{ij}$  with  $\delta_{ij}$  the Kronecker symbol and  $\epsilon_{ij}$  the generator of counter-clock wise rotations (see main text). Proofs of these relations are presented in Appendix F.

where the perturbations of the vector fields  $\Xi$  are

$$\delta\Xi_0 = (\nabla \cdot \delta\mathbf{p})\mathbf{p}^* + (\nabla \times \delta\mathbf{p}) \times \mathbf{p}^*, \quad (4.4)$$

$$\delta\Xi_1 = (\mathbf{p}^* \cdot \nabla)\nabla^2\delta\mathbf{p} + (\mathbf{p}^* \times \nabla) \times \nabla^2\delta\mathbf{p} \quad (4.5)$$

and that of the nematic tensor  $\mathbf{Q}^{(1)}$  is specified by

$$\begin{aligned} \delta Q_j^{(1)} &= -B_0\mathbb{D}^\alpha\delta M_{jl}p_l^* - B_0\mathbb{D}^\alpha M_{jl}^*\delta p_l \\ &+ \frac{\lambda_1}{2}\mathbb{I}^{1-\alpha}T_{jl}\delta p_l - \frac{\lambda_2}{4}\mathbb{I}^{2-\alpha}T_{jl}\partial_l\delta\rho \\ &+ \frac{\lambda_3}{4}\mathbb{I}^{3-\alpha}T_{jl}\nabla^2\delta p_l - B_4\mathbb{I}^{4-\alpha}T_{jl}\delta\Xi_{1l} \end{aligned} \quad (4.6)$$

with the short-hand notations  $\delta M_{jl} \equiv (\delta p_x\delta_{jl} + \delta p_y\epsilon_{jl})$  and  $M_{jl}^* \equiv (p_x^*\delta_{jl} + p_y^*\epsilon_{jl})$ . In this equation, we adopt the same index convention defined in Sec. III. To further simplify the notation, in the next paragraphs, we will suppress all explicit dependencies on the homogeneous density  $\rho^*$ .

#### A. Disordered fluid state

In the disordered phase we set  $\mathbf{p}^* = \mathbf{0}$  and choose  $\rho^*$  such as  $\kappa_0(\rho^*) < 0$ . Therefore, Eqs. (4.2, 4.3) reduce to

$$\frac{\partial}{\partial t}\delta\rho = -\Upsilon_0\mathbb{D}^\alpha\delta\rho + 2\Upsilon_1\mathbb{I}^{1-\alpha}(\nabla \cdot \delta\mathbf{p}), \quad (4.7)$$

$$\frac{\partial}{\partial t}\delta\mathbf{p} = [\kappa_0 - \Upsilon_0\mathbb{D}^\alpha]\delta\mathbf{p} + \Upsilon_1\mathbb{I}^{1-\alpha}\nabla\delta\rho - \Upsilon_2\mathbb{I}^{2-\alpha}\nabla^2\delta\mathbf{p}. \quad (4.8)$$

We apply the ansatz (4.1) and compute the corresponding fractional terms by taking their Fourier transforms. Recalling that  $\mathcal{F}\{e^{i\mathbf{q}\cdot\mathbf{r}}\} = 2\pi\delta(\mathbf{k} + \mathbf{q})$ , we can write, e.g., for the terms in the first equation,

$$\begin{aligned} \mathbb{D}^\alpha\delta\rho &= \mathcal{F}^{-1}\{k^\alpha[2\pi e^{st}\delta(\mathbf{k} + \mathbf{q})]\delta\rho_0\} \\ &= \mathcal{F}^{-1}\{q^\alpha[2\pi e^{st}\delta(\mathbf{k} + \mathbf{q})]\delta\rho_0\} = q^\alpha\delta\rho, \end{aligned} \quad (4.9)$$

where we denote  $q \equiv |\mathbf{q}|$ , and

$$\begin{aligned} \mathbb{I}^{1-\alpha}(\nabla \cdot \delta\mathbf{p}) &= \mathcal{F}^{-1}\{k^{\alpha-1}(-i\mathbf{k} \cdot \delta\mathbf{p}_0)[2\pi e^{st}\delta(\mathbf{k} + \mathbf{q})]\} \\ &= \mathcal{F}^{-1}\{q^{\alpha-1}(i\mathbf{q} \cdot \delta\mathbf{p}_0)[2\pi e^{st}\delta(\mathbf{k} + \mathbf{q})]\} \\ &= q^{\alpha-1}(i\mathbf{q} \cdot \delta\mathbf{p}). \end{aligned} \quad (4.10)$$

Thus, after eliminating the multiplicative factor  $e^{st+i\mathbf{q}\cdot\mathbf{r}}$ , we obtain the equation

$$(s + \Upsilon_0q^\alpha)\delta\rho_0 - 2\Upsilon_1q^{\alpha-1}(i\mathbf{q} \cdot \delta\mathbf{p}_0) = 0. \quad (4.11)$$

Likewise, for the terms in the second equation we obtain

$$\begin{aligned} \mathbb{I}^{1-\alpha}\nabla\delta\rho &= \mathcal{F}^{-1}\{k^{\alpha-1}(-i\mathbf{k})[2\pi e^{st}\delta(\mathbf{k} + \mathbf{q})]\delta\rho_0\} \\ &= \mathcal{F}^{-1}\{q^{\alpha-1}(i\mathbf{q})[2\pi e^{st}\delta(\mathbf{k} + \mathbf{q})]\delta\rho_0\} \\ &= q^{\alpha-1}(i\mathbf{q})\delta\rho, \end{aligned} \quad (4.12)$$

and

$$\begin{aligned} \mathbb{I}^{2-\alpha}\nabla^2\delta\mathbf{p} &= \mathcal{F}^{-1}\{k^{\alpha-2}(-i\mathbf{k})^2[2\pi e^{st}\delta(\mathbf{k} + \mathbf{q})]\delta\mathbf{p}_0\} \\ &= \mathcal{F}^{-1}\{-q^\alpha[2\pi e^{st}\delta(\mathbf{k} + \mathbf{q})]\delta\mathbf{p}_0\} \\ &= -q^\alpha\delta\mathbf{p}. \end{aligned} \quad (4.13)$$

Therefore, the second equation yields

$$[s - \kappa_0 + (\Upsilon_0 - \Upsilon_2)q^\alpha]\delta\mathbf{p}_0 = \Upsilon_1q^{\alpha-1}(i\mathbf{q})\delta\rho_0. \quad (4.14)$$

Multiplying Eq. (4.14) by  $(i\mathbf{q})$  and solving it for  $i\mathbf{q} \cdot \delta\mathbf{p}_0$  we obtain

$$i\mathbf{q} \cdot \delta\mathbf{p}_0 = \frac{-\Upsilon_1q^{1+\alpha}\delta\rho_0}{[s - \kappa_0 + (\Upsilon_0 - \Upsilon_2)q^\alpha]}, \quad (4.15)$$

which can be combined with Eq. (4.11) to yield the dispersion relation

$$\begin{aligned} s^2 + s[-\kappa_0 + (2\Upsilon_0 - \Upsilon_2)q^\alpha] + 2\Upsilon_1^2q^{2\alpha} \\ + \Upsilon_0q^\alpha[-\kappa_0 + (\Upsilon_0 - \Upsilon_2)q^\alpha] = 0. \end{aligned} \quad (4.16)$$

Because by definition  $\Upsilon_0 > \Upsilon_2$  (for all  $0 < \alpha < 1$ ) and  $\kappa_0 < 0$  by assumption, the coefficient of the linear term is always positive. The solutions of Eq. (4.16) are then given by

$$s_{\pm} = \frac{1}{2} \left[ \kappa_0 - (2\Upsilon_0 - \Upsilon_2)q^\alpha \pm \sqrt{\Delta} \right], \quad (4.17)$$

with the discriminant given by

$$\Delta = [\kappa_0 - (2\Upsilon_0 - \Upsilon_2)q^\alpha]^2 + 4\Upsilon_0\kappa_0q^\alpha - 4[\Upsilon_0(\Upsilon_0 - \Upsilon_2) + 2\Upsilon_1^2]q^{2\alpha}. \quad (4.18)$$

The last three terms in its rhs are negative for all  $\alpha$ , i.e., the inequality  $\sqrt{\Delta} < -\kappa_0 + (2\Upsilon_0 - \Upsilon_2)q^\alpha$  holds. This relation implies that  $s_+ < 0$ . Therefore, the disordered fluid phase is stable with respect to perturbations in all directions, as in conventional polar active fluids.

### B. Ordered fluid state

In the ordered phase, we assume the stationary homogeneous flow  $\mathbf{p}^* \equiv p^* \mathbf{e}_\parallel$  with the unit vector  $\mathbf{e}_\parallel \equiv (\cos \vartheta_\parallel, \sin \vartheta_\parallel)$  specifying the arbitrary direction of symmetry breaking. We denote the corresponding orthogonal direction with the unit vector  $\mathbf{e}_\perp \equiv (-\sin \vartheta_\parallel, \cos \vartheta_\parallel)$ . These two vectors form a basis on which we can project the wave amplitude  $\delta \mathbf{p}_0$ , such that we can write  $\delta \mathbf{p}_0 = \delta p_{0\parallel} \mathbf{e}_\parallel + \delta p_{0\perp} \mathbf{e}_\perp$ . Furthermore, we assume the wave number vector  $\mathbf{q} = q \mathbf{e}_\vartheta$  with the angle  $\vartheta$  defined with respect to  $\mathbf{e}_\parallel$ . Therefore, the unit vector is  $\mathbf{e}_\vartheta \equiv \cos \vartheta \mathbf{e}_\parallel + \sin \vartheta \mathbf{e}_\perp$ . Under these assumptions Eqs. (4.2, 4.3) can be solved similarly to the disordered phase. For the first equation in particular the only term left to be calculated is  $\mathbb{I}^{2-\alpha}(\nabla \cdot \delta \Xi_0)$  with  $\delta \Xi_0$  specified by Eq. (4.4), which is given by (see Appendix G 1)

$$\mathbb{I}^{2-\alpha}(\nabla \cdot \delta \Xi_0) = -q^\alpha p^* [(\mathbf{e}_\vartheta \cdot \mathbf{e}_\parallel)(\delta \mathbf{p} \cdot \mathbf{e}_\vartheta) + (\mathbf{e}_\vartheta \cdot \mathbf{e}_\perp)(\delta \mathbf{p} \cdot \mathbf{e}_{\vartheta+\frac{\pi}{2}})]. \quad (4.19)$$

All other terms have been already computed in the previous paragraph (see Eqs. (4.9, 4.10)). Combining all these equations and removing the multiplicative factor  $e^{st+i\mathbf{q}\cdot\mathbf{r}}$ , we derive the following relation between  $\delta \rho_0$  and  $\delta \mathbf{p}_0$

$$(s + \Upsilon_0 q^\alpha) \delta \rho_0 = 2q^\alpha [i\Upsilon_1 + \lambda_2 p^* (\mathbf{e}_\vartheta \cdot \mathbf{e}_\parallel)] (\delta \mathbf{p}_0 \cdot \mathbf{e}_\vartheta) + 2q^\alpha \lambda_2 p^* (\mathbf{e}_\vartheta \cdot \mathbf{e}_\perp) (\delta \mathbf{p}_0 \cdot \mathbf{e}_{\vartheta+\frac{\pi}{2}}). \quad (4.20)$$

For the second equation, instead, by applying the same technique we calculate the terms (see Appendix G)

$$\mathbb{I}^{1-\alpha} \delta \Xi_0 = iq^\alpha p^* [(\delta \mathbf{p} \cdot \mathbf{e}_\vartheta) \mathbf{e}_\parallel + (\delta \mathbf{p} \cdot \mathbf{e}_{\vartheta+\frac{\pi}{2}}) \mathbf{e}_\perp], \quad (4.21)$$

$$\mathbb{I}^{3-\alpha} \delta \Xi_1 = -iq^\alpha p^* \left[ (\mathbf{e}_\vartheta \cdot \mathbf{e}_\parallel) \delta \mathbf{p} + (\mathbf{e}_\vartheta \cdot \mathbf{e}_\perp) \mathbf{R} \left( \frac{\pi}{2} \right) \delta \mathbf{p} \right] \quad (4.22)$$

with  $\mathbf{R}$  denoting a two-dimensional rotation matrix. Substituting these expressions into Eq. (4.3) and again eliminating the exponential multiplicative factor yields

$$\begin{aligned} s \delta \mathbf{p}_0 = & \left[ \frac{\gamma}{2} \delta \rho_0 - 2\xi p^* (\delta \mathbf{p}_0 \cdot \mathbf{e}_\parallel) \right] p^* \mathbf{e}_\parallel + \Upsilon_1 iq^\alpha \delta \rho_0 \mathbf{e}_\vartheta \\ & - \Upsilon_0 q^\alpha \delta \mathbf{p}_0 + \Upsilon_2 q^\alpha \delta \mathbf{p}_0 + 2\lambda_1 iq^\alpha p^* [(\delta \mathbf{p}_0 \cdot \mathbf{e}_\vartheta) \mathbf{e}_\parallel \\ & + (\delta \mathbf{p}_0 \cdot \mathbf{e}_{\vartheta+\frac{\pi}{2}}) \mathbf{e}_\perp] - \lambda_3 iq^\alpha p^* [(\mathbf{e}_\vartheta \cdot \mathbf{e}_\parallel) \delta \mathbf{p}_0 \\ & + (\mathbf{e}_\vartheta \cdot \mathbf{e}_\perp) \mathbf{R} \left( \frac{\pi}{2} \right) \delta \mathbf{p}_0] - p^* \delta \mathbf{Q}^{(1)} \mathbf{e}_\parallel, \end{aligned} \quad (4.23)$$

where the components of the tensor  $\delta \mathbf{Q}^{(1)}$  are given by (see Appendix G)

$$\begin{aligned} \delta Q_j^{(1)} = & -2B_0 q^\alpha p^* \delta p_{0l} + i \frac{\lambda_1}{2} q^\alpha R_{jl} (\vartheta + \vartheta_\parallel) \delta p_{0l} \\ & + \frac{\lambda_2}{4} q^\alpha \delta \rho_0 R_{jl} (\vartheta + \vartheta_\parallel) e_{\vartheta l} - i \frac{\lambda_3}{4} q^\alpha R_{jl} (\vartheta + \vartheta_\parallel) \delta p_{0l} \\ & - B_4 q^\alpha p^* (\mathbf{e}_\vartheta \cdot \mathbf{e}_\perp) R_{jm} (\vartheta + \vartheta_\parallel) R_{ml} \left( \frac{\pi}{2} \right) \delta p_{0l} \\ & - B_4 q^\alpha p^* (\mathbf{e}_\vartheta \cdot \mathbf{e}_\parallel) R_{jl} (\vartheta + \vartheta_\parallel) \delta p_{0l}. \end{aligned} \quad (4.24)$$

#### 1. Longitudinal perturbations

We first investigate the linear stability of the ordered phase in the case of longitudinal perturbations. We thus set  $\vartheta = 0$  (i.e.,  $\mathbf{e}_\vartheta = \mathbf{e}_\parallel$  and  $\mathbf{e}_{\vartheta+\frac{\pi}{2}} = \mathbf{e}_\perp$ ) in Eqs. (4.20, (4.23) and (4.24). In addition, because also  $\delta \mathbf{p}_0 \propto \mathbf{e}_\parallel$ , we set  $\delta p_{0\perp} = 0$ . Under these assumptions, we obtain the reduced equations

$$(s + \Upsilon_0 q^\alpha) \delta \rho_0 = 2q^\alpha (i\Upsilon_1 + \lambda_2 p^*) \delta p_{0\parallel}, \quad (4.25)$$

$$[s + 2\kappa_0 + (\Upsilon_0 - \Upsilon_2 - \Lambda_\parallel p^{*2}) q^\alpha] \delta p_{0\parallel} = \quad (4.26)$$

$$\left[ \frac{p^*}{2} \left( \gamma - \frac{\lambda_2}{2} q^\alpha \right) + i\Upsilon_1 q^\alpha \right] \delta \rho_0 + iq^\alpha p^* \zeta_\parallel \delta p_{0\parallel}$$

with auxiliary parameters  $\Lambda_\parallel \equiv B_4 + 2B_0 \cos \phi_\parallel$  and  $\zeta_\parallel = 3(2\lambda_1 - \lambda_3)/4$ . Solving the first equation for  $\delta p_{0\parallel}/\delta \rho_0$  and substituting it in the second one, we obtain the dispersion relation

$$\begin{aligned} s^2 + s [2\kappa_0 + (2\Upsilon_0 - \Upsilon_2 - \Lambda_\parallel p^{*2}) q^\alpha - iq^\alpha p^* \zeta_\parallel] \\ - iq^{2\alpha} p^* \Upsilon_0 \zeta_\parallel + \Upsilon_0 q^\alpha [2\kappa_0 + (\Upsilon_0 - \Upsilon_2 - \Lambda_\parallel p^{*2}) q^\alpha] \\ - 2q^\alpha (i\Upsilon_1 + \lambda_2 p^*) \left[ \frac{p^*}{2} \left( \gamma - \frac{\lambda_2}{2} q^\alpha \right) + i\Upsilon_1 q^\alpha \right] = 0. \end{aligned} \quad (4.27)$$

The real part of its solutions can be calculated. In detail,

$$\begin{aligned} \text{Re}(s_{\pm}) = & -\frac{1}{2} [2\kappa_0 + (2\Upsilon_0 - \Upsilon_2 - \Lambda_\parallel p^{*2}) q^\alpha] \\ & \pm \frac{1}{2} \sqrt{\frac{1}{2} \left( J_1 + \sqrt{J_1^2 + J_2^2} \right)} \end{aligned} \quad (4.28)$$

with auxiliary functions

$$J_1 = [2\kappa_0 + (2\Upsilon_0 - \Upsilon_2 - \Lambda_{\parallel} p^{*2})q^\alpha]^2 - 8(\Upsilon_0 - 2\Upsilon_2)\kappa_0 q^\alpha + 4\Upsilon_0(\Upsilon_2 - \Upsilon_0 + \Lambda_{\parallel} p^{*2})q^{2\alpha} - (8\Upsilon_1^2 + \zeta_{\parallel}^2 p^{*2} + 2\lambda_2^2 p^{*2})q^{2\alpha}, \quad (4.29)$$

$$J_2 = 4p^* q^\alpha [\gamma\Upsilon_1 - \zeta_{\parallel}\kappa_0] + 2p^* q^{2\alpha} [3\Upsilon_1\lambda_2 + \zeta_{\parallel}(\Upsilon_2 + \Lambda_{\parallel} p^{*2})]. \quad (4.30)$$

In the hydrodynamic limit  $q \rightarrow 0$ , we can expand these equations up to terms  $\mathcal{O}(q^{2\alpha})$  consistently with the order of the expansion employed to derive the full set of hydrodynamic equations. At this order of approximation, therefore, the linear stability of the model can only be assessed for long wavelength perturbations. In details, we find the asymptotic behaviour

$$\text{Re}(s_-) \simeq -2\kappa_0 - (\Upsilon_0 + \Upsilon_2 - \Lambda_{\parallel} p^{*2})q^\alpha \quad (4.31)$$

$$\text{Re}(s_+) \simeq (-\Upsilon_0 + 2\Upsilon_2)q^\alpha. \quad (4.32)$$

For comparison, we recover the stability picture of ordinary active fluids. Setting  $\alpha = 1$  and expanding Eqs. (4.28–4.30) up to terms  $\mathcal{O}(q^4)$  (in this case the expansion is valid because the only higher order term in the hydrodynamic equation,  $\nabla^2 \mathbf{p}$ , can be shown relevant only for short wavelength perturbations), we find  $\text{Re}(s_-) \simeq -2\kappa_0(\rho^*)$  and  $\text{Re}(s_+) \simeq \frac{\sigma}{16\kappa_0^2} [4 - 7\frac{\kappa_0}{\sigma}] q^2$ . The mode  $s_-$  has negative real part such that it represents the fast relaxation of small perturbations from the stationary solution  $\mathbf{p}^*$ . For the mode  $s_+$ , instead, by writing  $4 - 7\kappa_0/\sigma = 11 - 7\sigma_t/\sigma$ , we can see that its real part is negative for  $\sigma < 7\sigma_t/11$ . In this region of the parameter space, the ordered phase is thus stable against longitudinal perturbations at the linear level. Conversely, when  $7\sigma_t/11 \leq \sigma < \sigma_t$  the mode becomes unstable and the perturbation can destabilize the system. The eigenmode  $s_+$  thus corresponds to the banding instability characteristic of ordinary active fluids, which renders the transition first-order [61–64].

In the Lévy case  $\alpha \neq 1$ , the mode  $s_-$  only differs by a term of higher order  $\sim q^\alpha$ , which is thus negligible in the hydrodynamic limit. In contrast, the mode  $s_+$  exhibits a term of lower order  $\sim q^\alpha$ , which is thus dominant in the hydrodynamic limit. Because  $\Upsilon_0 > 2\Upsilon_2$  for all  $0 < \alpha < 1$  (not shown), this term has negative sign and thus exerts a stabilizing effect on the perturbed phase. Therefore, in ALM the banding instability is suppressed, such that the critical behaviour of the order-disorder phase transition predicted by the mean field theory can manifest.

This stabilization of the order phase in ALM is caused by the terms in the hydrodynamic EOM representing the enhanced diffusion of the fields  $\rho$  and  $\mathbf{p}$ . In fact, if we switched them off by setting  $\Upsilon_0 = 0$ , the sign of Eq. (4.32) would still be positive in the hydrodynamic limit. The banding instability would thus still disrupt the order phase at the onset of collective motion, and the phase transition would remain first-order as in ordinary active fluids.

We remark that the previous results on the stability of the order phase at the onset of collective motion are strictly valid only in the hydrodynamic limit, i.e., for long-wavelength perturbations. This calculation as is, thus, can not rule out the possibility that other instabilities could emerge in the order phase for intermediate wavelength perturbations. To perform a reliable linear stability analysis in this regime, in fact, the hydrodynamic equations (3.36) and (3.37) must be first corrected to account for, potentially, the entire hierarchy of higher-order expansion terms. This analysis, however, goes beyond the scope of the present manuscript and will not be pursued. Further definite validation of the previous predictions will be provided, instead, through numerical simulations of the microscopic dynamics (see Sec. V).

## 2. Transversal perturbations

We now study the stability of the ordered phase against perturbations orthogonal to the direction of the collective motion. Therefore, we set  $\vartheta = \pi/2$  (such that  $\mathbf{e}_\vartheta = \mathbf{e}_\perp$  and  $\mathbf{e}_{\vartheta+\frac{\pi}{2}} = -\mathbf{e}_\parallel$ ) in Eqs. (4.20) and (4.23). Furthermore, because also  $\delta \mathbf{p}_0 \propto \mathbf{e}_\perp$ , we assume  $\delta p_{0\parallel} = 0$ . With these assumptions, the contribution from the alignment tensor  $\delta \mathbf{Q}^{(1)}$  is determined by the relations  $\mathbf{e}_\perp \cdot [\delta \mathbf{Q}^{(1)} \mathbf{e}_\parallel] = \cos(2\vartheta_\parallel) \delta Q_{xy}^{(1)} - \sin(2\vartheta_\parallel) \delta Q_{xx}^{(1)}$ ,  $\mathbf{R}(\vartheta_\parallel + \pi/2) \mathbf{e}_\perp = -(\cos 2\vartheta_\parallel, \sin 2\vartheta_\parallel)$  and  $\mathbf{R}(\vartheta_\parallel + \pi/2) \mathbf{e}_\parallel = (\sin 2\vartheta_\parallel, -\cos 2\vartheta_\parallel)$ . Finally, we obtain the equations

$$(s + \Upsilon_0 q^\alpha) \delta \rho_0 = 2\Upsilon_1 i q^\alpha \delta p_{0\perp}, \quad (4.33)$$

$$[s + (\Upsilon_0 - \Upsilon_2 + \Lambda_\perp p^{*2})q^\alpha] \delta p_{0\perp} = \Upsilon_1 i q^\alpha \delta \rho_0 \quad (4.34)$$

with the auxiliary parameter  $\Lambda_\perp \equiv 2B_0 \cos \vartheta_\parallel - B_4$ . Solving Eq. (4.33) for  $\delta p_{0\perp}/\delta \rho_0$  and substituting it into Eq. (4.34) yields the dispersion relation

$$s^2 + s(2\Upsilon_0 - \Upsilon_2 - \Lambda_\perp p^{*2})q^\alpha + [\Upsilon_0(\Upsilon_0 - \Upsilon_2 - \Lambda_\perp p^{*2}) + 2\Upsilon_1^2]q^{2\alpha} = 0. \quad (4.35)$$

This equation can be solved similarly to the previous case. The real parts of its solutions are thus given by

$$\text{Re}(s_\pm) = -\frac{q^\alpha}{2} [(2\Upsilon_0 - \Upsilon_2 - \Lambda_\perp p^{*2}) \pm \sqrt{\Delta}] \quad (4.36)$$

with  $\Delta$  prescribed as

$$\Delta = [(\Upsilon_2 + \Lambda_\perp p^{*2})^2 - 8\Upsilon_1^2]. \quad (4.37)$$

At the onset of collective motion, where  $\kappa_0 \approx 0$ , we find that  $\Delta \approx \Upsilon_2^2 - 8\Upsilon_1^2$ , which is negative for all  $0 < \alpha < 1$  (not shown). Consequently, we obtain

$$\text{Re}[s_\pm] \approx -\left(\frac{2\Upsilon_0 - \Upsilon_2}{2}\right) q^\alpha, \quad (4.38)$$

which is negative as for longitudinal perturbations. Therefore, in ALM, at the onset of collective motion, the

ordered phase is stable against long-wavelength transversal perturbations from the stationary fields. This result agrees with the picture valid for ordinary active matter, where one obtains non authorized modes (i.e., imaginary; set  $\alpha = 1$  above) indicating that no instabilities whatsoever can arise from perturbations in this direction [45].

## V. FINITE SIZE SCALING ANALYSIS AND CRITICAL PROPERTIES OF THE TRANSITION

The potential criticality of the order-disorder phase transition in ALM, which is consequence of the suppression of the long-wavelength banding instability at the onset of collective motion, can be further ascertained by performing a finite size scaling analysis of the microscopic model (2.1) [137]. For this purpose, we perform numerical simulations of this dynamics in a square box of edge length  $L$  with periodic boundary conditions (see Appendix B for details on the numerical implementation). We choose model parameters:  $\rho = 2$ ,  $\gamma = 0.25$  and  $\alpha = 1/2$ , which are kept fixed throughout the analysis. Conversely, in order to identify the critical noise strength, which we denote as  $\sigma_*$ , we scan through a wide range of values of  $\sigma$  and repeat all simulations for different system sizes  $L = \{48, 56, 64, 72\}$ . Each simulation is initialized in the homogeneously disorder phase and updated for  $T$  time sweeps, with  $T$  sufficiently large that the system can equilibrate (see below). At each time step  $t_j = j\Delta t$ , we calculate the polar order parameter

$$\varphi(t_j) \equiv \frac{1}{N} \left| \sum_{i=1}^N \mathbf{n}(\theta_i(t_j)) \right|, \quad (5.1)$$

which measures the time-evolution of the average orientation of the active Lévy particles. Furthermore, we define the time-averaged polar order parameter

$$\varphi \equiv \frac{1}{T - j_0 + 1} \sum_{j=j_0}^T \varphi(t_j), \quad (5.2)$$

again with  $j_0$  large enough for the system to equilibrate. In our simulations, we choose  $T = 2.5 \times 10^6$  and  $j_0 = 2.45 \times 10^6$  (i.e., the time average is made over the last  $5 \times 10^4$  time steps). We can confirm, in fact, that these time sweeps are sufficient for the system to equilibrate. This is shown in Fig. 5, where we plot the pair correlation function  $G$  (a) and the correlation function for the unit vector  $\mathbf{n}$  (b) as a function of the inter-particle distance  $r \equiv |\mathbf{r}_i - \mathbf{r}_j|$  ( $i, j = 1, \dots, N$ ;  $i \neq j$ ) for several different values of  $T$  at the critical point (estimated numerically; see below) and for the largest system size considered  $L = 72$ . We note that, if the system is equilibrated in these conditions, it is also equilibrated for any different  $\sigma$  and/or smaller  $L$ . While the pair correlation function is equilibrated for all  $T$  considered (and is thus not informative in this sense), the correlation function of the orientation vector suggests that the equilibration

time is about  $T = 10^5$ , where the different curves start overlapping. The value that we use in our simulations is, in fact, one order of magnitude larger than this estimate, which thus allows us to safely assume the system to be equilibrated when we perform the time averaging (5.2).

The conventional technique to assess numerically the criticality of a phase transition, and simultaneously locate the critical point, consists in the estimation of the Binder cumulant, in our case of the time-averaged polar order parameter, for different system sizes  $L$ . This observable is defined as

$$U_4^{(L)} \equiv \frac{\langle \varphi^2 \rangle_L^2}{\langle \varphi^4 \rangle_L}, \quad (5.3)$$

where  $\langle \cdot \rangle_L$  denotes the ensemble average taken at finite system size. Specifically, if the phase transition is of second order (i.e., continuous), the Binder cumulant curves for different  $L$  must cross at the critical point [138]. Evidently, by measuring the intersection point of these curves, if it exists, we can also obtain an estimate of the critical point. We plot the Binder cumulant  $U_4^{(L)}$  for our microscopic model of ALM in Fig. 6a. Remarkably, the curves intersect, thus highlighting that the order-disorder phase transition in ALM is indeed critical, in agreement with the prediction of the linear stability analysis on the hydrodynamic EOM at the onset (see Sec. IV). Furthermore, by identifying the crossing point, we obtain the numerical estimate of the asymptotic critical noise strength

$$\sigma_* = 0.239816(2), \quad (5.4)$$

where the error denotes 1 s.e.m..

Having established the criticality of the transition, and the critical point (at fixed density), we can now characterize numerically the critical exponents. To estimate the static exponent  $\nu$ , we use the scaling relation for the gradient of Binder cumulant at the onset of the transition

$$\left| \frac{\partial U_4^{(L)}}{\partial \tau} \right|_{\tau \simeq 0} \propto L^{1/\nu}, \quad (5.5)$$

with the distance from the critical noise strength  $\tau \equiv -1 + \sigma/\sigma_*$ . To estimate the gradient, we fit  $U_4^{(L)}$  around the critical point with a quadratic polynomial. The coefficient of the linear term thus estimates  $\partial U_4^{(L)}/\partial \tau$ . Fits for all considered  $L$  are shown in Fig. 6a. The fit of the relation (5.5) to these estimates of the Binder cumulant gradient is presented in Fig. 7a. The other static critical exponents,  $\gamma$  and  $\beta$ , can be also estimated as ratios by the exponent just calculated,  $\nu$ . In fact, we can determine the ratio  $\gamma/\nu$  from the scaling relation for the susceptibility of the time-averaged polar order parameter at criticality,  $\varphi_*$ , which is defined (in two spatial dimensions) as

$$\chi_L \equiv L^2 (\langle \varphi_*^2 \rangle_L - \langle \varphi_* \rangle_L^2). \quad (5.6)$$

This observable scales with the system size  $L$  as

$$\chi_L \propto L^{\gamma/\nu}. \quad (5.7)$$

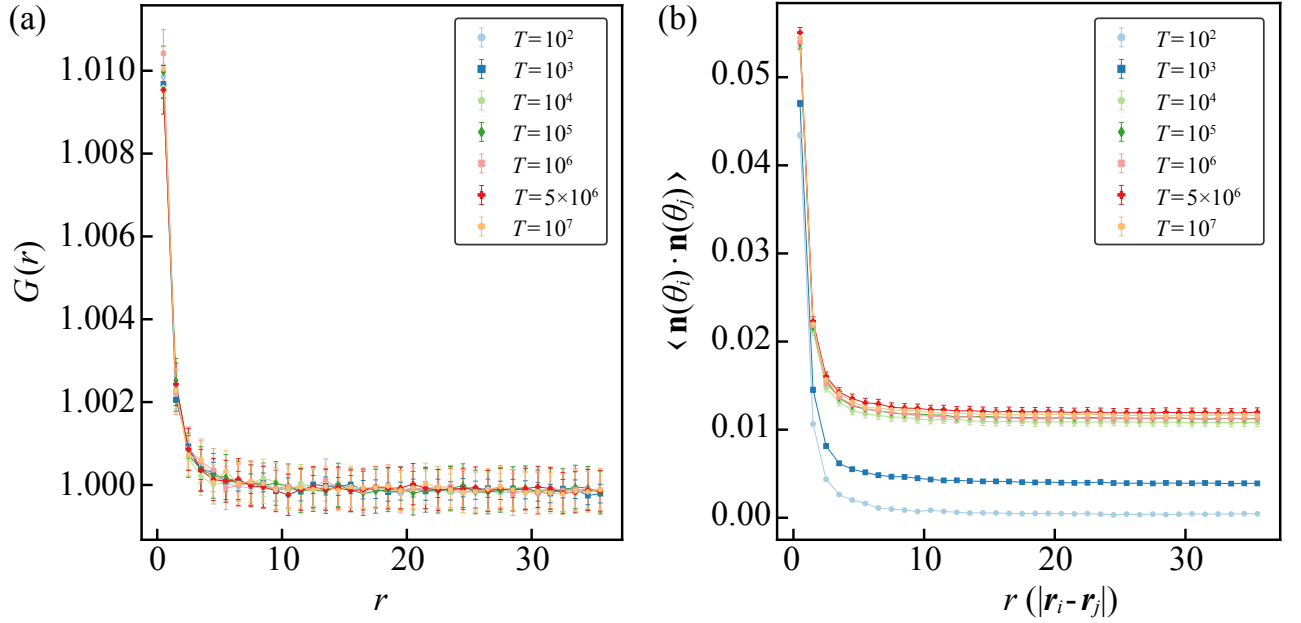


FIG. 5. Determination of the equilibration timescale of the microscopic model (2.1) of active Lévy matter at criticality. Other model parameters are  $\rho = 2$ ,  $\gamma = 0.25$  and  $\alpha = 1/2$ . The model is initialized in the homogeneously disorder phase and updated for different total time sweeps  $T$ . For each data point, we run 300 independent simulations. Error bars are 1 s.e.m; lines are also plotted as a guide to the eye. (a) Pair correlation function  $G$  at criticality vs. the inter-particle distance  $r$ . (b) Correlation function of the orientation vector  $\mathbf{n}(\theta_i) \equiv (\cos \theta_i, \sin \theta_i)$  at criticality vs. the distance between active particles.

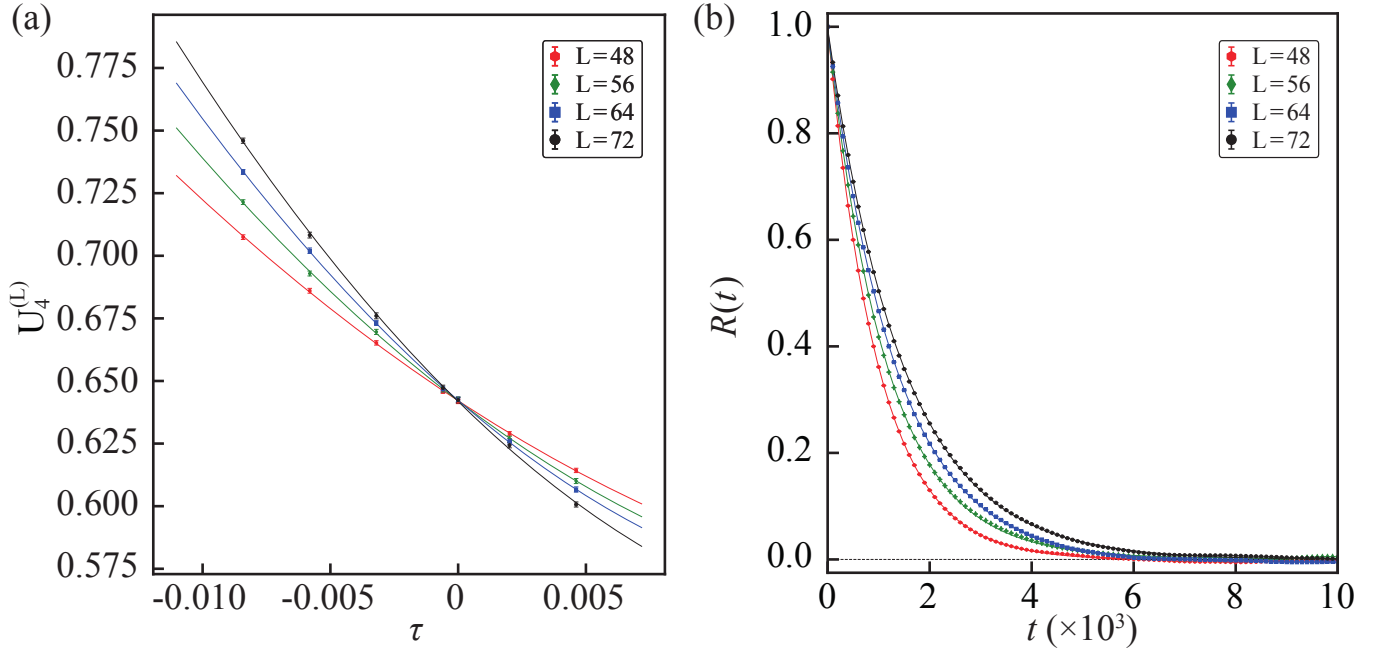


FIG. 6. Finite size scaling analysis of the microscopic model (2.1) of active Lévy matter. Model parameters are  $\rho = 2$ ,  $\gamma = 0.25$  and  $\alpha = 1/2$ . For each data point, we run 300 independent simulations of the microscopic model. (a) Estimation of the critical point through quadratic fits of Binder cumulant curves for different system sizes  $L$  as a function of the distance from criticality  $\tau \equiv -1 + \sigma/\sigma_*$ . (b) Estimation of the correlation time of the polar order parameter at criticality through exponential fits of the relaxation function  $R$  for different system sizes  $L$ . The fits are obtained by using the first 75 data points until the curve for the largest  $L$  starts oscillating. In both panels, we plot error bars denoting 1 s.e.m. and 95% confidence bands on the fit parameters. Fits are performed by applying a weighted least square method.

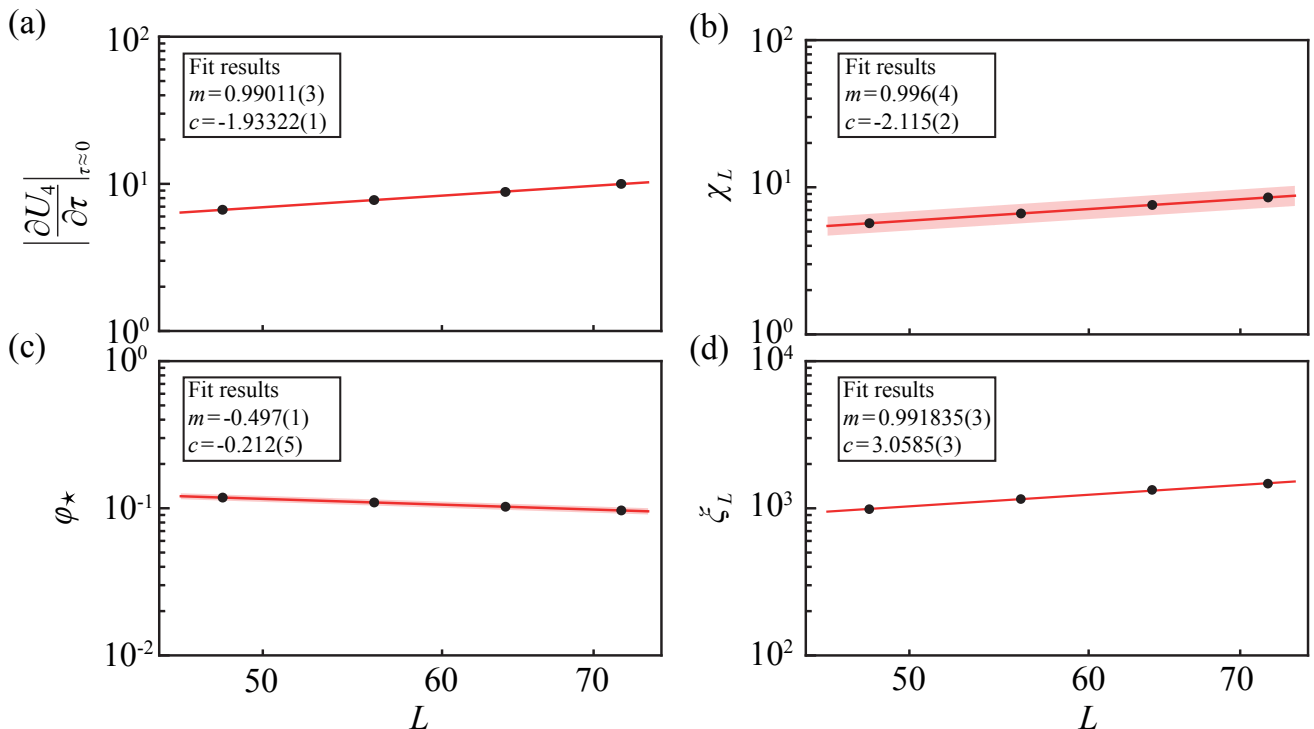


FIG. 7. Numerical estimation of static and dynamic critical exponents for the order-disorder phase transition in active Lévy matter. Model parameters are  $\rho = 2$ ,  $\gamma = 0.25$  and  $\alpha = 0.5$ . The simulation data (in logarithmic scales) are fitted with the linear function  $mL + c$  by using a weighted least squares method. We plot error bars denoting 1 s.e.m. and 95% confidence bands on fit parameters. (a) Gradient of the Binder cumulant at criticality  $|\partial U_4^{(L)}/\partial \tau|_{\tau \approx 0}$  vs. the system size  $L$ . (b) Susceptibility at criticality  $\chi_L$  vs.  $L$ . (c) Polar order parameter at criticality  $\phi_*$  vs.  $L$ . (d) Correlation time of the polar order parameter  $\xi_L$  at criticality vs.  $L$ .

The fit of the relation (5.7) to numerical estimates of  $\chi_L$  from simulation data is presented in Fig. 7b. To determine the ratio  $\beta/\nu$ , instead, we use the scaling relation of the time-averaged polar order parameter at criticality

$$\phi_* \propto L^{-\beta/\nu}. \quad (5.8)$$

The fit of the relation (5.8) to numerical estimates of  $\phi_*$  from simulation data is presented in Fig. 7c. Finally, we can estimate the dynamic critical exponent  $z$ , by applying the technique illustrated in [137]. From simulation data at criticality, we measure the relaxation function  $R$ , defined for a general time lag  $t > 0$  as

$$R(t) \equiv \frac{\langle \phi_*(t) \phi_*(0) \rangle_L - \langle \phi_*(0) \rangle_L^2}{\langle \phi_*^2(0) \rangle_L - \langle \phi_*(0) \rangle_L^2}. \quad (5.9)$$

By definition,  $R(0) = 1$  and  $R(t) \rightarrow 0$  for  $t \gg 1$ . In addition, this quantity is expected to decay exponentially, i.e.,  $R(t) \propto e^{-t/\xi}$ . By fitting our numerical data with this exponential function, we can then estimate the correlation length of the time-averaged polar order parameter at criticality,  $\xi_L$ , which obeys the scaling relation

$$\xi_L \propto L^z. \quad (5.10)$$

Therefore, we can use this expression to estimate directly the exponent  $z$ . Relaxation functions and corresponding exponential fits for all  $L$  considered are presented in Fig. 6b. Finally, we present the fit of the relation (5.10) to numerical estimates in Fig. 7d. This finite size scaling analysis is also repeated for a different microscopic step size distribution,  $\alpha = 3/4$ , (Fig. 8). In this case, we obtain the estimate for the critical noise strength

$$\sigma_* = 0.24343(6). \quad (5.11)$$

All the numerical estimates of static and dynamic critical exponents obtained are summarized in Table II.

$\alpha$	$\nu$	$\beta/\nu$	$\gamma/\nu$	$z$
1/2	1.00999(3)	0.497(1)	0.996(4)	0.991835(4)
3/4	1.0163(1)	0.496(1)	1.011(4)	0.991333(2)

TABLE II. Numerical estimates of the critical exponents for two exemplary values of the parameter  $\alpha$ . Errors are expressed as 1 s.e.m..

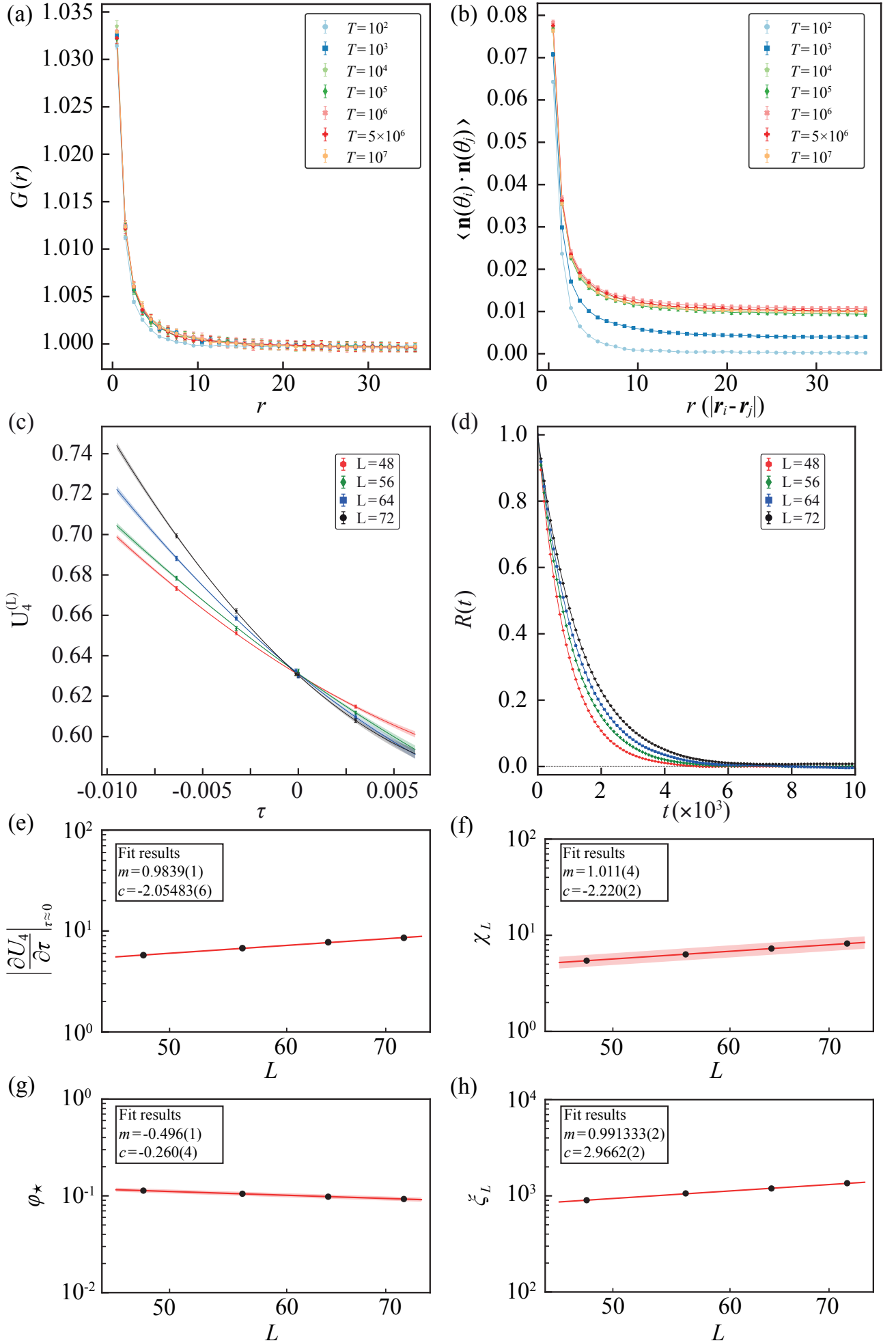


FIG. 8. (Caption on page 20.)

Intriguingly, the estimates obtained for the static critical exponents (at least for the first case,  $\alpha = 1/2$ ) suggest that the critical properties of ALM may be related to those of equilibrium two-dimensional models with long-range interaction energy  $\propto 1/|\mathbf{r}_{ij}|^{2+2\alpha}$  and  $n$ -component isotropic order parameter [139, 140]. For these systems, two regimes with distinct critical properties, separated by the threshold  $\alpha_c \equiv d/4$  ( $d$  are the spatial dimensions; thus, in our specific case,  $\alpha_c = 1/2$ ), have been demonstrated: For  $\alpha < \alpha_c$ , the so called *classical* regime, the critical exponents are

$$\gamma = 1, \quad \beta = \frac{1}{2}, \quad \nu = \frac{1}{2\alpha}. \quad (5.12)$$

These formulas are valid also at the threshold  $\alpha_c$ , except for logarithmic corrections for both the correlation length and susceptibility of the order parameter. The case  $\alpha = 1/2$ , therefore, belongs to this regime, and Eqs. (5.12) predict exponents  $\gamma = 1$ ,  $\beta = 1/2$  and  $\nu = 1$ . Our numerical estimates are clearly consistent with these predictions (see Table II).

For  $\alpha_c < \alpha < 1$ , the *nonclassical* regime, to which our second numerical case study,  $\alpha = 3/4$ , belongs, the critical exponents have been characterized as expansions in the distance from the threshold  $\Delta\alpha \equiv \alpha - \alpha_c$ . In details, setting  $n = 2$  for our polar order parameter, the following results hold to order  $\Delta\alpha^2$  [139]

$$\gamma \simeq 1 + \frac{8}{5}\Delta\alpha + \frac{668}{125}\Delta\alpha^2, \quad \beta = \frac{\gamma}{2} \left( \frac{1-\alpha}{\alpha} \right), \quad \nu = \frac{\gamma}{2\alpha}, \quad (5.13)$$

which predict  $\gamma = 1.734$ ,  $\beta = 0.289$  and  $\nu = 1.156$ . Our estimates are thus inconsistent with these predictions.

Having established the criticality of the disorder-to-collective motion transition in our model of ALM, we now compare the associated critical behaviour to other critical phenomena previously discussed in this context. Critical phenomena have been analyzed, either analytically or computationally, in the following active matter systems: (i) self-propelled particles with long-ranged metric alignment interactions [74, 75] (ii) incompressible active fluids [141–143], (iii) critical motility-induced phase separation [144–146], (iv) self-propelled particles with velocity reversals and alignment interactions [94], and (v) dense collections of active particles with contact inhibition of locomotion [147]. Our results indicate that the critical behavior in ALM is different from all of the above systems because our critical exponents depend on the parameter  $\alpha$  that quantifies the scaling properties of the Lévy particle dynamics, and such a parameter does not exist in the aforementioned systems. In addition, our observations seem to suggest that this dependence on  $\alpha$  may relate the static critical properties of ALM to the universality class of long-range attractive interactions in the classical regime. In contrast, they do not support this relation in the non classical regime. However, our numerical considerations are not exhaustive in this matter. To

further elucidate this connection, in fact, an analytical derivation of the critical exponents for general  $\alpha$  from the hydrodynamic equations must be developed by employing dynamic renormalisation group methods. This is an interesting open problem that we aim to elucidate in future investigations.

## VI. CONCLUSIONS

In this paper we studied in details a microscopic model of ALM [116], where the active particles perform superdiffusive motion, akin to a Lévy flight [117–119], with short-range interactions that promote the polar alignment of their velocity directions [7, 46]. First, we switched off the inter-particle interactions and characterized the diffusion process of individual active particles by their position mean-square displacement and statistics. We then switched on the alignment interactions and applied a coarse-graining procedure, based on the BBGKY hierarchical method [122] and on the expansion of the reduced single-particle probability density in terms of Fourier angular modes [45, 46, 48–50, 52], to derive the hydrodynamic EOM of the model. We then solved these equations at mean-field level, which yielded disordered and ordered phases similarly to ordinary active matter, and then studied the linear stability of these solutions.

On the one hand, we found that the disordered phase is stable at the linear level against small perturbations in an arbitrary direction. This prediction agrees with the conventional theory of active fluids [45–48]. On the other hand, we found that the ordered phase at the onset of collective motion is also stable at linear level against small perturbations in the longitudinal direction. This is fundamentally different from ordinary active fluids, where a characteristic banding instability has been shown to emerge both analytically and numerically [45–50, 61–64]. This instability, which makes the phase transition first-order in ordinary active matter, is thus suppressed in ALM, thus allowing for a critical disordered-ordered phase transition [116]. Finally, we validated this prediction by finite size scaling analysis of simulation data and estimated numerically the critical exponents of the transition, which revealed an intriguing relation between the static properties of our ALM model and the equilibrium  $n$ -component system with long-range attractive interactions (in the classical regime).

The derivation of the hydrodynamic EOM for ALM, the linear stability analysis on the order and disorder phases, and the numerical characterization of the critical properties of the phase transition are our most important results, even more so because they elucidate the novel physics of active matter integrating anomalous diffusive motility and inter-particle interactions. In particular, the connection with the universality class of long-range attractive interactions will need to be further elucidated with analytical arguments; for instance, by deriving general formulas for the critical exponents as a

FIG. 8. Summary of the finite size scaling analysis of the microscopic model (2.1) of active Lévy matter for  $\alpha = 3/4$ . Other model parameters are  $\rho = 2$  and  $\gamma = 0.25$ . We refer to the main text and to the captions of Figs. 5, 6 and 7 for details on the numerical protocol and statistical analysis employed. (a) Pair correlation function  $G$  at criticality vs. the inter-particle distance  $r$ . (b) Correlation function of the orientation vector  $\mathbf{n}(\theta_i) \equiv (\cos \theta_i, \sin \theta_i)$  at criticality vs. the distance between active particles. (c) Estimation of the critical point. (d) Estimation of the correlation time of the polar order parameter at criticality. (e) Gradient of the Binder cumulant at criticality  $|\partial U_4^{(L)} / \partial \tau|_{\tau \simeq 0}$  vs. the system size  $L$ . (f) Susceptibility at criticality  $\chi_L$  vs.  $L$ . (g) Polar order parameter at criticality  $\varphi_*$  vs.  $L$ . (h) Correlation time of the polar order parameter  $\xi_L$  at criticality vs.  $L$ .

function of the characteristic model parameter  $\alpha$ . One viable method to achieve this task can be to apply a dynamic renormalisation group approach, similarly to that recently introduced to study the universality class of the ordered phase and of the disorder-to-collective motion phase transition of incompressible active fluids [141–143].

Another important result relates to the structure of the hydrodynamic EOM for ALM (see Eqs. (3.36, 3.37)), which we obtained by coarse-graining the microscopic dynamical model (2.1). Our calculation shows that these equations contain: (a) terms that have a counterpart in the hydrodynamic EOM of ordinary active matter and are integrated across the domain weighted by probability measures that can be easily interpreted; (b) higher order terms in the Fourier angular expansion that are absent from the hydrodynamic EOM of ordinary active matter, which not only can depend on highly non-linear fields but can also exhibit a non local integral structure specified by non trivial probability measures. While the former terms can be understood straightforwardly also by applying a first principles approach, the latter ones pose considerable challenge because in general they may require complex and non intuitive jump statistics to be formulated correctly. Our discussion can thus potentially serve as a starting point to develop a systematic first-principles derivation of the hydrodynamic equations for ALM systems.

Overall, our results highlight that anomalous diffusion at single-particle level can fundamentally change the collective properties of active systems. Therefore, it will be interesting to apply considerations similar to those developed in this paper to other paradigmatic examples of collective behaviour, such as active turbulence [11–19] and motility-induced phase separation [20–23], and to further elucidate their relevance to the biological realm [99].

## VII. ACKNOWLEDGEMENTS

A.C. gratefully acknowledges funding under the Science Research Fellowship granted by the Royal Commission for the Exhibition of 1851 and the High Throughput Computing service provided by Imperial College Research Computing Service, DOI: 10.14469/hpc/2232.

## Appendix A: Diffusional features of the dynamical model (1.1) with Lévy stable distributed step sizes

We first calculate the position statistics of non-interacting active Lévy particles projected along the arbitrary direction  $\mathbf{n}(\psi) \equiv (\cos \psi, \sin \psi)$ , which is defined as  $P(x, t) \equiv \langle \delta(x - \mathbf{r}'(t) \cdot \mathbf{n}(\psi)) \rangle$  with  $\mathbf{r}'(t) \equiv \mathbf{r}(t) - \mathbf{r}(0)$  and  $\mathbf{r}$  prescribed by the Langevin equations (1.1). Taking its Fourier transform, we can write

$$\begin{aligned} \hat{P}(k, t) &= \langle e^{ik\mathbf{r}'(t) \cdot \mathbf{n}(\psi)} \rangle \\ &= \langle e^{ik \int_0^t \eta(t') \cos(\theta(t') - \psi) dt'} \rangle. \end{aligned} \quad (\text{A.1})$$

Exploiting the independence of  $\eta$  and  $\xi$ , we can calculate the average over the Lévy noise first by using Eq. (1.5) with  $h(t') \equiv H(t - t')(-ik) \cos(\theta(t') - \psi)$  ( $H$  is the Heaviside function; i.e.,  $H(x) = 1$  for  $x \geq 0$ ;  $H(x) = 0$  otherwise). Therefore, we obtain  $\hat{P}(k, t) = \langle e^{-k^\alpha D(t)} \rangle$  with the auxiliary function

$$D(t) \equiv \int_0^t |\cos(\theta(t') - \psi)|^\alpha e^{-i\frac{\alpha\pi}{2} \text{sign}(\cos(\theta(t') - \psi))} dt'. \quad (\text{A.2})$$

The remaining Brownian average can be calculated with the Feynman-Kac equation [148] (not shown). The projected statistics is thus formally given by

$$P(x, t) = \frac{1}{\pi} \text{Re} \int_0^\infty e^{-ikx} \langle e^{-|k|^\alpha D(t)} \rangle dk. \quad (\text{A.3})$$

To get its asymptotic tail behaviour, we expand the Brownian functional and rescale the Fourier variable as

$$\begin{aligned} P(x, t) - \delta(x) &\sim |x|^{-(1+\alpha)} \lim_{\epsilon \rightarrow 0} \left[ -\frac{1}{\pi} \text{Re} \int_0^\infty e^{-ik - \epsilon k} |k|^\alpha \langle D(t) \rangle dk \right] \\ &\sim -|x|^{-(1+\alpha)} \Gamma(1 + \alpha) \frac{1}{\pi} \text{Re} \left[ e^{-i\frac{\pi}{2}(1+\alpha)} \langle D(t) \rangle \right] \\ &\sim |x|^{-(1+\alpha)} \Gamma(1 + \alpha) \frac{\sin(\pi\alpha)}{\pi^2} C(t), \end{aligned} \quad (\text{A.4})$$

where the infinitesimal coefficient  $e^{-\epsilon k}$  ensures the convergence of the expansion [136] and  $C(t)$  is the positive real coefficient

$$C(t) \equiv \int_0^t \int_0^{\pi/2} \int_0^{2\pi} (\cos \phi)^\alpha \frac{e^{-\frac{(\phi - \phi')^2}{2\sigma t'}}}{\sqrt{2\pi\sigma t'}} d\phi' d\phi dt'. \quad (\text{A.5})$$

This is calculated by assuming uniformly distributed initial angles for the active particles and by recalling that the transition probability for the angular variables is Gaussian. This argument shows that the projected position statistics exhibits power-law asymptotic tail behaviour  $P(x, t) \sim |x|^{-(1+\alpha)}$  for  $|x| \gg 1$ .

Similarly, we can calculate the two-dimensional position statistics  $P(\mathbf{x}, t) \equiv \prec \langle \delta(\mathbf{x} - \mathbf{r}'(t)) \rangle \succ$ . Its Fourier transform is

$$\begin{aligned} \hat{P}(\mathbf{k}, t) &= \prec \langle e^{i\mathbf{k} \cdot \mathbf{r}'(t)} \rangle \succ \\ &= \prec \langle e^{i \int_0^t \eta(t') [\mathbf{k} \cdot \mathbf{n}(\theta(t'))] dt'} \rangle \succ. \end{aligned} \quad (\text{A.6})$$

Setting  $h(t') \equiv H(t - t')[-i\mathbf{k} \cdot \mathbf{n}(\theta(t'))]$  in Eq. (1.5) we obtain

$$\hat{P}(\mathbf{k}, t) = \langle e^{-\int_0^t [-i\mathbf{k} \cdot \mathbf{n}(\theta(t'))]^\alpha dt'} \rangle. \quad (\text{A.7})$$

Taking its inverse Fourier transform, and setting  $\mathbf{k} \equiv k\mathbf{n}(\psi)$ , we obtain the formal equation for the distribution

$$P(\mathbf{x}, t) = \frac{1}{2\pi} \int_{\mathbb{R}^2} d^2\mathbf{k} e^{-i\mathbf{k} \cdot \mathbf{x}} \langle e^{-k^\alpha D(t)} \rangle. \quad (\text{A.8})$$

Using this result, we can calculate the fractional moments  $\prec \langle |\mathbf{x}|^\delta \rangle \succ \equiv \int_{\mathbb{R}^2} |\mathbf{x}|^\delta P(\mathbf{x}, t) d^2\mathbf{x}$  for  $0 < \delta < \alpha$ . In details, using polar coordinates for both integrals, and performing the change of variables  $k' \equiv k[D(t)]^{1/\alpha}$ ,  $x' \equiv x/[D(t)]^{1/\alpha}$  we obtain

$$\begin{aligned} \prec \langle |\mathbf{x}|^\delta \rangle \succ &= \frac{1}{2\pi} \int_0^\infty dx' x'^{1+\delta} \int_0^{2\pi} d\phi \int_0^\infty k' dk' \times \\ &\times \int_0^{2\pi} d\phi' e^{-ik' x' \cos(\phi - \phi') - k'^\alpha} \langle [D(t)]^{\delta/\alpha} \rangle. \end{aligned} \quad (\text{A.9})$$

To solve this equation analytically, one needs to calculate the full statistics of the corresponding Brownian functional  $W(y, t) \equiv \langle \delta(y - D(t)) \rangle$ , which however we do not pursue here. Nevertheless, recalling that Brownian functionals scale linearly for long times [149], i.e., in Laplace space  $\mathcal{L}\{W(y, t)\}(s) = g(ys)$  with  $g$  a suitable scaling function, we can write  $\mathcal{L}\{\langle [D(t)]^{\delta/\alpha} \rangle\}(s) = s^{-1-\delta/\alpha} \int_{-\infty}^\infty y^{\delta/\alpha} g(y) dy$ . The inverse Laplace transform of this equation yields the scaling behaviour  $\langle [D(t)]^{\delta/\alpha} \rangle \sim t^{\delta/\alpha}$ . Upon rescaling the fractional moment, we obtain that the pseudo mean-square displacement  $\prec \langle |\mathbf{x}|^\delta \rangle \succ^{2/\delta}$  scales as  $t^{2/\alpha}$ .

## Appendix B: Details of the simulation protocol

### 1. Model numerical implementation

To simulate the dynamics of active Lévy particles from the initial time  $t_0 = 0$  to the final time  $t_T = M$ , we consider a time discretization  $\{t_m\}$  with time step  $\Delta t$  (thus  $m = 0, \dots, T$  with  $T \equiv M/\Delta t$ ). The Langevin

equations (2.1) are discretized as

$$\mathbf{r}_i(t_{m+1}) = \mathbf{r}_i(t_m) + \eta_i(t_m, \Delta t) \mathbf{n}(\theta_i(t_m)), \quad (\text{B.1})$$

$$\theta_i(t_{m+1}) = \theta_i(t_m) + F_i(t_m) \Delta t + \xi_i(t_m, \Delta t), \quad (\text{B.2})$$

where  $\eta_i(t_m, \Delta t)$  is a random variable sampled from a one-sided positive Lévy distribution with characteristic Lévy symbol generically specified by Eq. (1.2) (see below the algorithm for generating in particular stable variates with stability parameter  $0 < \alpha < 1$ ),  $\xi_i(t_m, \Delta t)$  is a Gaussian random variable with null mean and variance  $2\sigma\Delta t$ , and  $F_i(t_m)$  is the short-range alignment interaction exerted on particle  $i$ -th (see Eq. (2.2)). Note the choice of Itô prescription for the multiplicative noise term in the rhs of Eq. (B.1).

At each time step all particle trajectories are updated; in equivalent terms, for each simulation we then perform  $T$  particle sweeps (in the simulations presented  $\Delta t = 0.1$ ). Therefore, the predictions on the macroscopic behaviour of the model do not depend on  $\Delta t$ , as long as we account for a total number of particle sweeps sufficient to ensure that the system is equilibrated.

Let us consider, in full generality, that numerical simulations of the Eqs. (B.1, B.2) are performed in an asymmetric box of size  $2L_x \times 2L_y$  with periodic boundary conditions. Imposing these conditions for the dynamics described here requires more careful consideration with respect to the case of self-propelled particles (where one only needs to implement the rules presented, among other textbooks, in [150]). In fact, because the Lévy statistics allows for potentially large particle displacements between successive time steps, particles can jump from one time step to the next one in one of several consecutive adjacent boxes outside the simulation region (i.e., not only the first one) (see schematic in Fig. 9). Therefore, the rules to impose periodic boundary conditions in our microscopic ALM model are adapted as follows. Consider, e.g., the  $x$ -component of the  $i$ -th particle position vector  $r_{ix}$  that satisfies the condition  $-L_x \leq r_{ix} \leq L_x$ ; then,

- if  $r_{ix} \geq L_x$ , replace it by  $r_{ix} - (1+n)2L_x$  with the integer  $n = \lfloor (r_{ix} - L_x)/2L_x \rfloor$ ;
- otherwise, if  $r_{ix} < -L_x$ , replace it by  $r_{ix} + (1+n)2L_x$  with the integer  $n = \lfloor |r_{ix} + L_x|/2L_x \rfloor$ .

The same rules with  $L_x$  replaced by  $L_y$  hold for the  $y$ -component of the position vector  $r_{iy}$ , which is also assumed to satisfy the condition  $-L_y \leq r_{iy} \leq L_y$ . Similarly, when evaluating the distance between particles  $i$ -th

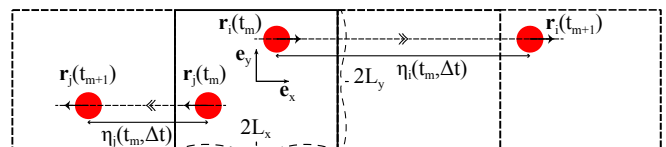


FIG. 9. Schematic of jump event for two active Lévy particles illustrating the rules to impose periodic boundary conditions.

and  $j$ -th, these rules are applied to each of the components of the distance vector  $\mathbf{r}_{ij} = \mathbf{r}_i - \mathbf{r}_j$  (clearly in this case  $n = 0$  [150]). Finally, to efficiently evaluate the inter-particle force  $F_i$  in the rhs of Eq. (B.2) we implement the cell subdivision method [150].

## 2. Generation of one-sided positive Lévy stable random variables

Random variates  $\eta(t_i, \Delta t)$  following a one-sided positive Lévy stable distribution with stability parameter  $0 < \alpha < 1$  are obtained by implementing the algorithm below [151, 152]:

- 1.A We generate a random variable  $V_i$  uniformly distributed on  $(-\pi/2, \pi/2)$ . This is realized by sampling a uniformly distributed variate  $u_i^{(1)}$  on  $(0, 1)$  (here we use the ran2 algorithm presented in [153]) and then setting  $V_i = \pi(u_i^{(1)} - 1/2)$ .
- 1.B We generate a second independent random variable  $W_i$  exponentially distributed with mean 1. This is obtained similarly by sampling another uniformly distributed variate  $u_i^{(2)}$  on  $(0, 1)$ , independent on  $u_i^{(1)}$ , and setting  $W_i = -\log(u_i^{(2)})$ .
- 1.C The Lévy distributed variate is given by

$$\eta(t_i, \Delta t) = (\Delta t)^{1/\alpha} \frac{\sin[\alpha(V_i + \frac{\pi}{2})]}{[\cos(V_i)]^{1/\alpha}} \times \left\{ \frac{\cos[V_i - \alpha(V_i + \frac{\pi}{2})]}{W_i} \right\}^{(1-\alpha)/\alpha}. \quad (\text{B.3})$$

This algorithm also applies to the special case  $\alpha = 1$ , where it yields  $\eta(t_i, \Delta t) = \Delta t$  as expected (see Sec. I).

To avoid sampling random variables too large for the double-precision floating point format of typical calculators, we introduce a tempering  $H \gg L$  by employing the rejection method [154] (in the simulations presented we set  $H = 10^{10}$ ):

- 2.A We generate the Lévy distributed variate  $\eta(t_i, \Delta t)$  as detailed above; then
- 2.B we sample a second random variable  $Y_i$  from an exponential distribution with mean  $1/H$  (again as detailed above);
- 2.C finally, if  $\eta(t_i, \Delta t) \leq Y_i$ , we keep it; otherwise, we reject both variables and repeat steps 2.A and 2.B.

We refer to the original references [151, 152, 154] for the numerical verification of these algorithms. An algorithm similar to 1.A – 1.C yielding fully general Lévy stable distributed random variables can be found in [155].

## Appendix C: Large-scale limit of the integral term (2.20)

To simplify the notation, we consider a general test function  $h$ . Since the probability density  $P$  is also a test function, the argument presented below also applies to it. We write the integral term as

$$\begin{aligned} & \frac{1}{\pi d^2} \int_{\mathbb{R}^2} d\mathbf{r} \int_{\mathbb{R}^2} d\mathbf{r}' H(d - |\mathbf{r} - \mathbf{r}'|) h(\mathbf{r}') \\ &= \frac{1}{2\pi d^2} \int_{\mathbb{R}^2} d\mathbf{r}_1 \int_{\mathbb{R}^2} d\mathbf{r}_2 H(d - |\mathbf{r}_2|) h\left(\frac{\mathbf{r}_1 - \mathbf{r}_2}{2}\right) \\ &= \frac{1}{2\pi d^2} \int_{\mathbb{R}^2} d\mathbf{r}_1 \int_0^d dr_2 r_2 \int_{-\pi}^{\pi} d\phi h\left(\frac{\mathbf{r}_1 - r_2 \mathbf{e}_r}{2}\right) \quad (\text{C.1}) \end{aligned}$$

where first we use the change of variables  $(\mathbf{r}_1, \mathbf{r}_2) \equiv (\mathbf{r} + \mathbf{r}', \mathbf{r} - \mathbf{r}')$  with Jacobian  $1/2$  and second we express the integral over  $\mathbf{r}_2$  in polar coordinates  $(r_2, \phi)$  with  $\mathbf{e}_r \equiv (\cos \phi, \sin \phi)$ . Again changing variables as  $r_2 \equiv dr'_2$ , we obtain

$$\begin{aligned} & \frac{1}{\pi d^2} \int_{\mathbb{R}^2} d\mathbf{r} \int_{\mathbb{R}^2} d\mathbf{r}' H(d - |\mathbf{r} - \mathbf{r}'|) h(\mathbf{r}') \\ &= \frac{1}{2\pi} \int_{\mathbb{R}^2} d\mathbf{r}_1 \int_0^1 dr'_2 r'_2 \int_{-\pi}^{\pi} d\phi h\left(\frac{\mathbf{r}_1 - dr'_2 \mathbf{e}_r}{2}\right). \quad (\text{C.2}) \end{aligned}$$

It is now straightforward to take the limit  $d \rightarrow 0$ . In this limit,  $h$  can be taken outside the polar integral, and this latter one can be solved exactly. Therefore, we demonstrate the following relation

$$\begin{aligned} & \lim_{d \rightarrow 0} \frac{1}{\pi d^2} \int_{\mathbb{R}^2} d\mathbf{r} \int_{\mathbb{R}^2} d\mathbf{r}' H(d - |\mathbf{r} - \mathbf{r}'|) h(\mathbf{r}') \\ &= \frac{1}{2} \int_{\mathbb{R}^2} d\mathbf{r}_1 h\left(\frac{\mathbf{r}_1}{2}\right) \equiv \int_{\mathbb{R}^2} d\mathbf{r} \int_{\mathbb{R}^2} d\mathbf{r}' \delta(\mathbf{r} - \mathbf{r}') h(\mathbf{r}'). \quad (\text{C.3}) \end{aligned}$$

As this relation holds for any test function  $h$ , the outer integral can be dropped; therefore, this relation is equivalent to

$$\lim_{d \rightarrow 0} \frac{1}{\pi d^2} \int_{\mathbb{R}^2} d\mathbf{r}' H(d - |\mathbf{r} - \mathbf{r}'|) h(\mathbf{r}') = \int_{\mathbb{R}^2} d\mathbf{r}' \delta(\mathbf{r} - \mathbf{r}') h(\mathbf{r}'). \quad (\text{C.4})$$

Applying this relation to Eq. (2.20) yields its large-scale limit (2.21).

## Appendix D: Exact formulas for the coefficients $\Upsilon$ for Lévy stable distributed step sizes

We consider Eq. (3.16) with  $\nu$  specified by Eq. (1.3), i.e.,

$$\Upsilon_m \equiv \frac{(-i)^m}{2\pi} \int_{-\pi}^{\pi} e^{i\phi' m} (-i \cos \phi')^\alpha d\phi'. \quad (\text{D.1})$$

The remaining angular integral can be solved analytically. For  $m = 0$  we find

$$\int_{-\pi}^{\pi} (-i \cos \phi')^\alpha d\phi' = 2\sqrt{\pi} \cos\left(\frac{\pi\alpha}{2}\right) \frac{\Gamma(\frac{1+\alpha}{2})}{\Gamma(1 + \frac{\alpha}{2})}, \quad (\text{D.2})$$

such that

$$\Upsilon_0(\alpha) = \frac{\cos\left(\frac{\pi\alpha}{2}\right)}{\sqrt{\pi}} \frac{\Gamma\left(\frac{1+\alpha}{2}\right)}{\Gamma\left(1+\frac{\alpha}{2}\right)}. \quad (\text{D.3})$$

For  $m \neq 0$  we can write

$$\begin{aligned} \int_{-\pi}^{\pi} e^{i\phi'm} (-i \cos \phi')^{\alpha} d\phi' = \\ 2(-i)^{\alpha} \int_0^{\pi/2} \cos(\phi'm) (\cos \phi')^{\alpha} d\phi' \\ + 2i^{\alpha} \int_{\pi/2}^{\pi} \cos(\phi'm) |\cos \phi'|^{\alpha} d\phi'. \end{aligned} \quad (\text{D.4})$$

The first integral in its rhs is equal to

$$\begin{aligned} \int_0^{\pi/2} \cos(\phi'm) (\cos \phi')^{\alpha} d\phi' = \\ \frac{i2^{-1-\alpha}}{m-\alpha} {}_2F_1\left(\frac{m-\alpha}{2}, -\alpha; 1+\frac{m-\alpha}{2}; -1\right) \\ - \frac{i2^{-1-\alpha}}{m+\alpha} {}_2F_1\left(-\frac{m+\alpha}{2}, -\alpha; 1-\frac{m+\alpha}{2}; -1\right) \\ + \frac{i^m}{2} \left(-\frac{i}{2}\right)^{1+\alpha} \frac{\Gamma(1+\alpha)\Gamma\left(\frac{m-\alpha}{2}\right)}{\Gamma\left(1+\frac{m+\alpha}{2}\right)} \\ + \frac{(-i)^m}{2} \left(-\frac{i}{2}\right)^{1+\alpha} \frac{\Gamma(1+\alpha)\Gamma\left(-\frac{m+\alpha}{2}\right)}{\Gamma\left(1-\frac{m-\alpha}{2}\right)}; \end{aligned} \quad (\text{D.5})$$

likewise, the second one is given by

$$\begin{aligned} \int_{\pi/2}^{\pi} \cos(\phi'm) |\cos \phi'|^{\alpha} d\phi' = \\ \frac{i2^{-1-\alpha}(-1)^{1+m}}{m-\alpha} {}_2F_1\left(\frac{m-\alpha}{2}, -\alpha; 1+\frac{m-\alpha}{2}; -1\right) \\ + \frac{i2^{-1-\alpha}(-1)^m}{m+\alpha} {}_2F_1\left(-\frac{m+\alpha}{2}, -\alpha; 1-\frac{m+\alpha}{2}; -1\right) \\ + \frac{i^m}{2} \left(\frac{i}{2}\right)^{1+\alpha} \frac{\Gamma(1+\alpha)\Gamma\left(\frac{m-\alpha}{2}\right)}{\Gamma\left(1+\frac{m+\alpha}{2}\right)} \\ + \frac{(-i)^m}{2} \left(\frac{i}{2}\right)^{1+\alpha} \frac{\Gamma(1+\alpha)\Gamma\left(-\frac{m+\alpha}{2}\right)}{\Gamma\left(1-\frac{m-\alpha}{2}\right)} \end{aligned} \quad (\text{D.6})$$

with  ${}_2F_1$  the Gaussian hypergeometric function. Combining these results into Eq. (D.4), we finally obtain:

$$\begin{aligned} \int_{-\pi}^{\pi} e^{i\phi'm} (-i \cos \phi')^{\alpha} d\phi' = \frac{i^{\alpha+1}}{2^{\alpha}} \left\{ \frac{[(-1)^{\alpha} - (-1)^m]}{m-\alpha} \times \right. \\ {}_2F_1\left(\frac{m-\alpha}{2}, -\alpha; 1+\frac{m-\alpha}{2}; -1\right) + \frac{[(-1)^m - (-1)^{\alpha}]}{m+\alpha} \\ \left. \times {}_2F_1\left(-\frac{m+\alpha}{2}, -\alpha; 1-\frac{m+\alpha}{2}; -1\right) \right\}. \end{aligned} \quad (\text{D.7})$$

Using the relations

$$i^{\alpha}[(-1)^m - (-1)^{\alpha}] = 2i^{1+m} \sin\left(\frac{\pi}{2}(m+\alpha)\right), \quad (\text{D.8a})$$

$$i^{\alpha}[(-1)^m - (-1)^{\alpha}] = 2(-i)^{1+m} \sin\left(\frac{\pi}{2}(m-\alpha)\right), \quad (\text{D.8b})$$

we finally obtain

$$\begin{aligned} \Upsilon_m(\alpha) \equiv \\ \frac{\sin\left(\frac{\pi}{2}(m+\alpha)\right)}{\pi 2^{\alpha}(m-\alpha)} {}_2F_1\left(\frac{m-\alpha}{2}, -\alpha; 1+\frac{m-\alpha}{2}; -1\right) \\ + (-1)^m \frac{\sin\left(\frac{\pi}{2}(m-\alpha)\right)}{\pi 2^{\alpha}(m+\alpha)} \times \\ \times {}_2F_1\left(-\frac{m+\alpha}{2}, -\alpha; 1-\frac{m+\alpha}{2}; -1\right). \end{aligned} \quad (\text{D.9})$$

### Appendix E: Derivation of the second angular mode (3.23)

Employing the approximation  $\partial_t \hat{f}_2 \approx 0$ , Eq. (3.22) can be cast into the following equation

$$(\Upsilon_0 k^{\alpha} + 4\sigma) \hat{f}_2 + \Upsilon_4 k^{\alpha} e^{i4\psi} \hat{f}_2^* = \hat{F}_1 + i\hat{F}_2, \quad (\text{E.1})$$

with the auxiliary complex function

$$\begin{aligned} \hat{F}_1 + i\hat{F}_2 = \gamma(\hat{f}_1 \star \hat{f}_1) - \Upsilon_1 i k^{\alpha} e^{i\psi} \hat{f}_1 \\ + \Upsilon_2 k^{\alpha} e^{i2\psi} \hat{f}_0 + \Upsilon_3 i k^{\alpha} e^{i3\psi} \hat{f}_1^*, \end{aligned} \quad (\text{E.2})$$

which can be solved by writing out real and imaginary parts of all the modes. Using the ansatz  $\hat{f}_n = \hat{a}_n + i\hat{b}_n$ , for  $n > 0$  (the mode  $n = 0$  is in fact real) yields the coupled linear equations

$$[\Upsilon_0 k^{\alpha} + 4\sigma + \Upsilon_4 k^{\alpha} \cos(4\psi)] \hat{a}_2 + \Upsilon_4 k^{\alpha} \sin(4\psi) \hat{b}_2 = \hat{F}_1, \quad (\text{E.3})$$

$$[\Upsilon_0 k^{\alpha} + 4\sigma - \Upsilon_4 k^{\alpha} \cos(4\psi)] \hat{b}_2 + \Upsilon_4 k^{\alpha} \sin(4\psi) \hat{a}_2 = \hat{F}_2. \quad (\text{E.4})$$

To obtain the solution of the set of equations (E.3, E.4) we write them in vector form

$$\mathbf{M} \begin{pmatrix} \hat{a}_2 \\ \hat{b}_2 \end{pmatrix} = \begin{pmatrix} \hat{F}_1 \\ \hat{F}_2 \end{pmatrix}, \quad \mathbf{M} = (4\sigma + \Upsilon_0 k^{\alpha}) \mathbf{1} + \Upsilon_4 k^{\alpha} \mathbf{R}(4\psi) \quad (\text{E.5})$$

with  $\mathbf{1}$  the identity matrix in two dimensions and  $\mathbf{R}$  the involutory matrix (i.e.,  $\mathbf{R}^2 = \mathbf{1}$ ) in two dimensions

$$\mathbf{R}(\phi) \equiv \begin{pmatrix} \cos \phi & \sin \phi \\ \sin \phi & -\cos \phi \end{pmatrix}. \quad (\text{E.6})$$

In fact, the solution of the linear system (E.5) is readily given by

$$\begin{pmatrix} \hat{a}_2 \\ \hat{b}_2 \end{pmatrix} = \mathbf{M}^{-1} \begin{pmatrix} \hat{F}_1 \\ \hat{F}_2 \end{pmatrix}, \quad \mathbf{M}^{-1} = [\hat{D}_0 \mathbf{1} - \hat{D}_4 \mathbf{R}(4\psi)] \quad (\text{E.7})$$

with the auxiliary  $(k, \alpha)$ -dependent coefficients

$$\hat{D}_0 \equiv \frac{4\sigma + \Upsilon_0 k^{\alpha}}{(4\sigma + \Upsilon_0 k^{\alpha})^2 - (\Upsilon_4 k^{\alpha})^2}, \quad (\text{E.8})$$

$$\hat{D}_4 \equiv \frac{\Upsilon_4 k^{\alpha}}{(4\sigma + \Upsilon_0 k^{\alpha})^2 - (\Upsilon_4 k^{\alpha})^2}. \quad (\text{E.9})$$

Thus, we obtain the solution

$$\begin{pmatrix} \hat{a}_2 \\ \hat{b}_2 \end{pmatrix} = \hat{D}_0 \begin{pmatrix} \hat{F}_1 \\ \hat{F}_2 \end{pmatrix} - \hat{D}_4 \begin{pmatrix} \cos(4\psi)\hat{F}_1 + \sin(4\psi)\hat{F}_2 \\ \sin(4\psi)\hat{F}_1 - \cos(4\psi)\hat{F}_2 \end{pmatrix}, \quad (\text{E.10})$$

or equivalently in compact notation

$$\hat{f}_2 = \hat{D}_0(\hat{F}_1 + i\hat{F}_2) - \hat{D}_4 e^{i4\psi}(\hat{F}_1 + i\hat{F}_2)^*. \quad (\text{E.11})$$

Finally, using Eq. (E.2) the solution (E.11) can be written explicitly in terms of the lower order angular modes, i.e.,

$$\begin{aligned} \hat{f}_2 = & \gamma \hat{D}_0(\hat{f}_1 \star \hat{f}_1) - \gamma \hat{D}_4 e^{i4\psi}(\hat{f}_1 \star \hat{f}_1)^* + \hat{D}_2 k^\alpha e^{i2\psi} \hat{f}_0 \\ & - \hat{D}_1 i k^\alpha e^{i\psi} \hat{f}_1 + \hat{D}_3 i k^\alpha e^{i3\psi} \hat{f}_1^* \end{aligned} \quad (\text{E.12})$$

with the additional  $(k, \alpha)$ -dependent coefficients

$$\hat{D}_1 \equiv \frac{4\Upsilon_1\sigma + (\Upsilon_0\Upsilon_1 - \Upsilon_4\Upsilon_3)k^\alpha}{(4\sigma + \Upsilon_0 k^\alpha)^2 - (\Upsilon_4 k^\alpha)^2}, \quad (\text{E.13})$$

$$\hat{D}_2 \equiv \frac{\Upsilon_2}{4\sigma + (\Upsilon_0 + \Upsilon_4)k^\alpha}, \quad (\text{E.14})$$

$$\hat{D}_3 \equiv \frac{4\Upsilon_3\sigma + (\Upsilon_0\Upsilon_3 - \Upsilon_4\Upsilon_1)k^\alpha}{(4\sigma + \Upsilon_0 k^\alpha)^2 - (\Upsilon_4 k^\alpha)^2}. \quad (\text{E.15})$$

In the hydrodynamic limit ( $k \rightarrow 0$ ), these coefficients satisfy the following asymptotic formulas:

$$\hat{D}_0 = \frac{1}{4\sigma} - \frac{\Upsilon_0}{(4\sigma)^2} k^\alpha + \frac{\Upsilon_0^2 + \Upsilon_4^2}{(4\sigma)^3} k^{2\alpha} + \mathcal{O}(k^{3\alpha}), \quad (\text{E.16})$$

$$\hat{D}_1 = \frac{\Upsilon_1}{4\sigma} - \frac{1}{(4\sigma)^2} (\Upsilon_0\Upsilon_1 + \Upsilon_3\Upsilon_4) k^\alpha + \mathcal{O}(k^{2\alpha}), \quad (\text{E.17})$$

$$\hat{D}_2 = \frac{\Upsilon_2}{4\sigma} - \frac{\Upsilon_2}{4\sigma} (\Upsilon_0 + \Upsilon_4) k^\alpha + \mathcal{O}(k^{2\alpha}), \quad (\text{E.18})$$

$$\hat{D}_3 = \frac{\Upsilon_3}{4\sigma} - \frac{1}{(4\sigma)^2} (\Upsilon_0\Upsilon_3 + \Upsilon_1\Upsilon_4) k^\alpha + \mathcal{O}(k^{2\alpha}), \quad (\text{E.19})$$

$$\hat{D}_4 = \frac{\Upsilon_4}{(4\sigma)^2} k^\alpha + \mathcal{O}(k^{2\alpha}). \quad (\text{E.20})$$

Conversely, in the opposite limit ( $k \rightarrow \infty$ ) we find

$$\hat{D}_0 = \frac{\Upsilon_0}{\Upsilon_0^2 - \Upsilon_2^2} \frac{1}{k^\alpha} + \mathcal{O}(1), \quad (\text{E.21})$$

$$\hat{D}_1 = \frac{\Upsilon_0\Upsilon_1 - \Upsilon_3\Upsilon_4}{\Upsilon_0^2 - \Upsilon_4^2} \frac{1}{k^\alpha} + \mathcal{O}(1), \quad (\text{E.22})$$

$$\hat{D}_2 = \frac{\Upsilon_2}{\Upsilon_0 + \Upsilon_4} \frac{1}{k^\alpha} + \mathcal{O}(1), \quad (\text{E.23})$$

$$\hat{D}_3 = \frac{\Upsilon_0\Upsilon_3 - \Upsilon_1\Upsilon_4}{\Upsilon_0^2 - \Upsilon_2^2} \frac{1}{k^\alpha} + \mathcal{O}(1), \quad (\text{E.24})$$

$$\hat{D}_4 = \frac{\Upsilon_4}{\Upsilon_0^2 - \Upsilon_2^2} \frac{1}{k^\alpha} + \mathcal{O}(1). \quad (\text{E.25})$$

## Appendix F: Derivation of the auxiliary relations presented in Table I

We will denote  $\mathbf{e}_i$  ( $i = \{x, y, z\}$ ) the standard basis of a Cartesian coordinate system. We also introduce the

complex differential operators  $\hat{\nabla}$  and  $\hat{\nabla}^*$  [45, 48, 52]

$$\hat{\nabla} = \frac{\partial}{\partial x} + i \frac{\partial}{\partial y}, \quad \hat{\nabla}^* = \frac{\partial}{\partial x} - i \frac{\partial}{\partial y}, \quad (\text{F.1})$$

whose Fourier transforms are

$$\hat{\nabla}_{\mathbf{k}} = -ik e^{i\psi}, \quad \hat{\nabla}_{\mathbf{k}}^* = -ik e^{-i\psi}. \quad (\text{F.2})$$

For later convenience, we also recall the Pauli matrices

$$\sigma_1 \equiv \begin{pmatrix} 0 & 1 \\ 1 & 0 \end{pmatrix}, \quad \sigma_2 \equiv \begin{pmatrix} 0 & i \\ -i & 0 \end{pmatrix}, \quad \sigma_3 \equiv \begin{pmatrix} 1 & 0 \\ 0 & -1 \end{pmatrix}. \quad (\text{F.3})$$

### 1. Equation (3.50)

This relation is easily obtained by employing Eqs. (F.2). In details,

$$\hat{\nabla}_{\mathbf{k}}^* \hat{f}_1 = -ik_x \hat{p}_x - ik_y \hat{p}_y + k_x \hat{p}_y - k_y \hat{p}_x \quad (\text{F.4})$$

$$\hat{\nabla}_{\mathbf{k}} \hat{f}_1^* = -ik_x \hat{p}_x - ik_y \hat{p}_y - k_x \hat{p}_y + k_y \hat{p}_x, \quad (\text{F.5})$$

such that

$$\hat{\nabla}_{\mathbf{k}}^* \hat{f}_1 + \hat{\nabla}_{\mathbf{k}} \hat{f}_1^* = -2i(k_x \hat{p}_x + k_y \hat{p}_y) = -2i\mathbf{k} \cdot \hat{\mathbf{p}}. \quad (\text{F.6})$$

Therefore, we can write

$$\begin{aligned} ik^\alpha (e^{-i\psi} \hat{f}_1 + e^{i\psi} \hat{f}_1^*) &= -k^{\alpha-1} (\hat{\nabla}_{\mathbf{k}}^* \hat{f}_1 + \hat{\nabla}_{\mathbf{k}} \hat{f}_1^*) \\ &= 2k^{\alpha-1} (i\mathbf{k} \cdot \hat{\mathbf{p}}), \end{aligned} \quad (\text{F.7})$$

whose inverse Fourier transform yields  $-2\mathbb{1}^{1-\alpha}(\nabla \cdot \mathbf{p})$ .

### 2. Equation (3.51)

Employing again the explicit definitions (F.2), we can show that  $k^2 e^{-i2\psi} \hat{h} = -\hat{\nabla}_{\mathbf{k}}^{*2} \hat{h}$  and that  $\hat{\nabla}_{\mathbf{k}}^2 \hat{h}^* = (\hat{\nabla}_{\mathbf{k}}^{*2} \hat{h})^*$  with  $\hat{h}$  the Fourier transform of an arbitrary complex function. Setting  $\hat{h} = \hat{f}_1 \star \hat{f}_1$ , we can then write

$$\begin{aligned} k^\alpha [e^{-i2\psi} (\hat{f}_1 \star \hat{f}_1) + e^{i2\psi} (\hat{f}_1 \star \hat{f}_1)^*] \\ = -k^{\alpha-2} [\hat{\nabla}_{\mathbf{k}}^{*2} (\hat{f}_1 \star \hat{f}_1) + \hat{\nabla}_{\mathbf{k}}^2 (\hat{f}_1 \star \hat{f}_1)^*] \\ = 2k^{\alpha-2} (i\mathbf{k} \cdot \hat{\Xi}_0), \end{aligned} \quad (\text{F.8})$$

where we employed Eq. (F.6) with  $\hat{f}_1$  substituted by  $\hat{\nabla}_{\mathbf{k}}^* (\hat{f}_1 \star \hat{f}_1)$  and we defined the auxiliary vector field  $\hat{\Xi}_0 = (\text{Re}(\hat{\nabla}_{\mathbf{k}}^* \hat{f}_1^2), \text{Im}(\hat{\nabla}_{\mathbf{k}}^* \hat{f}_1^2))$ . The inverse Fourier transform of Eq. (F.8) is thus  $-2\mathbb{1}^{2-\alpha}(\nabla \cdot \hat{\Xi}_0)$ . To obtain an analytical expression for  $\hat{\Xi}_0$ , we calculate the complex derivative

$$\hat{\nabla}_{\mathbf{k}}^* \hat{f}_1^2 = \left[ \frac{\partial}{\partial x} - i \frac{\partial}{\partial y} \right] (p_x^2 - p_y^2 + i2p_x p_y). \quad (\text{F.9})$$

Its real part can be manipulated as below

$$\begin{aligned} \text{Re}[\hat{\nabla}_{\mathbf{k}}^* \hat{f}_1^2] &= 2 \left( p_x \frac{\partial}{\partial x} + p_y \frac{\partial}{\partial y} \right) p_x + 2p_x \left( \frac{\partial p_x}{\partial x} + \frac{\partial p_y}{\partial y} \right) \\ &\quad - \frac{\partial}{\partial x} (p_x^2 + p_y^2), \end{aligned} \quad (\text{F.10})$$

which is clearly the  $x$ -component of Eq. (3.34). Likewise, the imaginary part of  $\hat{\nabla}^* f_1^2$  can be shown to be equal to its  $y$ -component. We note that this final calculation also proves Eq. (3.53).

### 3. Equation (3.54)

The inverse Fourier transform of Eq. (F.5) is given by

$$\hat{\nabla} f_1^* = \nabla \cdot \mathbf{p} + i \left( \frac{\partial p_x}{\partial y} - \frac{\partial p_y}{\partial x} \right). \quad (\text{F.11})$$

Applying again the complex derivative, we obtain

$$\hat{\nabla}^2 f_1^* = \hat{\nabla}(\nabla \cdot \mathbf{p}) + \left( -\frac{\partial}{\partial y} + i \frac{\partial}{\partial x} \right) \left( \frac{\partial p_x}{\partial y} - \frac{\partial p_y}{\partial x} \right). \quad (\text{F.12})$$

On the one hand, the first term is identified with the gradient of  $(\nabla \cdot \mathbf{p})$ ; on the other hand, the second term is identified with the curl of the vorticity vector  $\boldsymbol{\omega}$ , i.e., with the term  $-\nabla \times \boldsymbol{\omega}$ . In fact, we can calculate  $\boldsymbol{\omega} = (\partial_y p_x - \partial_x p_y) \mathbf{e}_z$ . Likewise, we can compute  $\nabla \times \boldsymbol{\omega} = (\mathbf{e}_x \partial_y - \mathbf{e}_y \partial_x)(\partial_y p_x - \partial_x p_y)$ , which corresponds in the complex plane representation to the term  $(\partial_y - i \partial_x)(\partial_y p_x - \partial_x p_y)$ . Therefore, we obtain the vector representation

$$\hat{\nabla}^2 f_1^* \rightarrow \nabla(\nabla \cdot \mathbf{p}) - \nabla \times \boldsymbol{\omega} = \nabla^2 \mathbf{p}, \quad (\text{F.13})$$

where we employed the identity

$$\nabla^2 \mathbf{p} = \nabla(\nabla \cdot \mathbf{p}) - \nabla \times \boldsymbol{\omega}. \quad (\text{F.14})$$

### 4. Equation (3.55)

The inverse Fourier transform of the manipulated term (3.55) is  $-\mathbb{I}^{1-\alpha}(\hat{\nabla} f_1)$ . Using the definition (F.1), we obtain

$$\hat{\nabla} f_1 = \frac{\partial p_x}{\partial x} - \frac{\partial p_y}{\partial y} + i \left( \frac{\partial p_y}{\partial x} + \frac{\partial p_x}{\partial y} \right). \quad (\text{F.15})$$

Its vector representation is given by

$$\hat{\nabla} f_1 \rightarrow \left( \frac{\partial}{\partial x} \mathbf{1} + i \frac{\partial}{\partial y} \boldsymbol{\sigma}_2 \right) \mathbf{p}. \quad (\text{F.16})$$

### 5. Equation (3.56)

The inverse Fourier transform of the manipulated term (3.56) yields  $-\mathbb{I}^{2-\alpha} \hat{\nabla}^2 f_0$ . Applying twice the complex derivative (F.1), we can calculate

$$\hat{\nabla}^2 f_0 = \left( \frac{\partial^2}{\partial x^2} - \frac{\partial^2}{\partial y^2} \right) f_0 + 2i \frac{\partial}{\partial x} \frac{\partial}{\partial y} f_0. \quad (\text{F.17})$$

Its vector representation is thus given by

$$\hat{\nabla}^2 f_0 \rightarrow \left( \frac{\partial}{\partial x} \mathbf{1} + i \frac{\partial}{\partial y} \boldsymbol{\sigma}_2 \right) \nabla \rho. \quad (\text{F.18})$$

### 6. Equation (3.57)

Recalling the definitions (F.2) and the relations obtained in Appendix F 2, we can show that

$$ik^\alpha e^{i3\psi} \hat{f}_1^* = k^{\alpha-3} \hat{\nabla}_{\mathbf{k}}^3 \hat{f}_1^*. \quad (\text{F.19})$$

The inverse Fourier transform of this equation is  $\mathbb{I}^{3-\alpha}(\hat{\nabla}^3 f_1^*)$ . This complex derivative can be computed analytically by applying Eq. (F.1) to (F.12). In details, we obtain

$$\begin{aligned} \hat{\nabla}^3 f_1^* = & \left( \frac{\partial^2}{\partial x^2} - \frac{\partial^2}{\partial y^2} \right) (\nabla \cdot \mathbf{p}) - 2 \frac{\partial}{\partial x} \frac{\partial}{\partial y} \left( \frac{\partial p_x}{\partial y} - \frac{\partial p_y}{\partial x} \right) \\ & + i \left[ \left( \frac{\partial^2}{\partial x^2} - \frac{\partial^2}{\partial y^2} \right) \left( \frac{\partial p_x}{\partial y} - \frac{\partial p_y}{\partial x} \right) + 2 \frac{\partial}{\partial x} \frac{\partial}{\partial y} (\nabla \cdot \mathbf{p}) \right]. \end{aligned} \quad (\text{F.20})$$

Its vector representation can thus be written as

$$\begin{aligned} \hat{\nabla}^3 f_1 \rightarrow & \left( \frac{\partial}{\partial x} \mathbf{1} + i \frac{\partial}{\partial y} \boldsymbol{\sigma}_2 \right) [\nabla(\nabla \cdot \mathbf{p}) - (\nabla \times \boldsymbol{\omega})] \\ \rightarrow & \left( \frac{\partial}{\partial x} \mathbf{1} + i \frac{\partial}{\partial y} \boldsymbol{\sigma}_2 \right) \nabla^2 \mathbf{p}. \end{aligned} \quad (\text{F.21})$$

### 7. Equation (3.58)

Analogously to the previous subsection, we can write

$$ik^\alpha e^{i3\psi} (\hat{f}_1 \star \hat{f}_1)^* = k^{\alpha-3} \hat{\nabla}_{\mathbf{k}}^3 (\hat{f}_1 \star \hat{f}_1)^*, \quad (\text{F.22})$$

whose Fourier inverse transform yields  $\mathbb{I}^{3-\alpha} \hat{\nabla}^3 f_1^{*2}$ . Thus, we only need to compute the complex derivative

$$\hat{\nabla}^3 f_1^{*2} = 2(3\hat{\nabla} f_1^* \hat{\nabla}^2 f_1^* + f_1^* \hat{\nabla}^3 f_1^*). \quad (\text{F.23})$$

For the first term, using Eqs. (F.11, F.12) we find

$$\begin{aligned} \hat{\nabla} f_1^* \hat{\nabla}^2 f_1^* = & (\nabla \cdot \mathbf{p}) \hat{\nabla}(\nabla \cdot \mathbf{p}) \\ & + (\nabla \cdot \mathbf{p}) \left( -\frac{\partial}{\partial y} + i \frac{\partial}{\partial x} \right) \left( \frac{\partial p_x}{\partial y} - \frac{\partial p_y}{\partial x} \right) \\ & + \left( \frac{\partial p_x}{\partial y} - \frac{\partial p_y}{\partial x} \right) \left( -\frac{\partial}{\partial y} + i \frac{\partial}{\partial x} \right) (\nabla \cdot \mathbf{p}) \\ & - \left( \frac{\partial p_x}{\partial y} - \frac{\partial p_y}{\partial x} \right) \hat{\nabla} \left( \frac{\partial p_x}{\partial y} - \frac{\partial p_y}{\partial x} \right). \end{aligned} \quad (\text{F.24})$$

The first and last terms are clearly identified with the gradient of the scalar field  $(\nabla \cdot \mathbf{p})^2 - |\boldsymbol{\omega}|^2$ ; the second term is identified with  $-(\nabla \cdot \mathbf{p})(\nabla \times \boldsymbol{\omega})$ , and the third one with  $\boldsymbol{\omega} \times \nabla(\nabla \cdot \mathbf{p})$ . Indeed, recalling that  $\nabla(\nabla \cdot \mathbf{p}) = (\mathbf{e}_x \partial_x + \mathbf{e}_y \partial_y)(\nabla \cdot \mathbf{p})$ , we can compute  $\boldsymbol{\omega} \times \nabla(\nabla \cdot \mathbf{p}) = (\partial_y p_x - \partial_x p_y)(-\mathbf{e}_x \partial_y + \mathbf{e}_y \partial_x)(\nabla \cdot \mathbf{p})$ , which in the complex plane representation corresponds to the term appearing in the equation. Therefore, we write

$$\begin{aligned} \hat{\nabla} f_1^* \hat{\nabla}^2 f_1^* \rightarrow & \frac{1}{2} \nabla [(\nabla \cdot \mathbf{p})^2 - |\boldsymbol{\omega}|^2] \\ & - (\nabla \cdot \mathbf{p})(\nabla \times \boldsymbol{\omega}) + \boldsymbol{\omega} \times \nabla(\nabla \cdot \mathbf{p}). \end{aligned} \quad (\text{F.25})$$

For the second term, multiplying Eq. (F.20) by  $f_1^*$  and rearranging the terms, we obtain

$$\begin{aligned} f_1^* \hat{\nabla}^3 f_1^* = & \left( p_y \frac{\partial}{\partial y} + p_x \frac{\partial}{\partial x} \right) \left( -\frac{\partial}{\partial y} + i \frac{\partial}{\partial x} \right) \left( \frac{\partial p_x}{\partial y} - \frac{\partial p_y}{\partial x} \right) \\ & + \left( p_y \frac{\partial}{\partial y} + p_x \frac{\partial}{\partial x} \right) \hat{\nabla} (\nabla \cdot \mathbf{p}) \\ & + \left( p_y \frac{\partial}{\partial x} - p_x \frac{\partial}{\partial y} \right) \hat{\nabla} \left( \frac{\partial p_x}{\partial y} - \frac{\partial p_y}{\partial x} \right) \\ & + \left( p_y \frac{\partial}{\partial x} - p_x \frac{\partial}{\partial y} \right) \left( \frac{\partial}{\partial y} - i \frac{\partial}{\partial x} \right) (\nabla \cdot \mathbf{p}). \end{aligned} \quad (\text{F.26})$$

The first two terms are identified with  $(\mathbf{p} \cdot \nabla)[-\nabla \times \boldsymbol{\omega} + \nabla(\nabla \cdot \mathbf{p})]$ . By using Eq. (F.14), this is equal to  $(\mathbf{p} \cdot \nabla) \nabla^2 \mathbf{p}$ . To determine the remaining terms, we introduce the vector operator  $\mathbf{p} \times \nabla = (p_x \partial_y - p_y \partial_x) \mathbf{e}_z$ , such that we can show that  $(\mathbf{p} \times \nabla) \times \nabla(\nabla \cdot \mathbf{p}) = (p_y \partial_x - p_x \partial_y)(\mathbf{e}_x \partial_y - \mathbf{e}_y \partial_x)(\nabla \cdot \mathbf{p})$  and that  $(\mathbf{p} \times \nabla) \times (\nabla \times \boldsymbol{\omega}) = -(p_y \partial_x - p_x \partial_y)(\mathbf{e}_x \partial_x + \mathbf{e}_y \partial_y)(\partial_y p_x - \partial_x p_y)$ . Therefore, the second term in the rhs of the equation is identified with  $(\mathbf{p} \times \nabla) \times \nabla(\nabla \cdot \mathbf{p}) - (\mathbf{p} \times \nabla) \times (\nabla \times \boldsymbol{\omega})$ , which is shown equal to  $(\mathbf{p} \times \nabla) \times \nabla^2 \mathbf{p}$  by recalling Eq. (F.14). Thus, we obtain

$$f_1^* \hat{\nabla}^3 f_1^* \rightarrow (\mathbf{p} \cdot \nabla) \nabla^2 \mathbf{p} + (\mathbf{p} \times \nabla) \times \nabla^2 \mathbf{p}. \quad (\text{F.27})$$

Combining Eqs. (F.25, F.27), we obtain the vector representation

$$\begin{aligned} \frac{1}{2} \hat{\nabla}^3 f_1^{*2} \rightarrow & \frac{3}{2} \nabla [(\nabla \cdot \mathbf{p})^2 - |\boldsymbol{\omega}|^2] + (\mathbf{p} \cdot \nabla) \nabla^2 \mathbf{p} \\ & + (\mathbf{p} \times \nabla) \times \nabla^2 \mathbf{p} - 3(\nabla \cdot \mathbf{p})(\nabla \times \boldsymbol{\omega}) \\ & + 3[\boldsymbol{\omega} \times \nabla(\nabla \cdot \mathbf{p})]. \end{aligned} \quad (\text{F.28})$$

This is further simplified by using the relations

$$(\nabla \cdot \mathbf{p})(\nabla \times \boldsymbol{\omega}) = \frac{1}{2} \nabla(\nabla \cdot \mathbf{p})^2 - (\nabla \cdot \mathbf{p}) \nabla^2 \mathbf{p}, \quad (\text{F.29})$$

$$\boldsymbol{\omega} \times \nabla(\nabla \cdot \mathbf{p}) = \boldsymbol{\omega} \times (\nabla \times \boldsymbol{\omega}) + \boldsymbol{\omega} \times \nabla^2 \mathbf{p}, \quad (\text{F.30})$$

$$\boldsymbol{\omega} \times (\nabla \times \boldsymbol{\omega}) = \frac{1}{2} \nabla |\boldsymbol{\omega}|^2 - (\boldsymbol{\omega} \cdot \nabla) \boldsymbol{\omega}, \quad (\text{F.31})$$

where the first and second one are derived by using Eq. (F.14) and the third one by using the identity of vector calculus

$$\begin{aligned} \nabla(\mathbf{A} \cdot \mathbf{B}) = & (\mathbf{A} \cdot \nabla) \mathbf{B} + (\mathbf{B} \cdot \nabla) \mathbf{A} \\ & + \mathbf{A} \times (\nabla \times \mathbf{B}) + \mathbf{B} \times (\nabla \times \mathbf{A}) \end{aligned} \quad (\text{F.32})$$

with  $\mathbf{A} = \mathbf{B} = \boldsymbol{\omega}$ . Using these relations we obtain the representation

$$\begin{aligned} \frac{1}{2} \hat{\nabla}^3 f_1^{*2} \rightarrow & (\mathbf{p} \cdot \nabla) \nabla^2 \mathbf{p} + (\mathbf{p} \times \nabla) \times \nabla^2 \mathbf{p} + 3[(\nabla \cdot \mathbf{p}) \nabla^2 \mathbf{p} \\ & + (\boldsymbol{\omega} \times \nabla^2 \mathbf{p}) - (\boldsymbol{\omega} \cdot \nabla) \boldsymbol{\omega}]. \end{aligned} \quad (\text{F.33})$$

## 8. Equation (3.59)

Using the first relation from Appendix F 2 we find

$$[k^\alpha e^{i4\psi} (\hat{f}_1 \star \hat{f}_1)^*] = k^{\alpha-4} [\hat{\nabla}_{\mathbf{k}}^4 (\hat{f}_1 \star \hat{f}_1)^*], \quad (\text{F.34})$$

whose Fourier inverse transform yields  $\mathbb{I}^{4-\alpha} (\hat{\nabla}^4 f_1^{*2})$ . Recalling that  $\hat{\nabla}^3 f_1^{*2} \rightarrow 2(\Xi_1 + 3\Xi_2)$  and applying to it the complex derivative  $\hat{\nabla}$ , we can write:

$$\begin{aligned} \hat{\nabla}^4 f_1^{*2} = & 2 \left[ \frac{\partial}{\partial x} (\Xi_{1x} + 3\Xi_{2x}) - \frac{\partial}{\partial x} (\Xi_{1y} + 3\Xi_{2y}) \right] \\ & + 2i \left[ \frac{\partial}{\partial x} (\Xi_{1y} + 3\Xi_{2y}) + \frac{\partial}{\partial y} (\Xi_{1x} + 3\Xi_{2x}) \right]. \end{aligned} \quad (\text{F.35})$$

Its representation is obtained straightforwardly as

$$\hat{\nabla}^4 f_1^{*2} \rightarrow 2 \left( \frac{\partial}{\partial x} \mathbf{1} + i \frac{\partial}{\partial y} \boldsymbol{\sigma}_2 \right) (\Xi_1 + 3\Xi_2). \quad (\text{F.36})$$

## Appendix G: Derivation of the auxiliary relations for the linear stability analysis

We denote  $\mathbf{e}_{\parallel} \equiv (\cos \vartheta_{\parallel}, \sin \vartheta_{\parallel})$  the unit vector specifying the direction of spontaneous symmetry breaking,  $\mathbf{e}_{\perp} \equiv (-\sin \vartheta_{\parallel}, \cos \vartheta_{\parallel})$  the corresponding orthogonal vector and  $\mathbf{e}_{\vartheta} \equiv \mathbf{R}(\vartheta) \mathbf{e}_{\parallel}$  the unit vector specifying the direction of the wave number vector  $\mathbf{q}$  with the two-dimensional rotation matrix  $\mathbf{R}$  (the angle  $\vartheta$  is thus defined with respect to the direction of collective motion).

### 1. Equations (4.19) and (4.21)

The Fourier transform of the term  $\mathbb{I}^{1-\alpha} \delta \Xi_0$  is

$$\mathcal{F}\{\mathbb{I}^{1-\alpha} \delta \Xi_0\} = k^{\alpha-1} \delta \hat{\Xi}_0, \quad (\text{G.1})$$

with  $\delta \Xi_0$  as in Eq. (4.4). Taking its Fourier transform and using the ansatz (4.1) we obtain for the first term

$$\begin{aligned} \mathcal{F}\{(\nabla \cdot \delta \mathbf{p}) \mathbf{p}^*\} = & (-i \mathbf{k} \cdot \delta \mathbf{p}_0) [2\pi e^{st} \delta(\mathbf{k} + \mathbf{q})] p^* \mathbf{e}_{\parallel} \\ = & i q p^* (\mathbf{e}_{\vartheta} \cdot \delta \mathbf{p}_0) [2\pi e^{st} \delta(\mathbf{k} + \mathbf{q})] \mathbf{e}_{\parallel} \end{aligned} \quad (\text{G.2})$$

and for the second one, analogously,

$$\mathcal{F}\{(\nabla \times \delta \mathbf{p}) \times \mathbf{p}^*\} = i q p^* (\mathbf{e}_{\vartheta+\frac{\pi}{2}} \cdot \delta \mathbf{p}_0) [2\pi e^{st} \delta(\mathbf{k} + \mathbf{q})] \mathbf{e}_{\perp}. \quad (\text{G.3})$$

Substituting these expressions into Eq. (G.1), we find the Fourier transform of Eq. (4.21)

$$\mathcal{F}\{\mathbb{I}^{1-\alpha} \delta \Xi_0\} = i q^{\alpha} p^* [(\mathbf{e}_{\vartheta} \cdot \hat{\delta} \mathbf{p}) \mathbf{e}_{\parallel} + (\mathbf{e}_{\vartheta+\frac{\pi}{2}} \cdot \hat{\delta} \mathbf{p}) \mathbf{e}_{\perp}]. \quad (\text{G.4})$$

Analogously, the Fourier transform of  $\mathbb{I}^{2-\alpha} (\nabla \cdot \delta \Xi_0)$  is

$$\mathcal{F}\{\mathbb{I}^{2-\alpha} (\nabla \cdot \delta \Xi_0)\} = k^{\alpha-2} [(-i \mathbf{k}) \cdot \delta \hat{\Xi}_0]. \quad (\text{G.5})$$

By employing the formulas just derived, we obtain

$$\begin{aligned} \mathcal{F}\{\mathbb{I}^{2-\alpha} (\nabla \cdot \delta \Xi_0)\} = & -q^{\alpha} p^* [(\mathbf{e}_{\vartheta} \cdot \hat{\delta} \mathbf{p})(\mathbf{e}_{\vartheta} \cdot \mathbf{e}_{\parallel}) \\ & + (\mathbf{e}_{\vartheta+\frac{\pi}{2}} \cdot \hat{\delta} \mathbf{p})(\mathbf{e}_{\vartheta} \cdot \mathbf{e}_{\perp})]. \end{aligned} \quad (\text{G.6})$$

## 2. Equation (4.21)

The Fourier transform of the term  $\mathbb{I}^{3-\alpha}\delta\Xi_1$  is given by

$$\mathcal{F}\{\mathbb{I}^{3-\alpha}\delta\Xi_1\} = k^{\alpha-3}\mathcal{F}\{\delta\Xi_1\}, \quad (\text{G.7})$$

with  $\delta\Xi_1$  as in Eq. (4.5). Taking its Fourier transform and using the ansatz (4.1), we obtain for the first term

$$\begin{aligned} \mathcal{F}\{(\mathbf{p}^* \cdot \nabla)\nabla^2\delta\mathbf{p}\} &= p^*(-i\mathbf{k} \cdot \mathbf{e}_{\parallel})(-i\mathbf{k})^2\delta\mathbf{p}_0[2\pi e^{st}\delta(\mathbf{k} + \mathbf{q})] \\ &= -iq^3p^*(\mathbf{e}_{\vartheta} \cdot \mathbf{e}_{\parallel})\delta\mathbf{p}_0[2\pi e^{st}\delta(\mathbf{k} + \mathbf{q})]; \end{aligned} \quad (\text{G.8})$$

and for the second one

$$\begin{aligned} \mathcal{F}\{(\mathbf{p}^* \times \nabla) \times \nabla^2\delta\mathbf{p}\} &= p^*k^2(i\mathbf{k} \cdot \mathbf{e}_{\perp}) \times \\ &\quad \times (-\delta p_{0y}\mathbf{e}_x + \delta p_{0x}\mathbf{e}_y)[2\pi e^{st}\delta(\mathbf{k} + \mathbf{q})] \\ &= -iq^3p^*(\mathbf{e}_{\vartheta} \cdot \mathbf{e}_{\perp})\mathbf{R}\left(\frac{\pi}{2}\right)\delta\mathbf{p}_0[2\pi e^{st}\delta(\mathbf{k} + \mathbf{q})]. \end{aligned} \quad (\text{G.9})$$

Substituting these expressions into Eq. (G.7), we find the Fourier transform of Eq. (4.21)

$$\mathcal{F}\{\mathbb{I}^{3-\alpha}\delta\Xi_1\} = -iq^{\alpha}p^*\left[(\mathbf{e}_{\vartheta} \cdot \mathbf{e}_{\parallel}) + (\mathbf{e}_{\vartheta} \cdot \mathbf{e}_{\perp})\mathbf{R}\left(\frac{\pi}{2}\right)\right]\delta\hat{\mathbf{p}}. \quad (\text{G.10})$$

## 3. Equation (4.24)

The Fourier transform of Eq. (4.6) can be written as

$$\begin{aligned} \mathcal{F}\{\delta Q_j^{(1)}\} &= -B_0k^{\alpha}\delta\hat{M}_{jl}p_l^* - B_0k^{\alpha}M_{jl}^*\delta\hat{p}_l \\ &\quad + \frac{\lambda_1}{2}k^{\alpha-1}\hat{T}_{jl}\delta\hat{p}_l - \frac{\lambda_2}{4}k^{\alpha-2}\hat{T}_{jl}(-ik_l)\delta\hat{\rho} \\ &\quad + \frac{\lambda_3}{4}k^{\alpha-3}\hat{T}_{jl}(-k^2)\delta\hat{p}_l - B_4k^{\alpha-4}\hat{T}_{jl}\delta\hat{\Xi}_{1l}. \end{aligned} \quad (\text{G.11})$$

This equation can be simplified if we recall that all Fourier transform of the vector fields are  $\propto \delta(\mathbf{q} + \mathbf{k})$ . Thus, we can make the substitution  $\mathbf{k} \rightarrow -q\mathbf{e}_{\vartheta}$  and write the Fourier transform of the differential operator  $\mathbf{T}$  as

$$\hat{\mathbf{T}} = iq \begin{pmatrix} \cos(\vartheta + \vartheta_{\parallel}) & -\sin(\vartheta + \vartheta_{\parallel}) \\ \sin(\vartheta + \vartheta_{\parallel}) & \cos(\vartheta + \vartheta_{\parallel}) \end{pmatrix}. \quad (\text{G.12})$$

Therefore, Eq. (G.11) simplifies to

$$\begin{aligned} \mathcal{F}\{\delta Q_j^{(1)}\} &= -B_0q^{\alpha}\delta\hat{M}_{jl}p_l^* - B_0q^{\alpha}M_{jl}^*\delta\hat{p}_l \\ &\quad + i\frac{\lambda_1}{2}q^{\alpha}R_{jl}(\vartheta + \vartheta_{\parallel})\delta\hat{p}_l + \frac{\lambda_2}{4}q^{\alpha}R_{jl}(\vartheta + \vartheta_{\parallel})e_{\vartheta l}\delta\hat{\rho} \\ &\quad - i\frac{\lambda_3}{4}q^{\alpha}R_{jl}(\vartheta + \vartheta_{\parallel})\delta\hat{p}_l - iB_4q^{\alpha-3}R_{jl}(\vartheta + \vartheta_{\parallel})\delta\hat{\Xi}_{1l}. \end{aligned} \quad (\text{G.13})$$

In addition, we can show that  $\delta\hat{M}_{jl}p_l^* + M_{jl}^*\delta\hat{p}_l = 2p^*\delta\hat{p}_l$ . Therefore, using also Eqs. (G.8, G.9), we obtain

$$\begin{aligned} \mathcal{F}\{\delta Q_j^{(1)}\} &= -2B_0q^{\alpha}p^*\delta\hat{p}_j + i\frac{\lambda_1}{2}q^{\alpha}R_{jl}(\vartheta + \vartheta_{\parallel})\delta\hat{p}_l \\ &\quad + \frac{\lambda_2}{4}q^{\alpha}\delta\hat{\rho}R_{jl}(\vartheta + \vartheta_{\parallel})e_{\vartheta l} - i\frac{\lambda_3}{4}q^{\alpha}R_{jl}(\vartheta + \vartheta_{\parallel})\delta\hat{p}_l \\ &\quad - B_4q^{\alpha}p^*(\mathbf{e}_{\vartheta} \cdot \mathbf{e}_{\perp})R_{jm}(\vartheta + \vartheta_{\parallel})R_{ml}\left(\frac{\pi}{2}\right)\delta\hat{p}_l \\ &\quad - B_4q^{\alpha}p^*(\mathbf{e}_{\vartheta} \cdot \mathbf{e}_{\parallel})R_{jl}(\vartheta + \vartheta_{\parallel})\delta\hat{p}_l. \end{aligned} \quad (\text{G.14})$$

- 
- [1] John Toner, Yuhai Tu, and Sriram Ramaswamy, “Hydrodynamics and phases of flocks,” *Ann. Phys.* **318**, 170–244 (2005).
  - [2] Frank Schweitzer, *Brownian agents and active particles: collective dynamics in the natural and social sciences* (Springer, 2007).
  - [3] Sriram Ramaswamy, “The mechanics and statistics of active matter,” *Annu. Rev. Condens. Matter Phys.* **1**, 323–345 (2010).
  - [4] M Cristina Marchetti, J F Joanny, S Ramaswamy, T B Liverpool, J Prost, Madan Rao, and R Aditi Simha, “Hydrodynamics of soft active matter,” *Rev. Mod. Phys.* **85**, 1143 (2013).
  - [5] M. J. B. Hauser and Lutz Schimansky-Geier, “Statistical physics of self-propelled particles,” *Eur. Phys. J. Spec. Top.* **202**, 1–162 (2012).
  - [6] Daniel Needleman and Zvonimir Dogic, “Active matter at the interface between materials science and cell

- biology,” *Nat. Rev. Mat.* **2**, 17048 (2017).
- [7] Tamás Vicsek, András Czirók, Eshel Ben-Jacob, Inon Cohen, and Ofer Shochet, “Novel type of phase transition in a system of self-driven particles,” *Phys. Rev. Lett.* **75**, 1226 (1995).
- [8] John Toner and Yuhai Tu, “Long-range order in a two-dimensional dynamical xy model: how birds fly together,” *Phys. Rev. Lett.* **75**, 4326 (1995).
- [9] John Toner and Yuhai Tu, “Flocks, herds, and schools: A quantitative theory of flocking,” *Phys. Rev. E* **58**, 4828 (1998).
- [10] Tamás Vicsek and Anna Zafeiris, “Collective motion,” *Phys. Rep.* **517**, 71–140 (2012).
- [11] Christopher Dombrowski, Luis Cisneros, Sunita Chatkaew, Raymond E Goldstein, and John O Kessler, “Self-concentration and large-scale coherence in bacterial dynamics,” *Phys. Rev. Lett.* **93**, 098103 (2004).

- [12] Juan P Hernandez-Ortiz, Christopher G Stoltz, and Michael D Graham, “Transport and collective dynamics in suspensions of confined swimming particles,” *Phys. Rev. Lett.* **95**, 204501 (2005).
- [13] Andrey Sokolov, Igor S Aranson, John O Kessler, and Raymond E Goldstein, “Concentration dependence of the collective dynamics of swimming bacteria,” *Phys. Rev. Lett.* **98**, 158102 (2007).
- [14] Igor S Aranson, Andrey Sokolov, John O Kessler, and Raymond E Goldstein, “Model for dynamical coherence in thin films of self-propelled microorganisms,” *Phys. Rev. E* **75**, 040901(R) (2007).
- [15] David Saintillan and Michael J Shelley, “Orientational order and instabilities in suspensions of self-locomoting rods,” *Phys. Rev. Lett.* **99**, 058102 (2007).
- [16] Charles W Wolgemuth, “Collective swimming and the dynamics of bacterial turbulence,” *Biophys. J.* **95**, 1564–1574 (2008).
- [17] Tim Sanchez, Daniel TN Chen, Stephen J DeCamp, Michael Heymann, and Zvonimir Dogic, “Spontaneous motion in hierarchically assembled active matter,” *Nature* **491**, 431 (2012).
- [18] Henricus H Wensink, Jörn Dunkel, Sebastian Heidenreich, Knut Drescher, Raymond E Goldstein, Hartmut Löwen, and Julia M Yeomans, “Meso-scale turbulence in living fluids,” *Proc. Natl. Acad. Sci.* **109**, 14308–14313 (2012).
- [19] Amin Doostmohammadi, Jordi Ignés-Mullol, Julia M Yeomans, and Francesc Sagués, “Active nematics,” *Nat. Commun.* **9**, 3246 (2018).
- [20] J Tailleur and M E Cates, “Statistical mechanics of interacting run-and-tumble bacteria,” *Phys. Rev. Lett.* **100**, 218103 (2008).
- [21] Yaouen Fily and M Cristina Marchetti, “Athermal phase separation of self-propelled particles with no alignment,” *Phys. Rev. Lett.* **108**, 235702 (2012).
- [22] Gabriel S Redner, Michael F Hagan, and Aparna Baskaran, “Structure and dynamics of a phase-separating active colloidal fluid,” *Phys. Rev. Lett.* **110**, 055701 (2013).
- [23] Michael E Cates and Julien Tailleur, “Motility-induced phase separation,” *Annu. Rev. Condens. Matter Phys.* **6**, 219–244 (2015).
- [24] Eric Lauga and Thomas R Powers, “The hydrodynamics of swimming microorganisms,” *Rep. Progr. Phys.* **72**, 096601 (2009).
- [25] Donald L. Koch and Ganesh Subramanian, “Collective hydrodynamics of swimming microorganisms: Living fluids,” *Annu. Rev. Fluid Mech.* **43**, 637–659 (2011).
- [26] Jens Elgeti, Roland G Winkler, and Gerhard Gompper, “Physics of microswimmers?single particle motion and collective behavior: a review,” *Rep. Progr. Phys.* **78**, 056601 (2015).
- [27] M. Poujade, E. Grasland-Mongrain, A. Hertzog, J. Jouanneau, P. Chavrier, B. Ladoux, A. Buguin, and P. Silberzan, “Collective migration of an epithelial monolayer in response to a model wound,” *Proc. Natl. Acad. Sci.* **104**, 15988–15993 (2007).
- [28] Thuan Beng Saw, Amin Doostmohammadi, Vincent Nier, Leyla Kocgozlu, Sumesh Thampi, Yusuke Toyama, Philippe Marcq, Chwee Teck Lim, Julia M Yeomans, and Benoit Ladoux, “Topological defects in epithelia govern cell death and extrusion,” *Nature* **544**, 212 (2017).
- [29] Kyogo Kawaguchi, Ryoichiro Kageyama, and Masaki Sano, “Topological defects control collective dynamics in neural progenitor cell cultures,” *Nature* **545**, 327 (2017).
- [30] C Blanch-Mercader, V Yashunsky, S Garcia, G Duclos, L Giomi, and P Silberzan, “Turbulent dynamics of epithelial cell cultures,” *Phys. Rev. Lett.* **120**, 208101 (2018).
- [31] Wang Xi, Thuan Beng Saw, Delphine Delacour, Chwee Teck Lim, and Benoit Ladoux, “Material approaches to active tissue mechanics,” *Nat. Rev. Mat.* **4**, 23–44 (2018).
- [32] Xavier Trepast and Erik Sahai, “Mesoscale physical principles of collective cell organization,” *Nat. Phys.* **14**, 671–682 (2018).
- [33] Frederick C MacKintosh and Christoph F Schmidt, “Active cellular materials,” *Curr. Opin. Cell Biol.* **22**, 29–35 (2010).
- [34] Jacques Prost, Frank Jülicher, and Jean-François Joanny, “Active gel physics,” *Nat. Phys.* **11**, 111 (2015).
- [35] Dirk Helbing, “Traffic and related self-driven many-particle systems,” *Rev. Mod. Phys.* **73**, 1067 (2001).
- [36] Jerome Buhl, David JT Sumpter, Iain D Couzin, Joe J Hale, Emma Despland, Edgar R Miller, and Steve J Simpson, “From disorder to order in marching locusts,” *Science* **312**, 1402–1406 (2006).
- [37] Michele Ballerini, Nicola Cabibbo, Raphael Candelier, Andrea Cavagna, Evaristo Cisbani, Irene Giardinà, Vivien Lecomte, Alberto Orlandi, Giorgio Parisi, Andrea Procaccini, M Viale, and V Zdravkovic, “Interaction ruling animal collective behavior depends on topological rather than metric distance: Evidence from a field study,” *Proc. Natl. Acad. Sci.* **105**, 1232–1237 (2008).
- [38] Ofer Feinerman, Itai Pinkoviezky, Aviram Gelblum, Ehud Fonio, and Nir S Gov, “The physics of cooperative transport in groups of ants,” *Nat. Phys.* **14**, 683–693 (2018).
- [39] Clemens Bechinger, Roberto Di Leonardo, Hartmut Löwen, Charles Reichhardt, Giorgio Volpe, and Giovanni Volpe, “Active particles in complex and crowded environments,” *Rev. Mod. Phys.* **88**, 045006 (2016).
- [40] Manuele Brambilla, Eliseo Ferrante, Mauro Birattari, and Marco Dorigo, “Swarm robotics: a review from the swarm engineering perspective,” *Swarm Intell.* **7**, 1–41 (2013).
- [41] FJ Ndlec, Thomas Surrey, Anthony C Maggs, and Stanislas Leibler, “Self-organization of microtubules and motors,” *Nature* **389**, 305 (1997).
- [42] Volker Schaller, Christoph Weber, Christine Semmrich, Erwin Frey, and Andreas R Bausch, “Polar patterns of driven filaments,” *Nature* **467**, 73 (2010).
- [43] Tariq Butt, Tabish Mufti, Ahmad Humayun, Peter B Rosenthal, Sohaib Khan, Shahid Khan, and Justin E Molloy, “Myosin motors drive long range alignment of actin filaments,” *J. Biol. Chem.* **285**, 4964–4974 (2010).
- [44] Paul M Chaikin, Tom C Lubensky, and Thomas A Witten, *Principles of condensed matter physics*, Vol. 1 (Cambridge University Press, 1995).
- [45] Eric Bertin, Michel Droz, and Guillaume Grégoire, “Boltzmann and hydrodynamic description for self-propelled particles,” *Phys. Rev. E* **74**, 022101 (2006).
- [46] F. Peruani, A. Deutsch, and M. Bär, “A mean-field theory for self-propelled particles interacting by velocity

- alignment mechanisms,” *Eur. Phys. J. Spec. Top.* **157**, 111–122 (2008).
- [47] Aparna Baskaran and M Cristina Marchetti, “Hydrodynamics of self-propelled hard rods,” *Phys. Rev. E* **77**, 011920 (2008).
- [48] Eric Bertin, Michel Droz, and Guillaume Grégoire, “Hydrodynamic equations for self-propelled particles: microscopic derivation and stability analysis,” *J. Phys. A* **42**, 445001 (2009).
- [49] Chiu Fan Lee, “Fluctuation-induced collective motion: A single-particle density analysis,” *Phys. Rev. E* **81**, 031125 (2010).
- [50] A. Peshkov, E. Bertin, F. Ginelli, and H. Chaté, “Boltzmann-Ginzburg-Landau approach for continuous descriptions of generic Vicsek-like models,” *Eur. Phys. J. Spec. Top.* **223**, 1315–1344 (2014).
- [51] Florian Thüroff, Christoph A Weber, and Erwin Frey, “Numerical treatment of the Boltzmann equation for self-propelled particle systems,” *Phys. Rev. X* **4**, 041030 (2014).
- [52] Eric Bertin, “Theoretical approaches to the steady-state statistical physics of interacting dissipative units,” *J. Phys. A* **50**, 083001 (2017).
- [53] Pawel Romanczuk, Markus Bär, Werner Ebeling, Benjamin Lindner, and Lutz Schimansky-Geier, “Active Brownian particles,” *Eur. Phys. J. Spec. Top.* **202**, 1–162 (2012).
- [54] John Toner, “Reanalysis of the hydrodynamic theory of fluid, polar-ordered flocks,” *Phys. Rev. E* **86**, 031918 (2012).
- [55] R Aditi Simha and Sriram Ramaswamy, “Hydrodynamic fluctuations and instabilities in ordered suspensions of self-propelled particles,” *Phys. Rev. Lett.* **89**, 058101 (2002).
- [56] Yashodhan Hatwalne, Sriram Ramaswamy, Madan Rao, and R Aditi Simha, “Rheology of active-particle suspensions,” *Phys. Rev. Lett.* **92**, 118101 (2004).
- [57] Karsten Kruse, Jean-François Joanny, Frank Jülicher, Jacques Prost, and Ken Sekimoto, “Asters, vortices, and rotating spirals in active gels of polar filaments,” *Phys. Rev. Lett.* **92**, 078101 (2004).
- [58] Karsten Kruse, Jean-François Joanny, Frank Jülicher, Jacques Prost, and Ken Sekimoto, “Generic theory of active polar gels: a paradigm for cytoskeletal dynamics,” *Eur. Phys. J. E* **16**, 5–16 (2005).
- [59] Frank Jülicher, Stephan W Grill, and Guillaume Salbreux, “Hydrodynamic theory of active matter,” *Rep Prog Phys* **81**, 076601 (2018).
- [60] Crispin Gardiner, *Stochastic Methods: A Handbook for the Natural and Social Sciences* (Springer, Berlin, Germany, 2009).
- [61] Guillaume Grégoire and Hugues Chaté, “Onset of collective and cohesive motion,” *Phys. Rev. Lett.* **92**, 025702 (2004).
- [62] Hugues Chaté, Francesco Ginelli, Guillaume Grégoire, and Franck Raynaud, “Collective motion of self-propelled particles interacting without cohesion,” *Phys. Rev. E* **77**, 046113 (2008).
- [63] A P Solon and Julien Tailleur, “Revisiting the flocking transition using active spins,” *Phys. Rev. Lett.* **111**, 078101 (2013).
- [64] Alexandre P Solon and Julien Tailleur, “Flocking with discrete symmetry: The two-dimensional active ising model,” *Phys. Rev. E* **92**, 042119 (2015).
- [65] Balint Szabo, GJ Szöllösi, B Gönci, Zs Jurányi, David Selmeczi, and Tamás Vicsek, “Phase transition in the collective migration of tissue cells: experiment and model,” *Phys. Rev. E* **74**, 061908 (2006).
- [66] András Czirók, H Eugene Stanley, and Tamás Vicsek, “Spontaneously ordered motion of self-propelled particles,” *J. Phys. A* **30**, 1375 (1997).
- [67] András Czirók, Albert-László Barabási, and Tamás Vicsek, “Collective motion of self-propelled particles: Kinetic phase transition in one dimension,” *Phys. Rev. Lett.* **82**, 209 (1999).
- [68] András Czirók and Tamás Vicsek, “Collective behavior of interacting self-propelled particles,” *Physica A* **281**, 17–29 (2000).
- [69] Maximino Aldana, Victor Dossetti, Christian Huepe, VM Kenkre, and Hernán Larralde, “Phase transitions in systems of self-propelled agents and related network models,” *Phys. Rev. Lett.* **98**, 095702 (2007).
- [70] Balázs Gönci, Máté Nagy, and Tamás Vicsek, “Phase transition in the scalar noise model of collective motion in three dimensions,” *Eur. Phys. J. Spec. Top.* **157**, 53–59 (2008).
- [71] Francesco Ginelli, “The Physics of the Vicsek model,” *Eur. Phys. J. Spec. Top.* **225**, 2099–2117 (2016).
- [72] Guillaume Grégoire, Hugues Chaté, and Yuhai Tu, “Comment on” particle diffusion in a quasi-two-dimensional bacterial bath,” *Phys. Rev. Lett.* **86**, 556 (2001).
- [73] Guillaume Grégoire, Hugues Chaté, and Yuhai Tu, “Active and passive particles: Modeling beads in a bacterial bath,” *Phys. Rev. E* **64**, 011902 (2001).
- [74] Francesco Ginelli and Hugues Chaté, “Relevance of metric-free interactions in flocking phenomena,” *Phys. Rev. Lett.* **105**, 168103 (2010).
- [75] A. Peshkov, S. Ngo, E. Bertin, H. Chaté and F. Ginelli, “Continuous theory of active matter systems with metric-free interactions,” *Phys. Rev. Lett.* **109**, 098101 (2012).
- [76] Sriram Ramaswamy, R Aditi Simha, and John Toner, “Active nematics on a substrate: Giant number fluctuations and long-time tails,” *EPL* **62**, 196 (2003).
- [77] Hugues Chaté, Francesco Ginelli, and Raúl Montagne, “Simple model for active nematics: quasi-long-range order and giant fluctuations,” *Phys. Rev. Lett.* **96**, 180602 (2006).
- [78] Sandrine Ngo, Francesco Ginelli, and Hugues Chaté, “Competing ferromagnetic and nematic alignment in self-propelled polar particles,” *Phys. Rev. E* **86**, 050101(R) (2012).
- [79] L Huber, R Suzuki, T Krüger, E Frey, and AR Bausch, “Emergence of coexisting ordered states in active matter systems,” *Science* **361**, 255–258 (2018).
- [80] ME Cates, D Marenduzzo, I Pagonabarraga, and J Tailleur, “Arrested phase separation in reproducing bacteria creates a generic route to pattern formation,” *Proc. Natl. Acad. Sci.* **107**, 11715–11720 (2010).
- [81] F D C Farrell, M C Marchetti, D Marenduzzo, and J Tailleur, “Pattern formation in self-propelled particles with density-dependent motility,” *Phys. Rev. Lett.* **108**, 248101 (2012).
- [82] Yutaka Sumino, Ken H Nagai, Yuji Shitaka, Dan Tanaka, Kenichi Yoshikawa, Hugues Chaté, and Kazuhiro Oiwa, “Large-scale vortex lattice emerging from collectively moving microtubules,” *Nature* **483**,

- 448 (2012).
- [83] Alessandro Attanasi, Andrea Cavagna, Lorenzo Del Castello, Irene Giardina, Tomas S Grigera, Asja Jelić, Stefania Melillo, Leonardo Parisi, Oliver Pohl, Edward Shen, *et al.*, “Information transfer and behavioural inertia in starling flocks,” *Nat. Phys.* **10**, 691 (2014).
  - [84] Andrea Cavagna, Lorenzo Del Castello, Irene Giardina, Tomas Grigera, Asja Jelic, Stefania Melillo, Thierry Mora, Leonardo Parisi, Edmondo Silvestri, Massimiliano Viale, *et al.*, “Flocking and turning: a new model for self-organized collective motion,” *J. Stat. Phys.* **158**, 601–627 (2015).
  - [85] Xingbo Yang and M Cristina Marchetti, “Hydrodynamics of turning flocks,” *Phys. Rev. Lett.* **115**, 258101 (2015).
  - [86] Ken H Nagai, Yutaka Sumino, Raul Montagne, Igor S Aranson, and Hugues Chaté, “Collective motion of self-propelled particles with memory,” *Phys. Rev. Lett.* **114**, 168001 (2015).
  - [87] Felix Kümmel, Borge ten Hagen, Raphael Wittkowski, Ivo Buttinoni, Ralf Eichhorn, Giovanni Volpe, Hartmut Löwen, and Clemens Bechinger, “Circular motion of asymmetric self-propelling particles,” *Phys. Rev. Lett.* **110**, 198302 (2013).
  - [88] A Kaiser and H Löwen, “Vortex arrays as emergent collective phenomena for circle swimmers,” *Phys. Rev. E* **87**, 032712 (2013).
  - [89] H H Wensink, V Kantsler, R E Goldstein, and J Dunkel, “Controlling active self-assembly through broken particle-shape symmetry,” *Phys. Rev. E* **89**, 010302(R) (2014).
  - [90] Nguyen H P Nguyen, Daphne Klotz, Michael Engel, and Sharon C Glotzer, “Emergent collective phenomena in a mixture of hard shapes through active rotation,” *Phys. Rev. Lett.* **112**, 075701 (2014).
  - [91] Jonas Denk, Lorenz Huber, Emanuel Reithmann, and Erwin Frey, “Active curved polymers form vortex patterns on membranes,” *Phys. Rev. Lett.* **116**, 178301 (2016).
  - [92] Benno Liebchen, Michael E Cates, and Davide Marenduzzo, “Pattern formation in chemically interacting active rotors with self-propulsion,” *Soft Matter* **12**, 7259–7264 (2016).
  - [93] Benno Liebchen and Demian Levis, “Collective behavior of chiral active matter: pattern formation and enhanced flocking,” *Phys. Rev. Lett.* **119**, 058002 (2017).
  - [94] B Mahault, X-c Jiang, E Bertin, Y-q Ma, A Patelli, X-q Shi, and H Chaté, “Self-propelled particles with velocity reversals and ferromagnetic alignment: Active matter class with second-order transition to quasi-long-range polar order,” *Phys. Rev. Lett.* **120**, 258002 (2018).
  - [95] Jean-Philippe Bouchaud and Antoine Georges, “Anomalous diffusion in disordered media: statistical mechanisms, models and physical applications,” *Phys. Rep.* **195**, 127–293 (1990).
  - [96] R. Metzler and J. Klafter, “The random walk’s guide to anomalous diffusion: a fractional dynamics approach,” *Phys. Rep.* **339**, 1–77 (2000).
  - [97] Ralf Metzler and Joseph Klafter, “The restaurant at the end of the random walk: recent developments in the description of anomalous transport by fractional dynamics,” *J. Phys. A* **37**, R161 (2004).
  - [98] R. Klages, G. Radons, and I. M. Sokolov, *Anomalous transport: foundations and applications* (John Wiley & Sons, 2008).
  - [99] V. Zaburdaev, S. Denisov, and J. Klafter, “Lévy walks,” *Rev. Mod. Phys.* **87**, 483 (2015).
  - [100] A. Cairoli and A. Baule, “Anomalous Processes with General Waiting Times: Functionals and Multipoint Structure,” *Phys. Rev. Lett.* **115**, 110601 (2015).
  - [101] Peter Dieterich, Rainer Klages, Roland Preuss, and Albrecht Schwab, “Anomalous dynamics of cell migration,” *Proc. Natl. Acad. Sci.* **105**, 459–463 (2008).
  - [102] Tajie H Harris, Edward J Banigan, David A Christian, Christoph Konradt, Elia D Tait Wojno, Kazumi Norose, Emma H Wilson, Beena John, Wolfgang Weninger, Andrew D Luster, *et al.*, “Generalized lévy walks and the role of chemokines in migration of effector cd8+ t cells,” *Nature* **486**, 545 (2012).
  - [103] Paul C Bressloff and Jay M Newby, “Stochastic models of intracellular transport,” *Rev. Mod. Phys.* **85**, 135 (2013).
  - [104] F. Höfling and T. Franosch, “Anomalous transport in the crowded world of biological cells,” *Rep. Progr. Phys.* **76**, 046602 (2013).
  - [105] Igor M Sokolov, “Models of anomalous diffusion in crowded environments,” *Soft Matter* **8**, 9043–9052 (2012).
  - [106] Yasmine Meroz and Igor M Sokolov, “A toolbox for determining subdiffusive mechanisms,” *Phys. Rep.* **573**, 1–29 (2015).
  - [107] Gandimohan M Viswanathan, Sergey V Buldyrev, Shlomo Havlin, MGE Da Luz, EP Raposo, and H Eugene Stanley, “Optimizing the success of random searches,” *Nature* **401**, 911 (1999).
  - [108] Michael A Lomholt, Koren Tal, Ralf Metzler, and Klafter Joseph, “Lévy strategies in intermittent search processes are advantageous,” *Proc. Natl. Acad. Sci.* (2008).
  - [109] Olivier Bénichou, C Loverdo, M Moreau, and R Voituriez, “Intermittent search strategies,” *Rev. Mod. Phys.* **83**, 81 (2011).
  - [110] Gandhimohan M Viswanathan, Marcos GE Da Luz, Ernesto P Raposo, and H Eugene Stanley, *The physics of foraging: an introduction to random searches and biological encounters* (Cambridge University Press, 2011).
  - [111] Andrea Cavagna, SM Duarte Queirós, Irene Giardina, Fabio Stefanini, and Massimiliano Viale, “Diffusion of individual birds in starling flocks,” *Proc. R. Soc. B* **280**, 20122484 (2013).
  - [112] Hisashi Murakami, Takayuki Niizato, Takenori Tomaru, Yuta Nishiyama, and Yukio-Pegio Gunji, “Inherent noise appears as a Lévy walk in fish schools,” *Sci. Rep.* **5** (2015).
  - [113] Gil Ariel, Amit Rabani, Sivan Benisty, Jonathan D Partridge, Rasika M Harshey, and Avraham Be’Er, “Swarming bacteria migrate by Lévy walk,” *Nat. Commun.* **6** (2015).
  - [114] Sergei Fedotov and Nickolay Korabel, “Emergence of lévy walks in systems of interacting individuals,” *Phys. Rev. E* **95**, 030107(R) (2017).
  - [115] B. V. Gnedenko and A. N. Kolmogorov, *Limit distributions for sums of independent random variables* (Addison-Wesley, Cambridge, United States, 1954).
  - [116] Andrea Cairoli and Chiu Fan Lee, “Hydrodynamics of active Lévy matter,” The accompanying Letter.

- [117] Benoit B Mandelbrot, *The fractal geometry of nature*, Vol. 2 (WH freeman New York, 1982).
- [118] Barry D Hughes, Michael F Shlesinger, and Elliott W Montroll, “Random walks with self-similar clusters,” *Proc. Natl. Acad. Sci.* **78**, 3287–3291 (1981).
- [119] Micheal F Shlesinger, George M Zaslavsky, and Uriel Frisch, *Lévy flights and related topics in Physics*, Lecture notes in Physics, Vol. 450 (Springer-Verlag, 1995).
- [120] R. Großmann, F. Peruani, and M. Bär, “Superdiffusion, large-scale synchronization, and topological defects,” *Phys. Rev. E* **93**, 040102(R) (2016).
- [121] Gissell Estrada-Rodriguez and Heiko Gimperlein, “Swarming of interacting robots with Lévy strategies: a macroscopic description,” *arXiv preprint arXiv:1807.10124* (2018).
- [122] Kerson Huang, *Statistical Mechanics*, 2nd ed. (New York: John Wiley & Sons, 1987).
- [123] David Applebaum, *Lévy processes and stochastic calculus* (Cambridge university press, 2009).
- [124] Peter Tankov, *Financial modelling with jump processes*, Vol. 2 (CRC press, 2003).
- [125] J Mikusinski, “On the function whose laplace transform is  $\exp^{-sa}$ ,” *Stud. Math.* **18**, 191 (1959).
- [126] John T Bendler, “Lévy (stable) probability densities and mechanical relaxation in solid polymers,” *J. Stat. Phys.* **36**, 625–637 (1984).
- [127] R Hilfer, “H-function representations for stretched exponential relaxation and non-Debye susceptibilities in glassy systems,” *Phys. Rev. E* **65**, 061510 (2002).
- [128] KA Penson and K Górska, “Exact and explicit probability densities for one-sided Lévy stable distributions,” *Phys. Rev. Lett.* **105**, 210604 (2010).
- [129] Hans C Fogedby, “Langevin equations for continuous time Lévy flights,” *Phys. Rev. E* **50**, 1657 (1994).
- [130] Nikolai V Brilliantov and Thorsten Pöschel, *Kinetic theory of granular gases* (Oxford University Press, 2010).
- [131] Anatoly Aleksandrovich Vlasov, “The vibrational properties of an electron gas,” *Phys.-Uspekhi* **10**, 721–733 (1968).
- [132] Stefan G Samko, Anatoly A Kilbas, Oleg I Marichev, *et al.*, *Fractional integrals and derivatives: Theory and Applications*, Vol. 1993 (Gordon and Breach, Yverdon, 1993).
- [133] Mark M Meerschaert, David A Benson, and Boris Bäumer, “Multidimensional advection and fractional dispersion,” *Phys. Rev. E* **59**, 5026 (1999).
- [134] Jake P Taylor-King, Rainer Klages, Sergei Fedotov, and Robert A Van Gorder, “Fractional diffusion equation for an n-dimensional correlated Lévy walk,” *Phys. Rev. E* **94**, 012104 (2016).
- [135] Vasily E Tarasov, *Fractional dynamics: applications of fractional calculus to dynamics of particles, fields and media* (Springer Science & Business Media, 2011).
- [136] Itzhak Fouxon, Sergey Denisov, Vasily Zaburdaev, and Eli Barkai, “Limit theorems for Lévy walks in d dimensions: rare and bulk fluctuations,” *J. Phys. A* **50**, 154002 (2017).
- [137] David P Landau and Kurt Binder, *A Guide to Monte Carlo Simulations in Statistical Physics* (Cambridge University Press, England, 2014).
- [138] Kurt Binder, “Finite size scaling analysis of ising model block distribution functions,” *Zeitschrift für Physik B Condensed Matter* **43**, 119–140 (1981).
- [139] Michael E Fisher, Shang-keng Ma, and BG Nickel, “Critical exponents for long-range interactions,” *Phys. Rev. Lett.* **29**, 917 (1972).
- [140] Masuo Suzuki, “Critical exponents for long-range interactions. i: Dimensionality, symmetry and potential-range,” *Prog. Theor. Phys.* **49**, 424–441 (1973).
- [141] Leiming Chen, John Toner, and Chiu Fan Lee, “Critical phenomenon of the order–disorder transition in incompressible active fluids,” *New J. Phys.* **17**, 042002 (2015).
- [142] Leiming Chen, Chiu Fan Lee, and John Toner, “Mapping two-dimensional polar active fluids to two-dimensional soap and one-dimensional sandblasting,” *Nat. Commun.* **7** (2016).
- [143] Leiming Chen, Chiu Fan Lee, and John Toner, “Incompressible polar active fluids in the moving phase in dimensions  $d \geq 2$ ,” *New J. Phys.* **20**, 113035 (2018).
- [144] B. Partridge, and C. F. Lee “Critical motility-induced phase separation belongs to the Ising universality class,” *Phys. Rev. Lett.* **123**, 068002 (2019).
- [145] J. T. Siebert, F. Dittrich, F. Schmid, K. Binder, T. Speck, and P. Virmau “Critical behavior of active Brownian particles,” *Phys. Rev. E* **98**, 030601(R) (2018).
- [146] F. Caballero, C. Nardini, and M. E. Cates “From bulk to microphase separation in scalar active matter: A perturbative renormalization group analysis,” *J. Stat. Mech.* **12**, 123208 (2018).
- [147] D. Nesbitt, G. Pruessner and C. F. Lee, “Using a lattice Boltzmann method to uncover novel phase transitions in dry polar active fluids,” *arXiv:1902.00530*.
- [148] Satya N Majumdar, “Brownian functionals in Physics and Computer Science,” *Curr. Sci.* **88** (2005).
- [149] C Godreche and JM Luck, “Statistics of the occupation time of renewal processes,” *J. Stat. Phys.* **104**, 489–524 (2001).
- [150] Dennis C Rapaport, *The art of molecular dynamics simulation* (Cambridge university press, 2004).
- [151] Aleksand Janicki and Aleksander Weron, *Simulation and chaotic behavior of alpha-stable stochastic processes*, Vol. 178 (CRC Press, 1993).
- [152] D Kleinhans and R Friedrich, “Continuous-time random walks: Simulation of continuous trajectories,” *Phys. Rev. E* **76**, 061102 (2007).
- [153] William H Press, Saul A Teukolsky, William T Vetterling, and Brian P Flannery, *Numerical recipes 3rd edition: The art of scientific computing* (Cambridge university press, 2007).
- [154] Boris Baeumer and Mark M Meerschaert, “Tempered stable lévy motion and transient super-diffusion,” *J. Comput. Appl. Math.* **233**, 2438–2448 (2010).
- [155] Rafał Weron, “On the Chambers-Mallows-Stuck method for simulating skewed stable random variables,” *Stat. Probabil. Lett.* **28**, 165–171 (1996).